Oamaru Diatoms

Scanning Electron Microscope Images
by Mary Ann Tiffany

Seam of Diatomite Adjacent to Collection Outcrop

Introduction

The rolling hills near the town of Oamaru, on the east coast of the South Island of New Zealand, are famous for their beds of Late Eocene-Early Oligocene diatomite, laid down about 32-35 million years ago. The beds are exposed at several sites sandwiched between igneous and limestone layers on farms around Oamaru (Dailey 2004). While the rolling hills of the Oamaru region are not especially remarkable, the diatomite found there is quite remarkable indeed! Some people mine the diatomite for products such as kitty litter while some of us appreciate these fossil beds for learning.

The climate during this period was much warmer than now with tropical seas dominating the planet, tropical forest common on land, and temperate forests reaching all the way to near the North and South Poles.

The beds were deposited in a shallow, tropical sea rich in nutrients which encouraged successive plankton blooms. The diatom flora speciated wildly, resulting in the fantastic diversity found in the diatomite, including some of the most exotic marine forms in the world. The beds are believed to have formed in a quiet basin about 50 kilometers offshore that received very little terrestrial sediment. The silica skeletons of the diatoms fell on the sea floor and were covered and compressed by overlying layers of plankton to form the soft rock, diatomite. Subsequently, they were covered by volcanic deposits and earth movements. Remarkably, many of these diatom shells remain intact and perfectly preserved over many millions of years.

This speciation resulted in perhaps the most diverse fossil marine diatom community ever recorded with over 700 species from about 120 genera. A few species have been recorded only from Oamaru (e.g. species of *Kittonia*). Others are known from widely dispersed Eocene-Oligocene fossil sites around the world, such as Barbados, providing evidence that tropical seas were interconnected during these epochs. Some species are still living today (Richman & Carter 2007, Charles 2017, Edwards 1991).

The specimens in this collection came from Bain's Farm near Oamaru in New Zealand (lat -45.100657 lon 170.888204, elevation ~ 100 meters). In 2003, friends of Bill Dailey collected samples at the outcrop of diatomite shown at the arrow in the illustration. Bill cleaned the samples and sent material to Mary Ann Tiffany (then at the Center for Inland Waters and Department of Biology of San Diego State University, California, US) who made the images in this collection. This collection is a tribute to their work.

This selection of images is certainly not an exhaustive inventory of Oamaru diatoms but it contains studies of genera such as *Kittonia*, *Gyrosigma*, and *Aulacodiscus*. Many of the genera, at least in the form of their shell, are still living after all this time since the Eocene-Oligocene epochs.

Image Gallery

Images are arranged by morphological groups adapted from Diatoms of North America. Centric diatoms have been split into radial and polar groups. Some genera defy these categories. For example, *Stictodiscus* is assigned to centric radials but contains members that have definite poles. Several specimens are identified to genus with a provisional species identifier until more is learned (e.g., *Stephanopyxis* sp1).

The file name of the image is included at the end of each the figure description. The number in the file name stands for magnification to be used in the table A Sense of Scale. "Tilt" signifies that the specimen was tilted at 45 degrees in the SEM. A letter before tilt or the magnification denotes the same specimen in a group of images.

To enlarge images, expand the file in Acrobat Reader.

A Sense of Scale

Magnification is the last part of the file name included with each figure.
Image widths in microns (µm), rounded to nearest whole number.

Magnification	200	250	300	350	400	450	500	600	700	800	900	1000	1100
Width (µm)	583	467	389	333	292	260	233	194	167	146	130	117	106
Magnification	1300	1500	1800	2000	2500	3000	3500	4000	4500	5000	6000	7000	
Width (µm)	90	78	65	58	47	39	33	29	26	23	19	17	

Plate 1

Biraphid Symmetric

Gyrosigma sp1

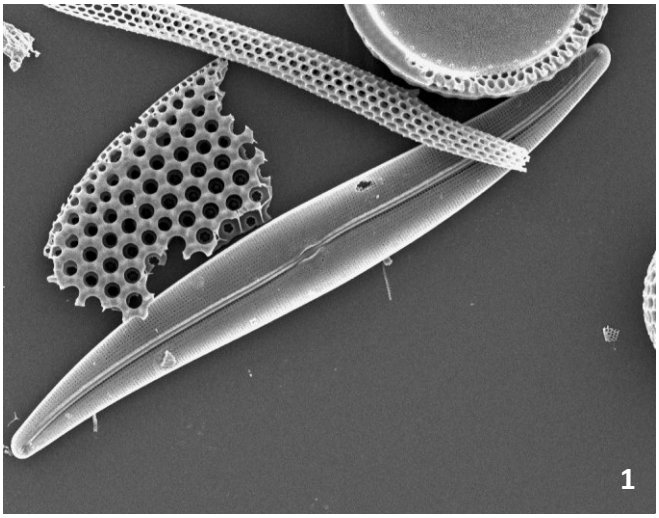

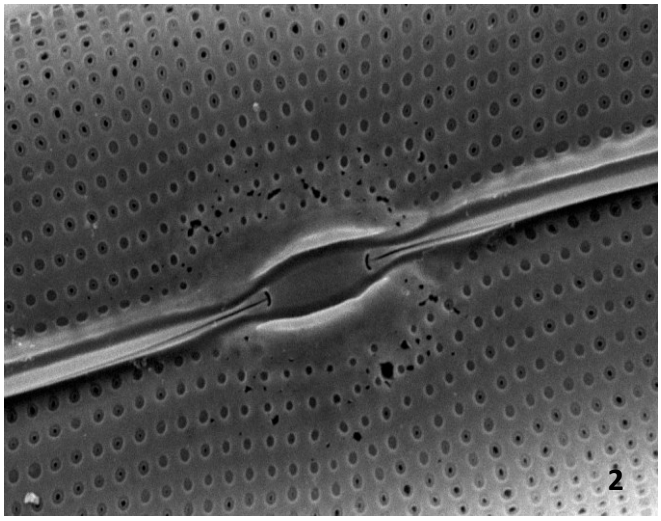

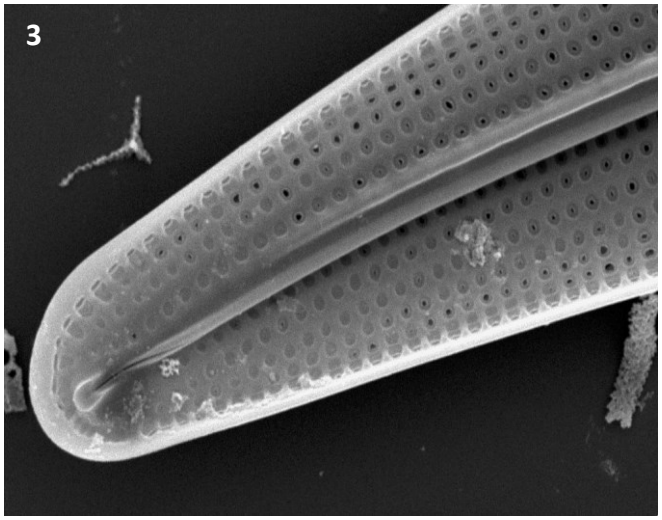

Refer to Round et al. (1990) for genus description; Witkowski (2023a); Edwards (1991) pg 3 for paleoenvironment.

Fig 1 Internal view. Length = 184 µm. It might be surprising to see a diatom associated with mud flats in this collection. This specimen might be an indicator of the volcanic shoals that occasionally formed in the basin where the sediments were accumulating. oamaru2i700gyrosigma.

Fig 2 Internal view of valve central area with proximal raphe ends. oamaru2i4500.

Fig 3 Internal view of apex with distal raphe ending in a helictoglossa. oamaru2ii4500.

Centric Polar

Entogoniopsis pseudonervata

Refer to Witkowski (2023a) for identification; Witkowski et al. (2015) fig 213 for LM image; D&S (1989) pl 127 fig 2,3,6,7 as *Trigonium pseudonervata*; DiatomBase for taxonomy (https://www.diatombase.org/aphia.php?p=taxdetails&id=1035025).

Fig 1 Pseudocelli on the poles have no rim. Mantles distinct and vertical. oamaru2utilt1000.

Entogoniopsis venosa

Refer to Witkowski (2023a) for identification; Witkowski et al. (2015) fig 52 for SEM image; DiatomBase (https://www.diatombase.org/aphia.php?p=taxdetails&id=987533).

Fig 2 Pseudocelli raised on elevations and have a plain rim. Areolae large near center, smaller beneath elevations. Mantles distinct and vertical. See images oamaru21100 and oamaru22000 for other views of this specimen. oamaru2ctilt1000.

Fig 3 Tilted view of image oamaru2ctilt1000. Pseudocelli raised on elevations and have a plain rim. Areolae large near center, smaller beneath elevations. Mantles distinct and vertical. oamaru21100.

Fig 4 Detail of a pole of oamaru21100. Pseudocellus raised on an elevation and having a plain rim. Areolae large near center of valve, smaller beneath elevations. Mantles distinct and vertical. oamaru22000.

Goniothecium decoratum

Refer to Charles (2017); D&S (1989) pg 156 and pl 66 fig 5,6,8, recorded from Bain's Farm.

Fig 5. Girdle view of two sibling valves linked by teeth. oamaru3_i1500.

Plate 2

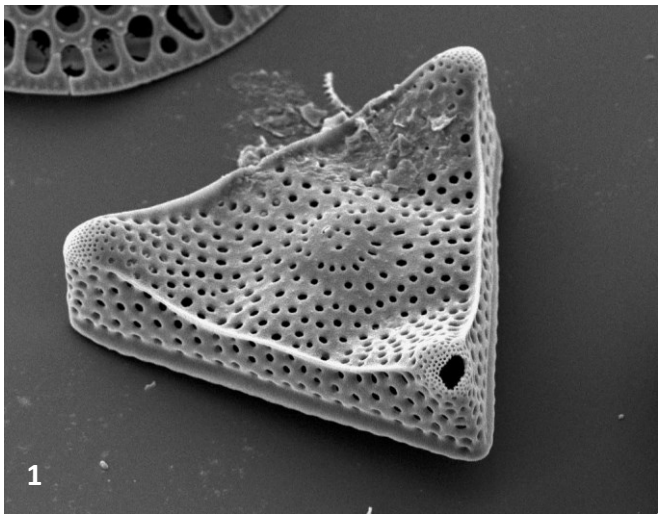

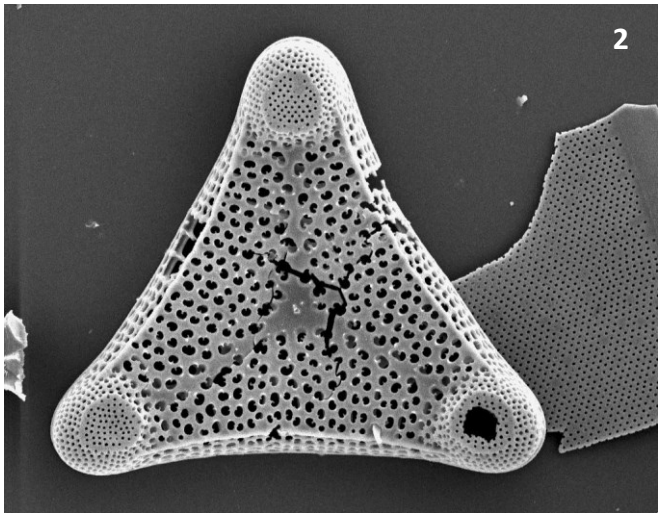

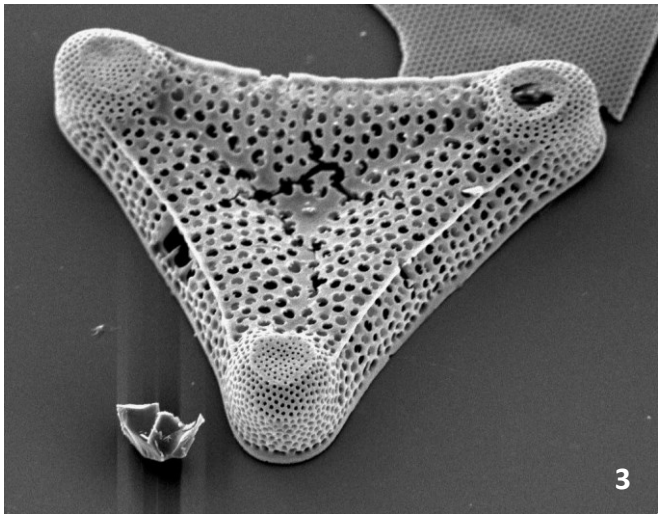

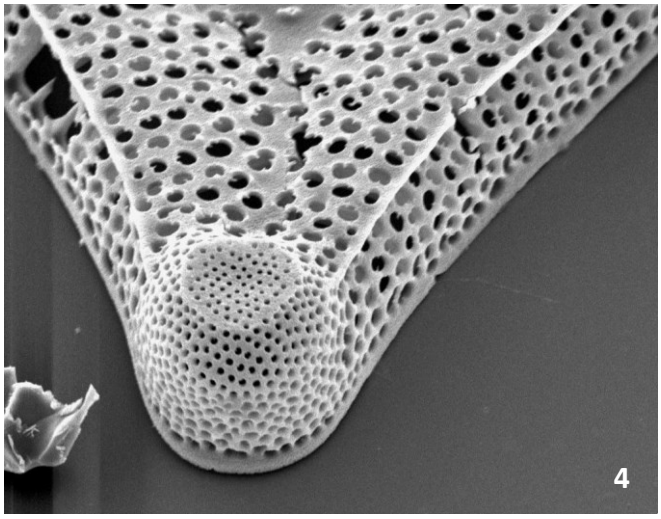

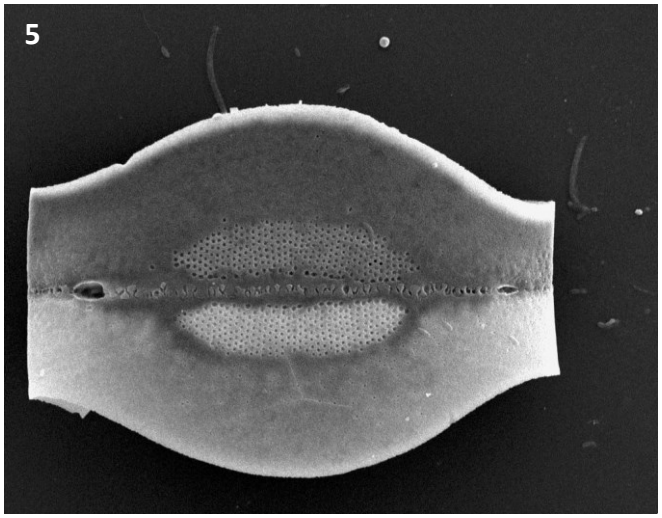

Plate 3

Hemiaulus sp1

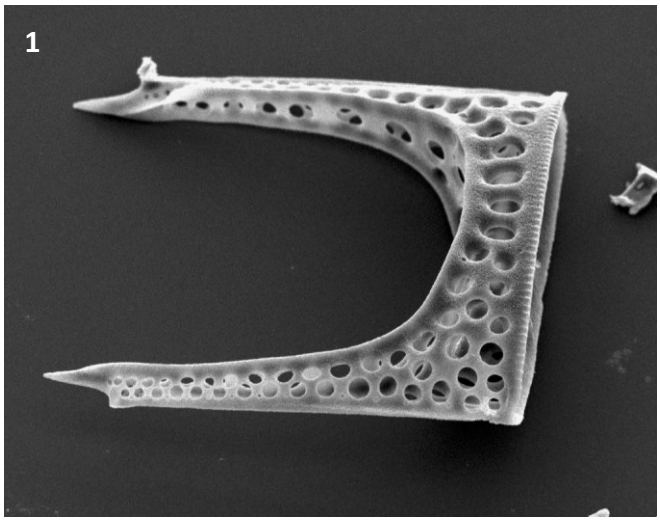

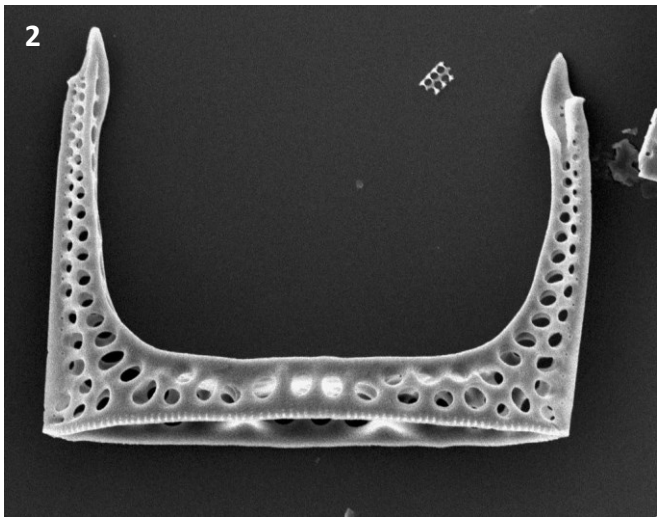

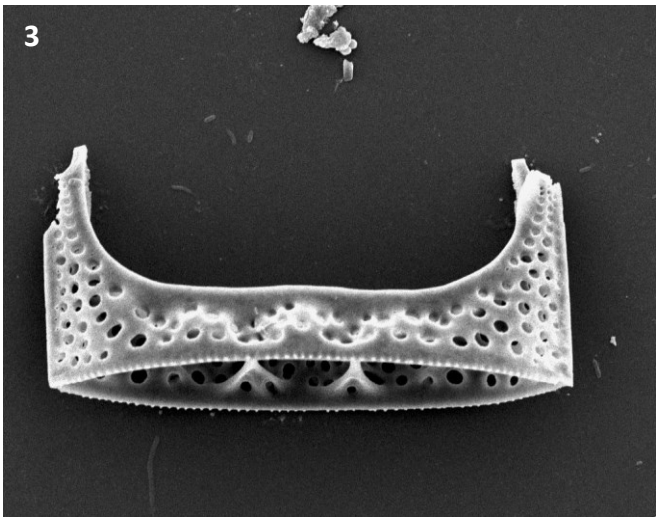

Refer to Round et al. (1990); Charles (2017).

Fig 1 Girdle view of valve tilted. oamaru2mtilt1800.

Fig 2 Girdle view of valve. oamaru2t1500.

Fig 3 Girdle view of valve. oamaru3_l1300.

Plate 4

Kittonia elaborata

Refer to Round et al. (1990) pg 278; Charles (2017); D&S (1989) pg 169 and pl 74 fig 1-9, recorded from Bain's Farm.

Fig 1 Internal view of valve. oamar3c800.

Fig 2 Detail of internal view of rimoportula openings in central area. oamar3c2500.

Fig 3 Internal view of opening to one of the tubular processes particular to this genus, here called a stalked ocellus. oamar3c3000.

Fig 4 External view of a stalked ocellus. oamaru_3f1300.

Fig 5 View of external openings of central rimoportulae. oamaru_3f2000.

Fig 6 External detail of stalked ocellus. oamaru_3f3000.

Plate 4

Kittonia elaborata

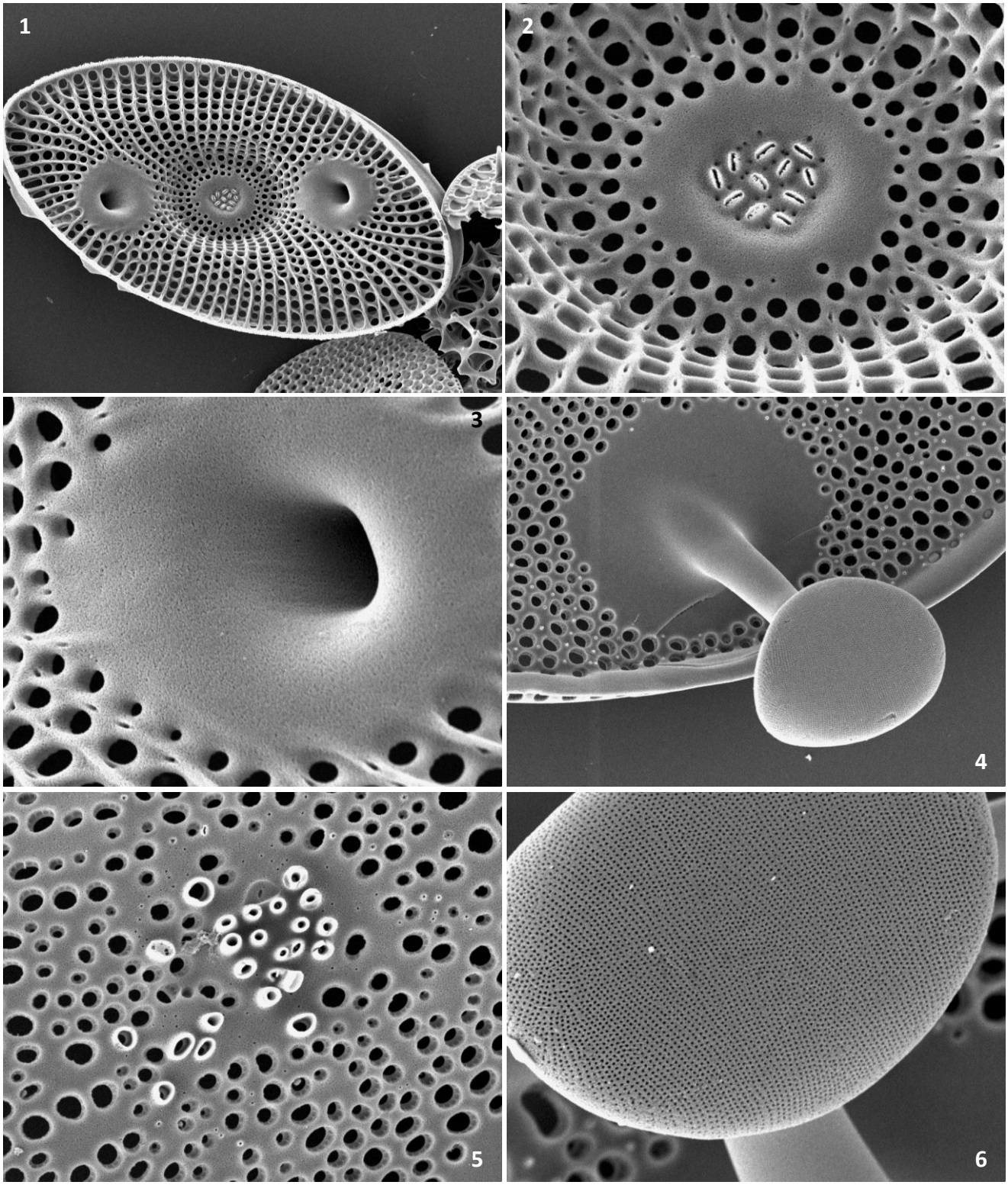

Plate 5

Kittonia elaborata

Fig 1 Complete external view of stalked ocellus. oamaru_3ff1300.

Fig 2 External view of valve tilted. oamaru_3fffftilt500.

Fig 3 External view of valve. oamaru_3ffftilt500.

Fig 4 External view of valve center and one pole. oamaru_3fftilt900.

Fig 5 External view of valve. oamaru_3ftilt500.

Fig 6 External view of valve center and one pole. oamaru_3ftilt900.

Oamaru Diatoms

Plate 5

Kittonia elaborata

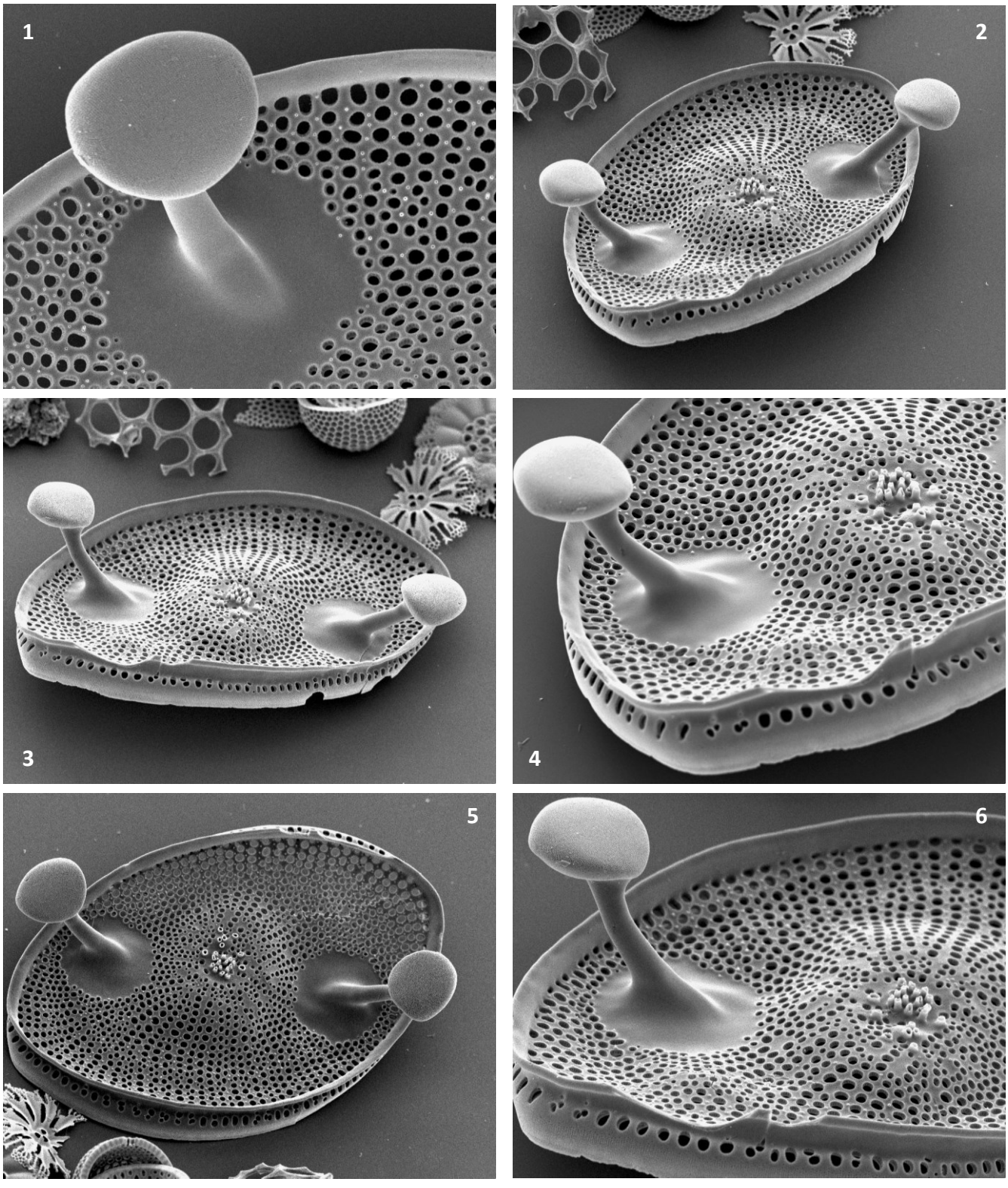

Plate 6

Kittonia elaborata

Fig 1 View of external openings of central rimoportulae. oamaru_3ftilt2500.

Fig 2 Internal view of openings of rimoportulae in central area. oamaru_3mtilt1300.

Fig 3 External openings of central rimoportulae. Detail of image oamaru_3tttilt600. oamaru_3ttilt2500.

Fig 4 External view of valve with fractured ocelli. oamaru_3tttilt600.

Fig 5 Fractured ocellus in detail of image oamaru_3tttilt600. oamaru_3tttilt2500.

Fig 6 External opening of fractured stem of ocellus in detail of image oamaru_3tttilt600. oamaru_3tttilt4000.

Plate 6

Kittonia elaborata

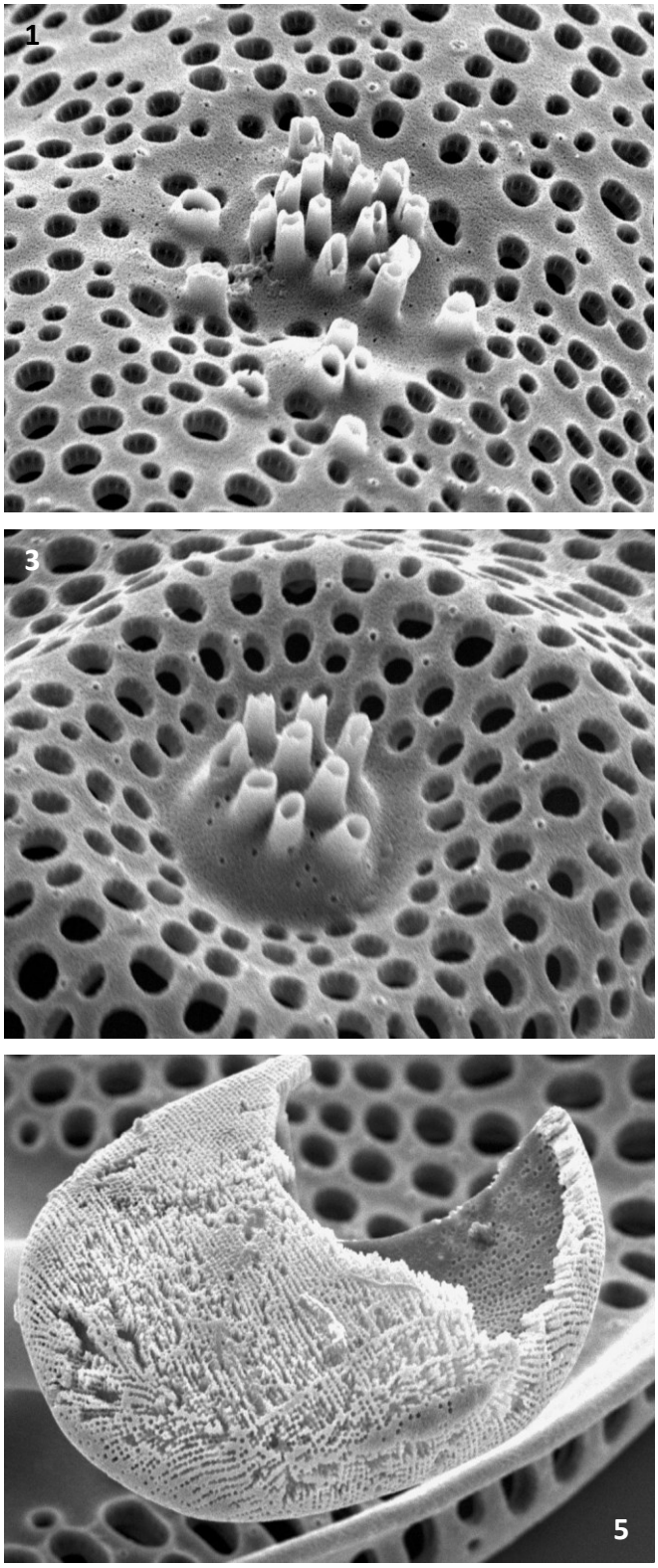

Pyxilla prolungata

Refer to Round et al. (1990); DiatomBase for name authority (https://www.diatombase.org/aphia.php?p=taxdetails&id=964841); Charles (2017) for illustration; D&S (1989) pg 220 and pl 93 fig 8 for description and illustration.

Fig 1 External view of a valve. oamaru2ntilt1000.

Rattrayella oamaruensis

Refer to Sims (2006); Guiry (2016); Heck (2015); Charles (2017); Schmidt (1874-1959) tafel 125 fig 20; D&S (1989) pg 221 and pl 94 fig 1-2.

Fig 2 External view. Large openings around the valve margin are ocelli with the coverings of small porelli eroded. Valve diameter 52 µm. Rimoportulae between the ocelli distinguish this from *Glyphodiscus*. oamaru3t1500.

Fig 3 External view of an ocellus with covering of small porelli eroded. Ocellus diameter 4 µm. oamaru3t7000.

Fig 4 External view of valve tilted. oamaru3ttilt1500.

Fig 5 External view of valve margin with ocelli and rimoportulae. Large openings along the margin are ocelli with the coverings of small porelli eroded. Remnants of the coverings visible around inner edge of an ocellus. Ocellus diameter 4 µm. Rimoportulae between the ocelli distinguish this from *Glyphodiscus*. oamaru3ttilt3500.

Plate 7

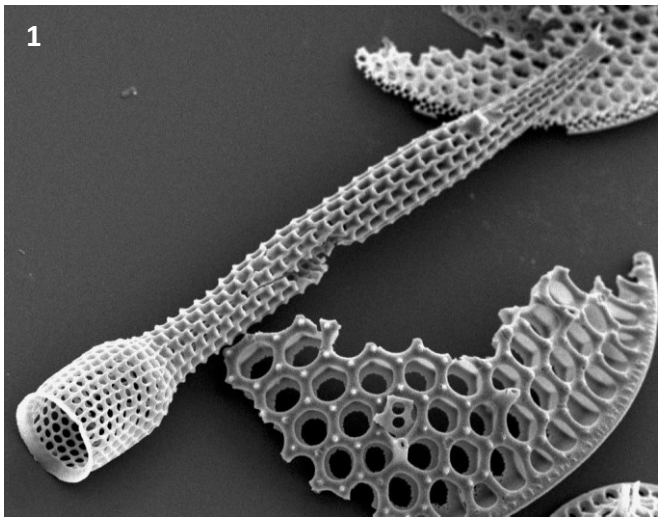

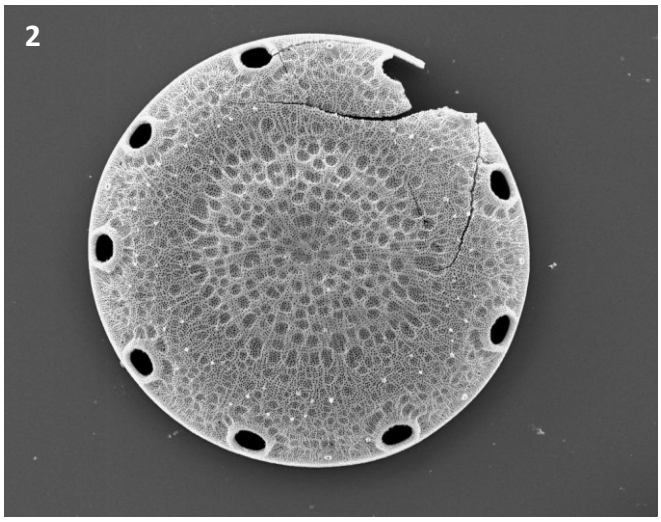

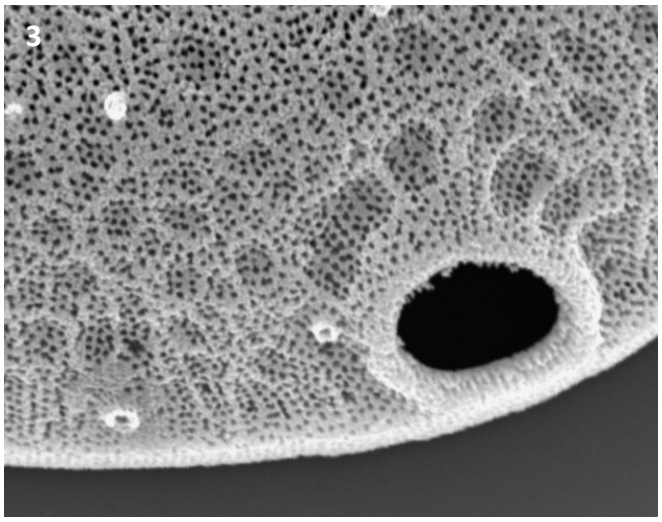

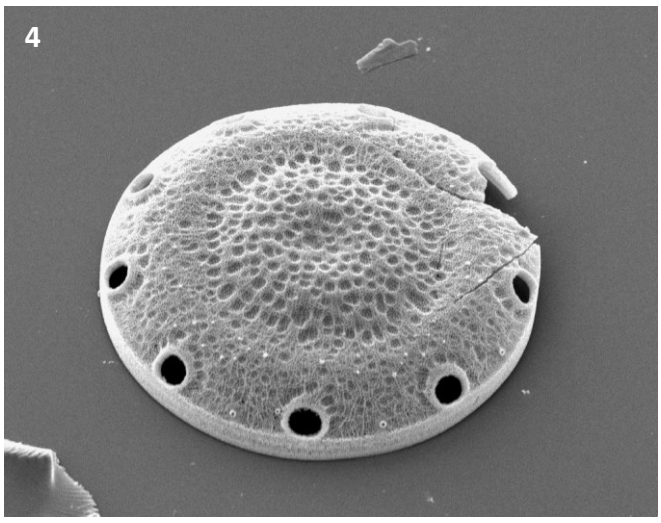

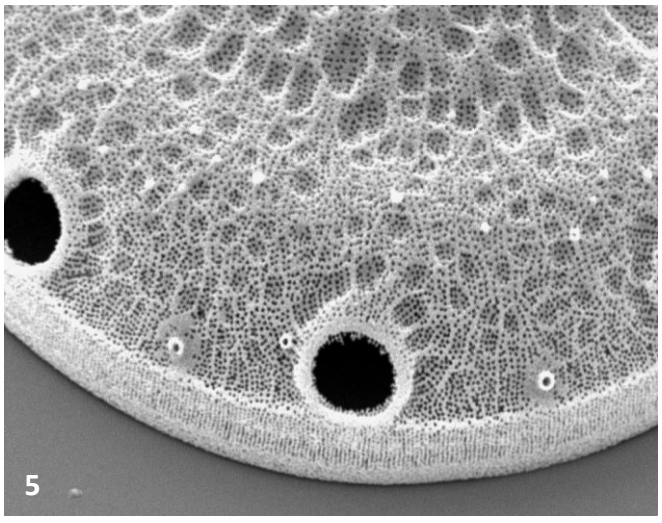

Plate 8

Rutilaria radiata

Refer to Charles (2017); D&S (1989) pg 250 and pl 118 fig 1-5, pl 122 fig 1,2,5, recorded from Bain's Farm.

Fig 1 External view of valve of a long form. Length 123 µm. Ocellus at one end is eroded. The opposite ocellus is missing. The twisted periplekton (a specialized rimoportula) arises from the center. oamaru2a1000.

Fig 2 Detail of external view of periplekton of image oamaru2a1000. Erosion in two locations has exposed the hollow interior. oamaru2a4000.

Fig 3 External view of valve tilted. Ocellus at one end is eroded. The opposite ocellus is missing. The twisted periplekton (a specialized rimoportula) arises from the center. oamaru2aatilt1000.

Fig 4 External view of valve tilted. Ocellus at one end is eroded. The opposite ocellus is missing. The twisted periplekton (a specialized rimoportula) arises from the center. oamaru2atilt1000.

Fig 5 Detail of periplekton. Erosion has exposed the hollow interior. oamaru2atilt2000.

Fig 6 Detail of periplekton. Erosion has exposed the hollow interior. oamaru2atilt4000.

Plate 8

Rutilaria radiata

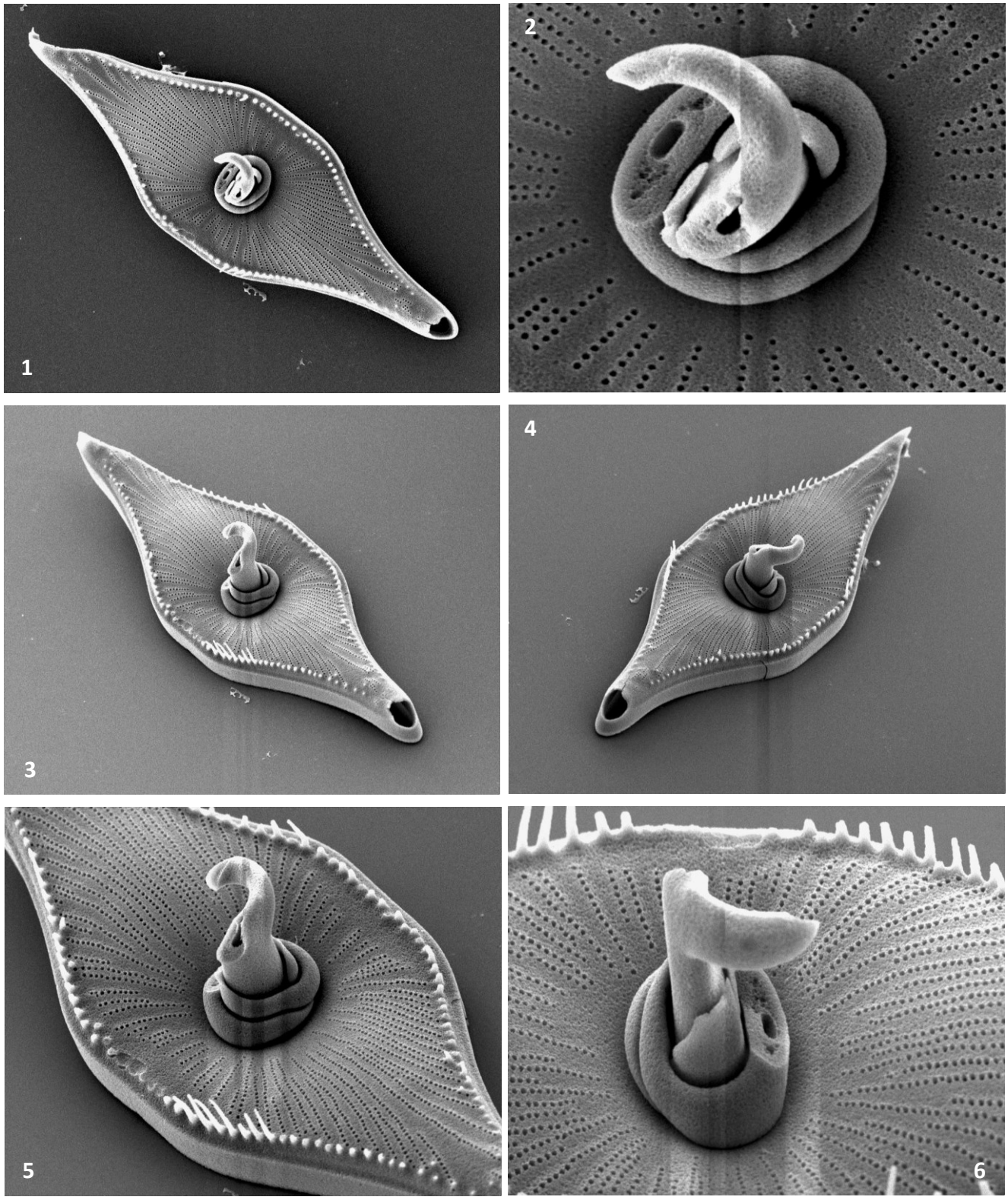

Plate 9

Rutilaria radiata

Fig 1 Detail of marginal spines. oamaru2atilt5000.

Fig 2 External valve view of a short form. Length 73 µm. Both ocelli, eroded, are visible at the poles. In the center, a fragment of the sibling valve shows the internal opening of the periplekton. oamaru2d1500.

Fig 3 Detail of eroded ocellus of image oamaru2d1500. oamaru2d5000.

Fig 4 External valve view of a short form, tilted. Length 73 µm. Both ocelli, eroded, are visible at the poles. In the center, a fragment of the sibling valve shows the internal opening of the periplekton. oamaru2dtilt_1500.

Fig 5 External valve view of a short form, tilted. Length 73 µm. Both ocelli, eroded, are visible at the poles. In the center, a fragment of the sibling valve shows the internal opening of the periplekton. oamaru2dtilt_1800.

Oamaru Diatoms

Plate 9

Rutilaria radiata

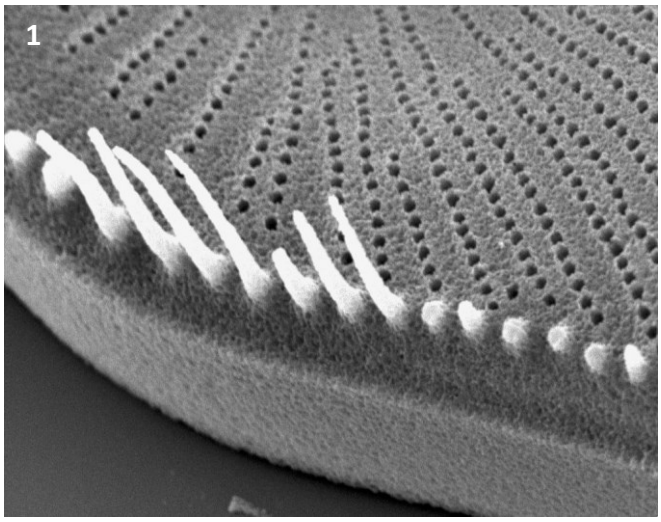

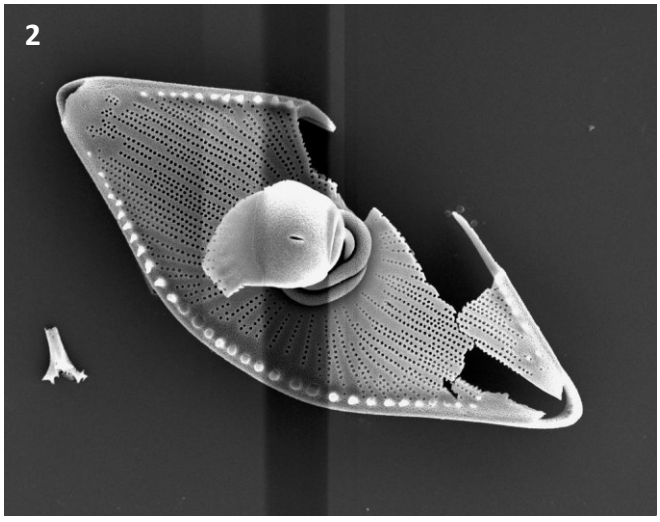

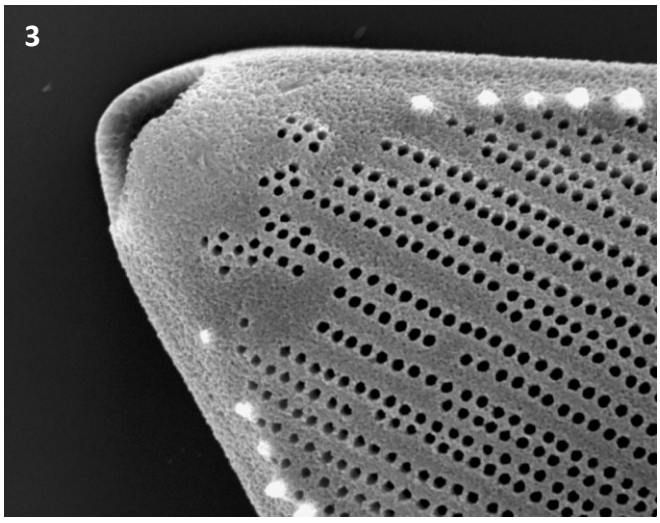

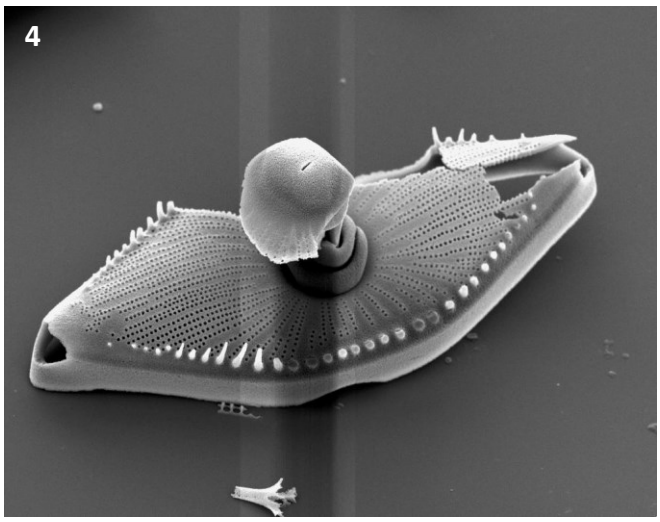

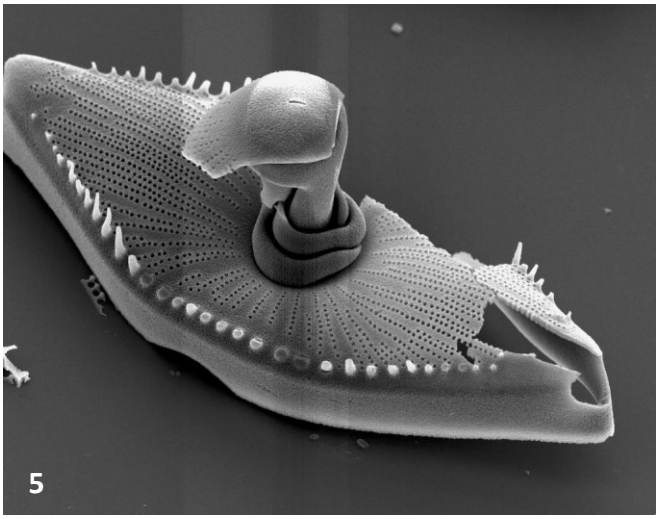

Plate 10

Sheshukovia castellifera

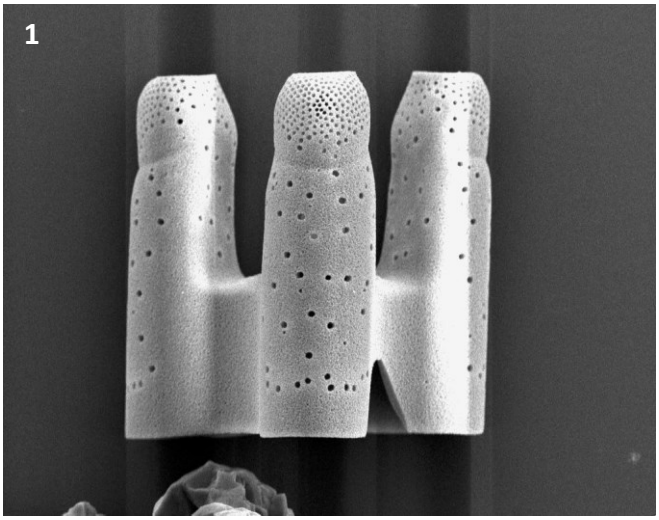

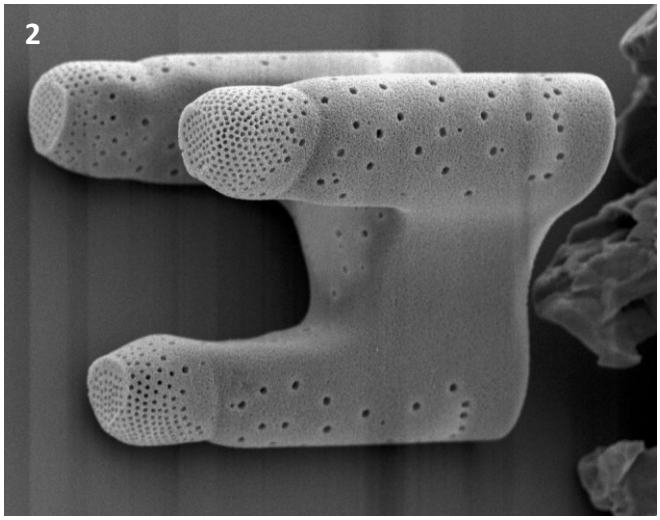

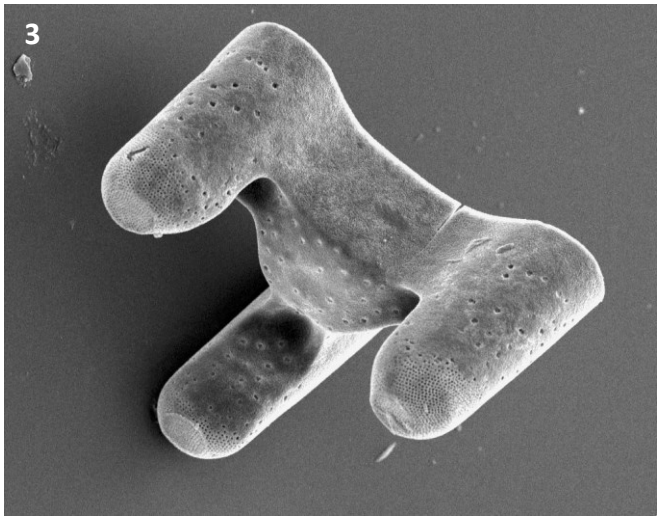

Refer to Witkowski (2023a); for current name see DiatomBase (https://www.diatombase.org/aphia.php?p=taxdetails&id=1595362); for older Triceratium castelliferum see Charles (2017); Heck (2015); D&S (1989), p.250, pl 115 fig 9,10; pl 117 fig 1-4,6,7.

Fig 1 Single valve. Girdle view. oamaru_3k1500.

Fig 2 Single valve. Girdle view. oamaru_3ktilt1800.

Fig 3 Single valve. Tilted view. oamaru_3ptilt1100.

Plate 11

Triceratium castellatum var. *fractum*

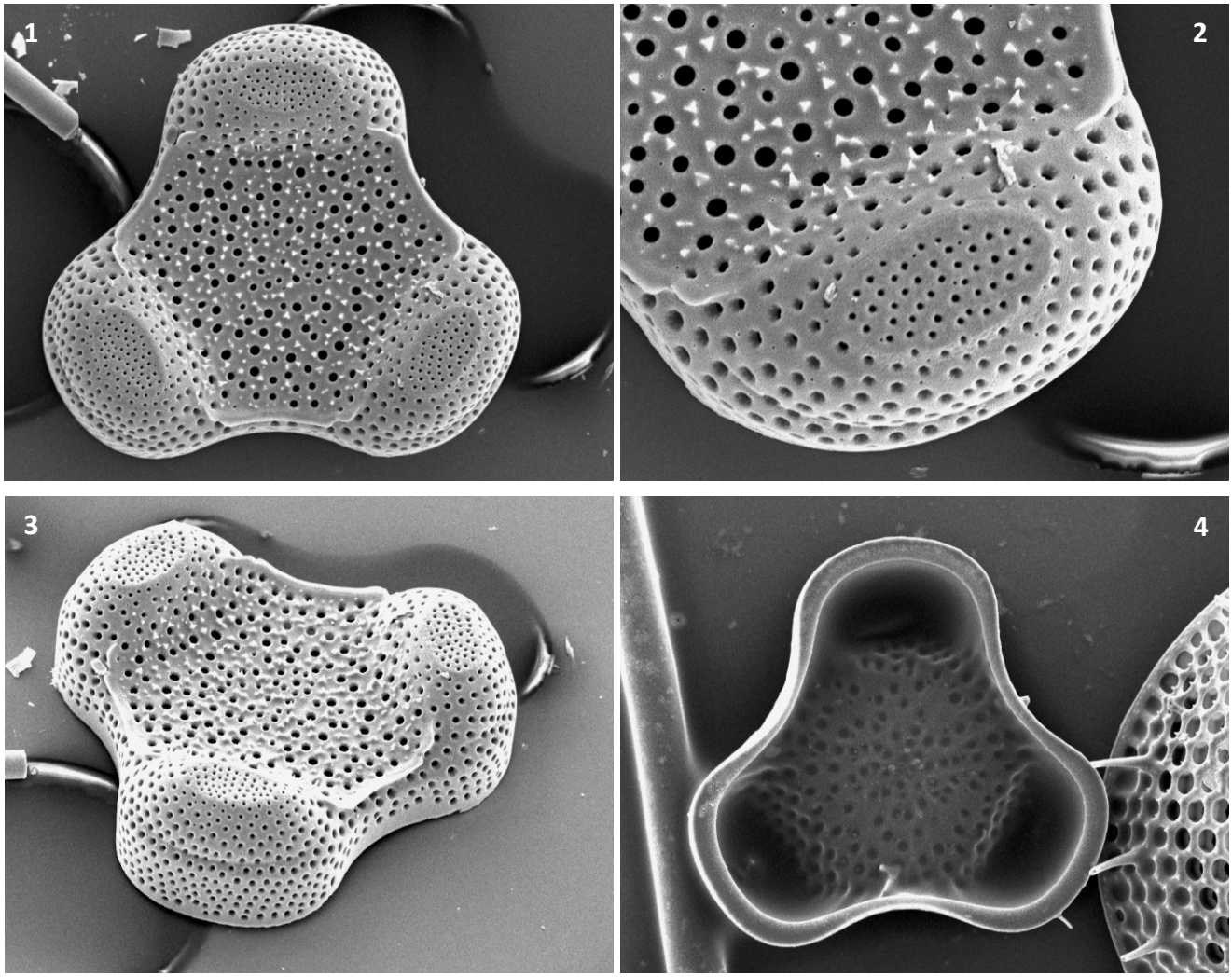

Refer to Charles (2017); D&S (1989) pg 250 and pl 118 fig 1-5, pl 122 fig 1,2,5, recorded from Bain's Farm.

Fig 1 External view of valve with raised porefields on the poles. oamaru_3s700.

Fig 2 Detail of a raised porefield at a pole. oamaru_3s1500.

Fig 3 External view of valve tilted with raised porefields on the poles. oamaru_3stilt700.

Fig 4 Internal view of valve. oamaru3_h800.

Plate 12

Triceratium favus var. *quadrata*

Refer to DiatomBase for name (https://www.diatombase.org/aphia.php?p=taxdetails&id=149326); Heck (2015) bild 512 for illustration; Round et al. (1990) for genus; Charles (2017) which uses *Triceratium favus* var. *favus* f. *quadrata*.

Fig 1 Internal view of valve. Clustered pores radiate from the center. oamaru2x900.

Fig 2 External view of valve tilted. oamaru2xtilt500.

Fig 3 Internal view of valve tilted. oamaru2xtilt800.

Fig 4 Detail of internal view of apex. oamaru2xtilt2500.

Fig 5 Internal view of an ocellus at an apex. oamaru2xxtilt2500.

Fig 6 External view of valve. oamaru3a600.

Plate 13

Triceratium favus var. *quadrata*

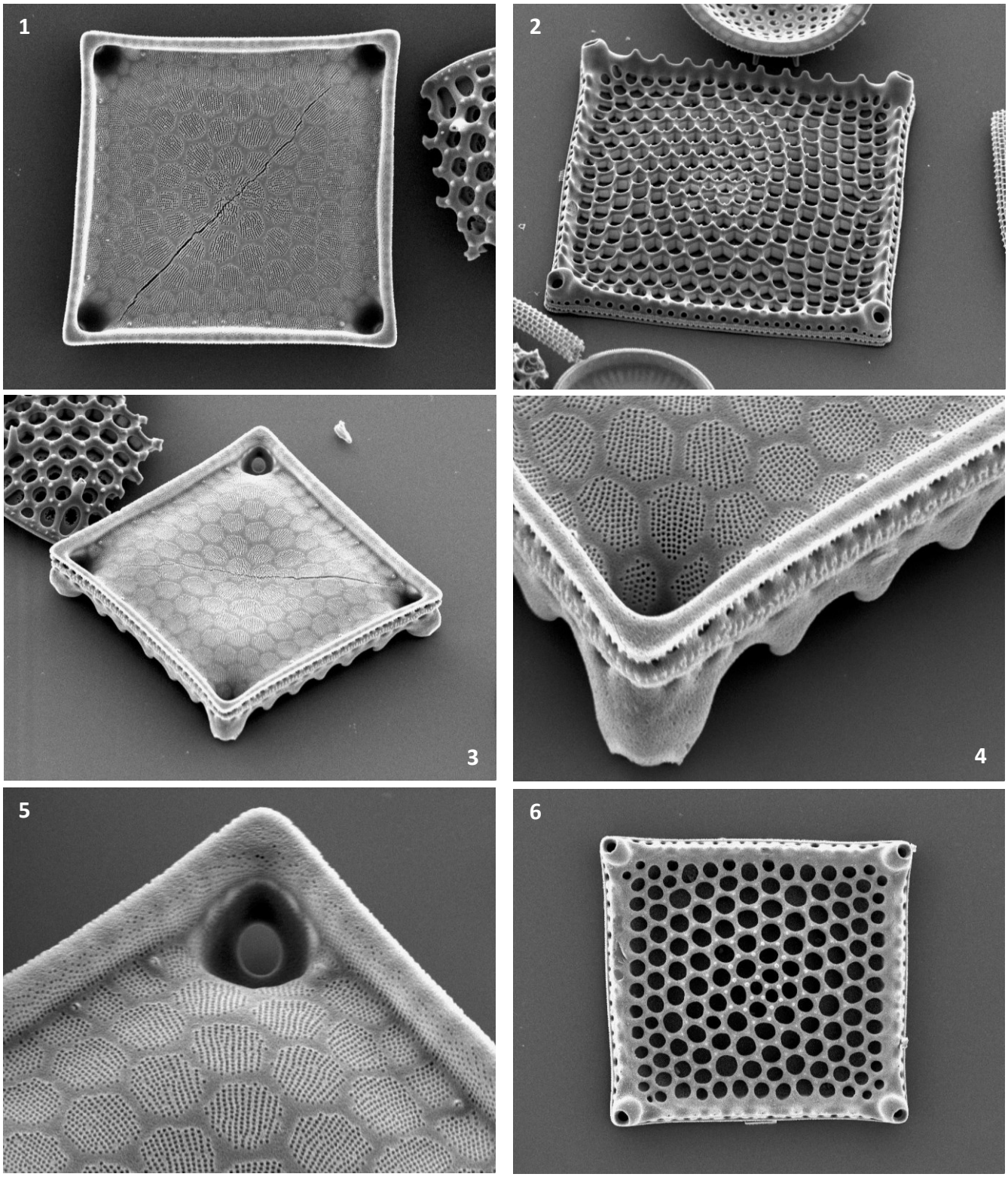

Triceratium favus var. *quadrata*

Fig 1 External view of valve tilted. oamaru3atilt600.

Fig 2 Detail of external view of ocellus. oamaru3atilt2500.

Triceratium pantocsekii

Refer to D&S (1989) pg 262 and pl 136 fig 3; Charles (2017); Heck (2015) bild 530.

Fig 3. External view. Straight sides separate this from *T. secedens*. oamaru3stilt700.

Triceratium pulvinar

Refer to D&S (1989) pg 264 and pl 127 fig 8, pl 128 fig 6-7, pl 129 fig 8 for description and illustrations; Heck (2015) bild 535; Charles (2017); Round et al. (1990) for genus.

Fig 4 Internal view of valve. Rows of pores clustered and radiating from center of valve. Distance between adjacent apices at top of image 100 μm. Compare to *T. unguiculatum*. oamaru2s800.

Fig 5 Detail of internal view of an apex. Rows of pores clustered and radiating from center of valve. Compare to *T. unguiculatum*. oamaru2s3000.

Triceratium secedens

Refer to Charles (2017); Heck (2015) bild 536; D&S (1989) pg 266 and pl 135 fig1,2,4.

Fig 6 External view. Convex sides separate this from *T. pantocsekii*. oamaru_3htilt350.

Plate 14

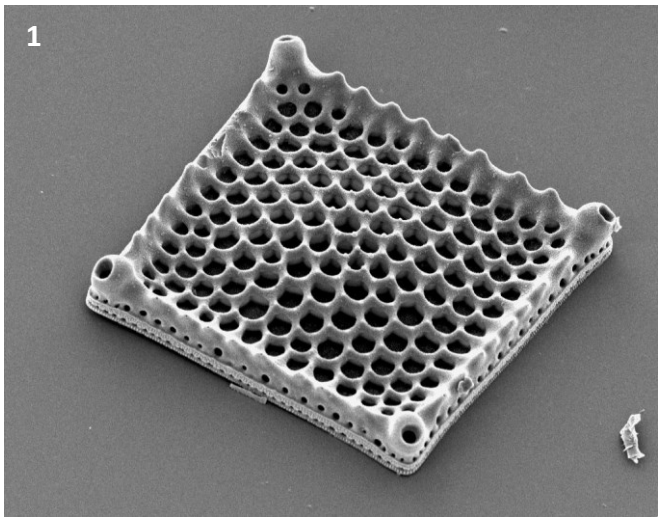

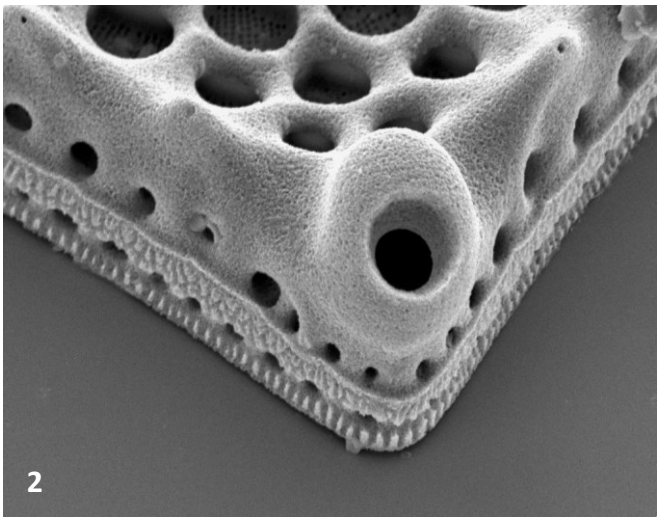

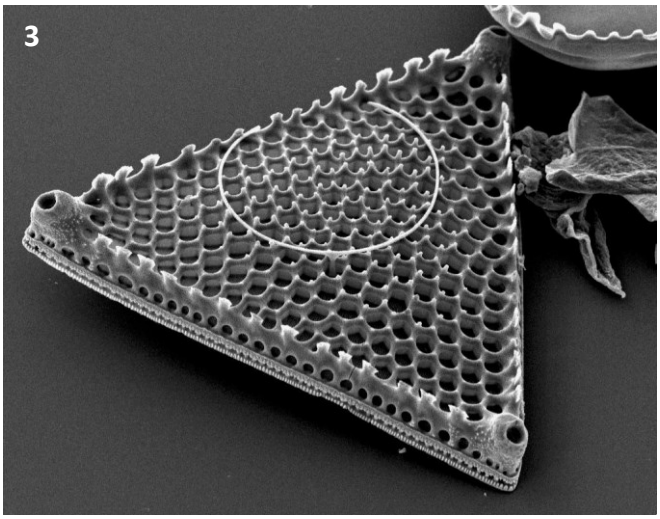

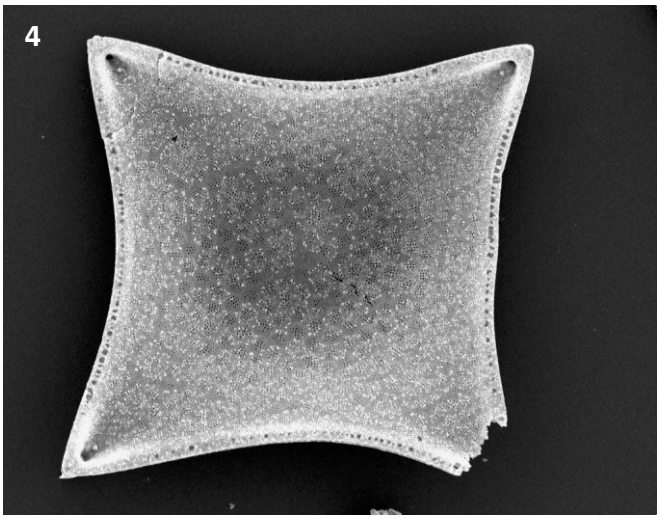

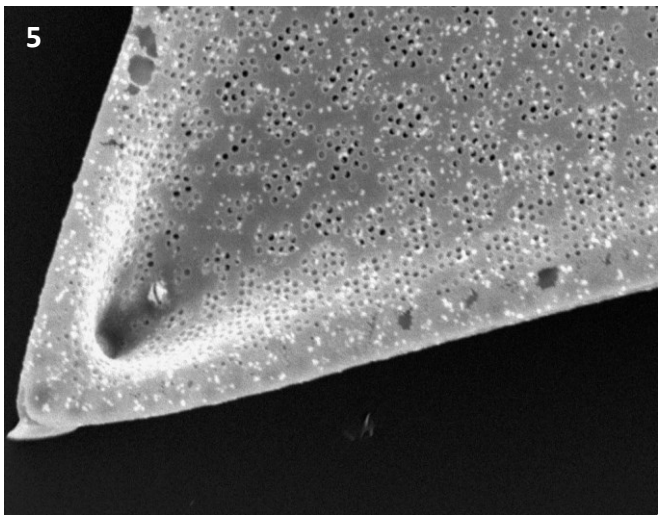

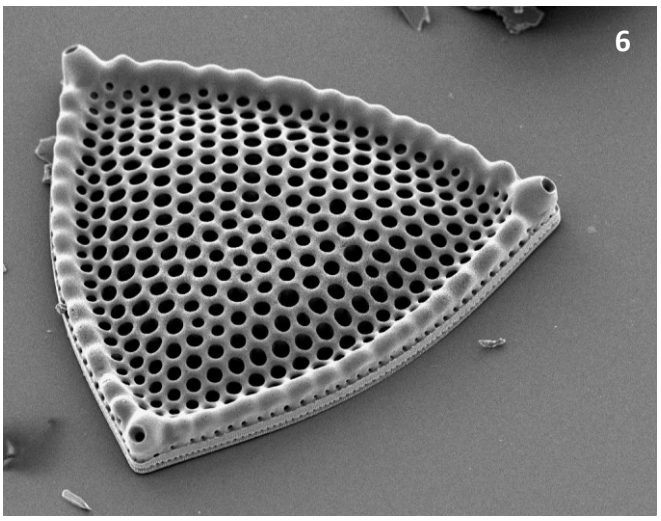

Plate 15

Trigonium glandiferum

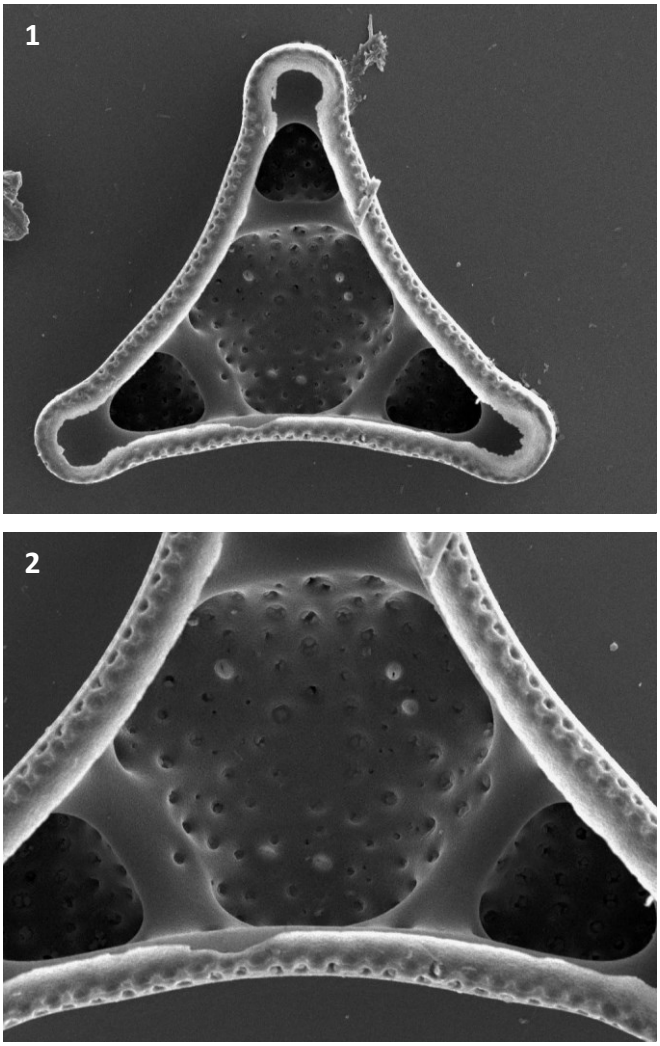

Refer to Schmidt (1874-1959) pl 127 fig 9-10; Charles (2017) for the genus; D&S (1989) pl 123 fig 2-5.

Fig 1 Internal view. Heavy internal costae, a septum in each corner, and internal openings of the scattered rimoportulae on the central area of the valve face. oamaru3_k700.

Fig 2 Internal view. Detail of image oamaru3_k700. Heavy internal costae and internal openings of the scattered rimoportulae on the central area of the valve face. oamaru3_k1300.

Trinacria excavata

Refer to Round et al. (1990) for genus; Witkowski (2023a) for the name; D&S (1989) pl 137 fig 8 for LM image. (Trinacria ligulata was considered but images were not found in Williams (1988) nor in DiatomBase.)

Fig 1 Genus distinguished by valves with 3 or 4 poles elevated at the corners. Elevations have spines which interlock neatly with the corresponding poles on sibling cells. oamaru2ktilt1100.

Fig 2 Detail of image oamaru2ktilt1100. Corner eroded. Linking spines visible. oamaru2ktilt4500.

Fig 3 Detail of image oamaru2ktilt1100. Linking spines clearly visible. oamaru2ktilt5000.

Trinacria ventricosa

Refer to Charles (2017); D&S (1989) pg 284 and pl 137 fig 9, pl 138 fig 1-5,7. Recorded from Bain's Farm.

Fig 4 Internal valve view. oamaru3_j900.

Fig 5 Internal view of a pole. oamaru3_j3500.

Williamriedelia tenuicornis

Refer to Witkowski (2023b) for LM image (https://fossil-diatoms.com/atlas/index.php?page=entry&id=65&genus=Williamriedelia&requestedBy=taxa-list); Round et al. (1990) Hemiaulus, the former genus; Charles (2017); Kociolek et al. (2023) for name changes.

Fig 6 Girdle view of complete valve. Similar to *Hemiaulus.* May also be placed in genus *Riedelia*. oamaru2otilt1500.

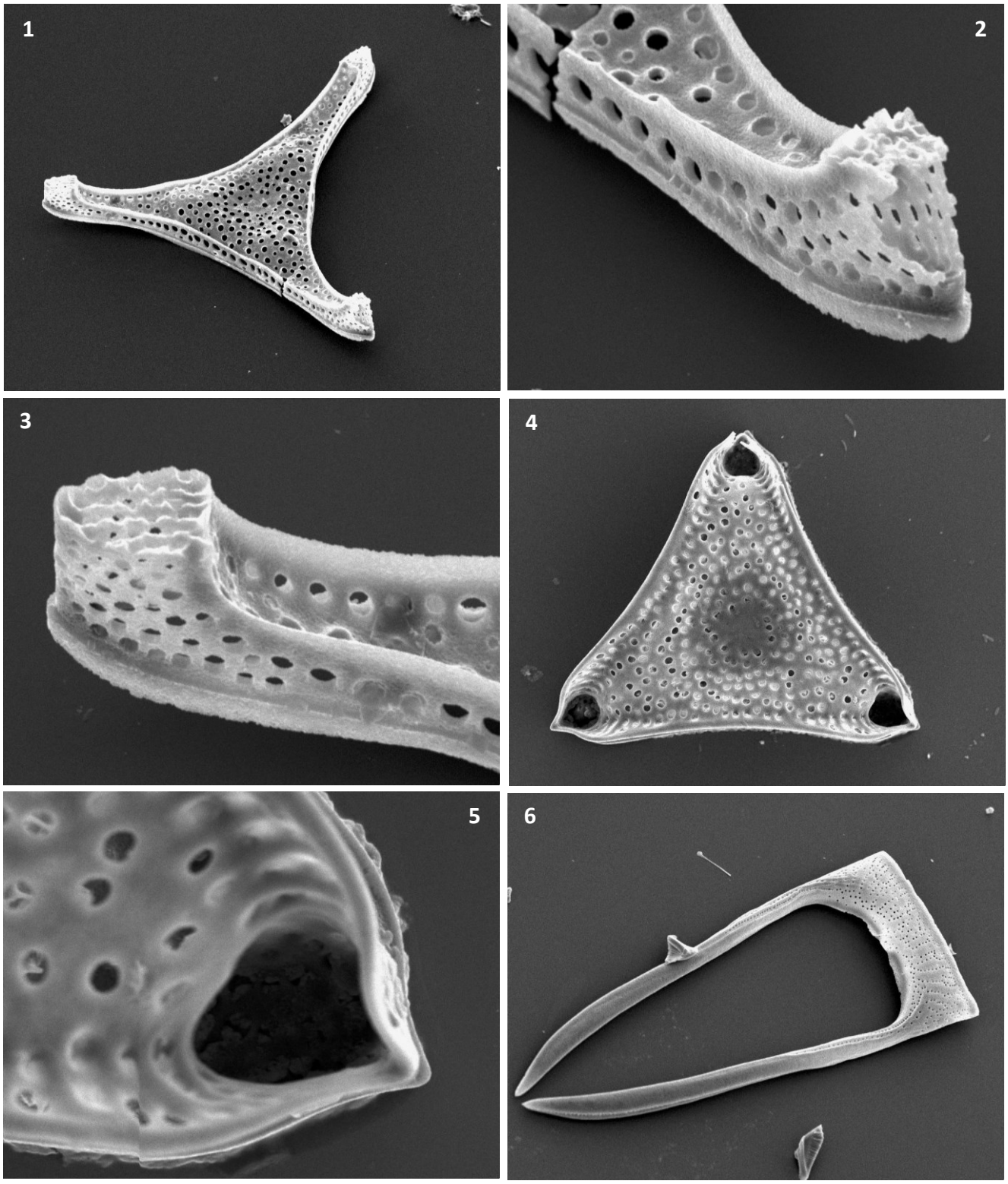
1
2
3
4
5
6

Plate 17

Centric Radial

Arachnoidiscus oamaruensis

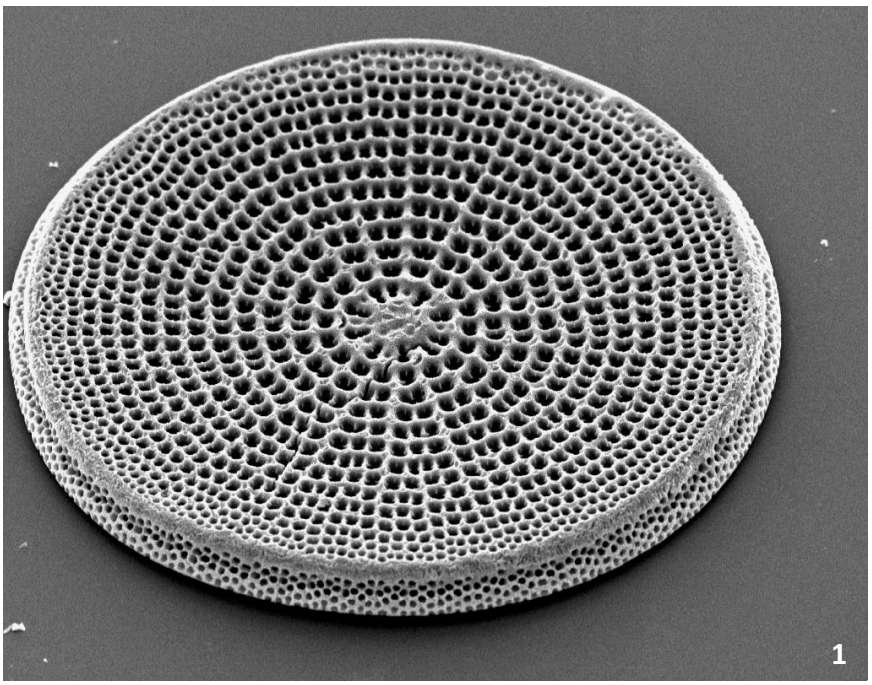

Refer to Charles (2017); Heck (2015) bild 73; Brown (1933) pl 1 fig 1,6.

Fig 1 External view of tilted valve. Diameter 95 µm. Species epithet *oamaruensis* was chosen by (1) key in Brown 1933, lead 17: primary rays slender, penetrating to the fourth, third, or second circle of areolae; and (2) the central area in this SEM which could be interpreted as hyaline, matching image in Charles 2017 and Brown 1933. oamaru2htilt_1100.

Plate 18

Asterolampra insignis

Refer to Round et al. (1990) for genus; Tiffany and Hernández-Becerril (2005) pl 11 fig 1-4; D&S (1989) pg 54 pl 17 fig 1,3,6,7, recorded from Bain's Farm.

Fig 1 External view of valve. Diameter 93 µm. Raised rays lie between blocks of areoale. Species distinguished by trapezoidal blocks of areolae at the margin between the rays. oamaru_3g1000.

Fig 2 External view of central area. oamaru_3g2000.

Fig 3 External view of valve margin. oamaru_3g3500.

Fig 4 External valve view tilted. Illustrates ray holes with tiny rimoportula at the base of each ray hole. oamaru_3gtilt1100.

Fig 5 Detail of external view of valve margin. Illustrates eroded ray holes with tiny rimoportula at the base of each ray hole. oamaru_3gtilt3500.

Fig 6 Internal view of valve. Open chambers of the raised rays appear as black bars. Species distinguished by trapezoidal blocks of areolae at the margin between the rays. oamar3a800.

Plate 18

Asterolampra insignis

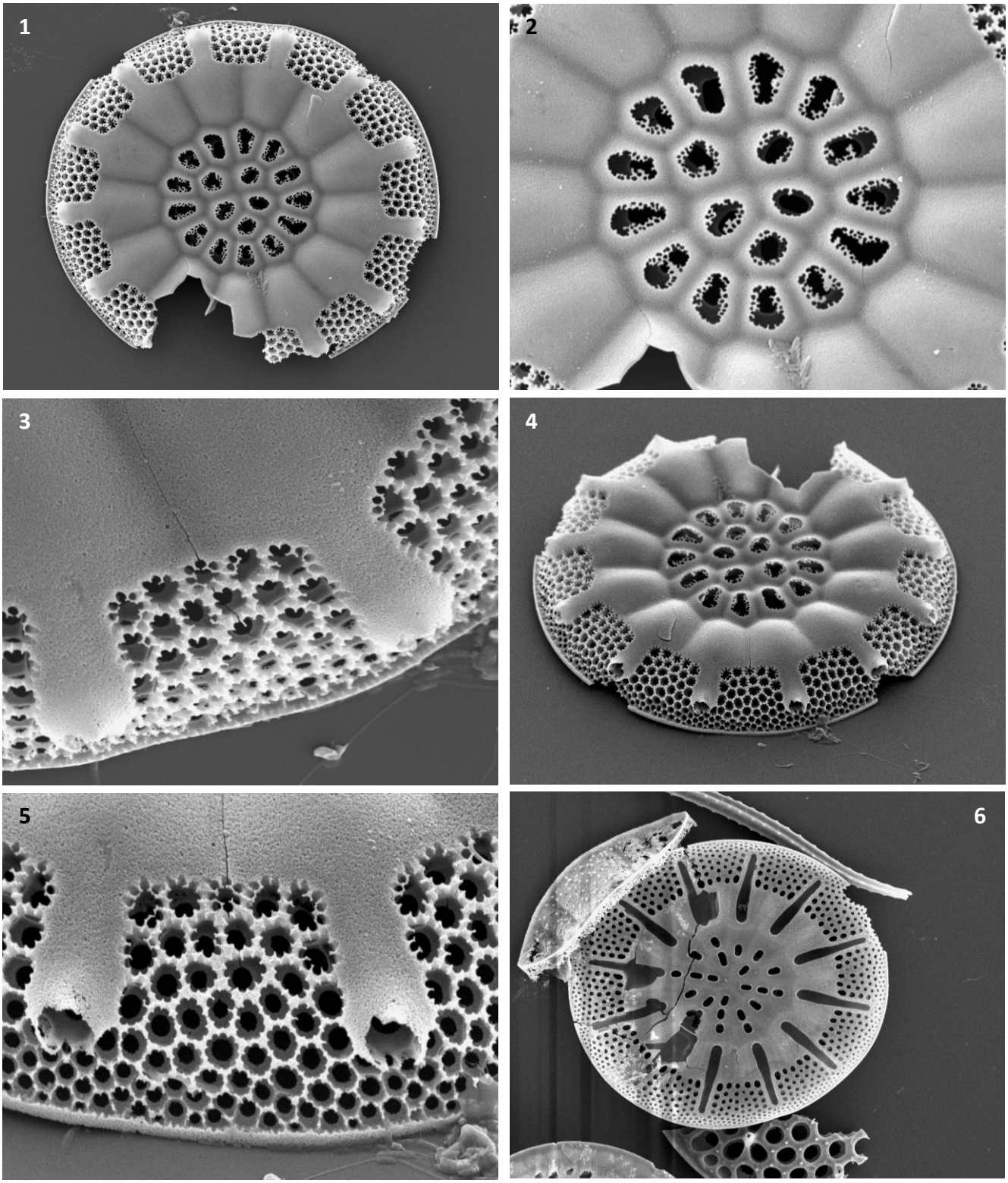

Plate 19

Asterolampra insignis

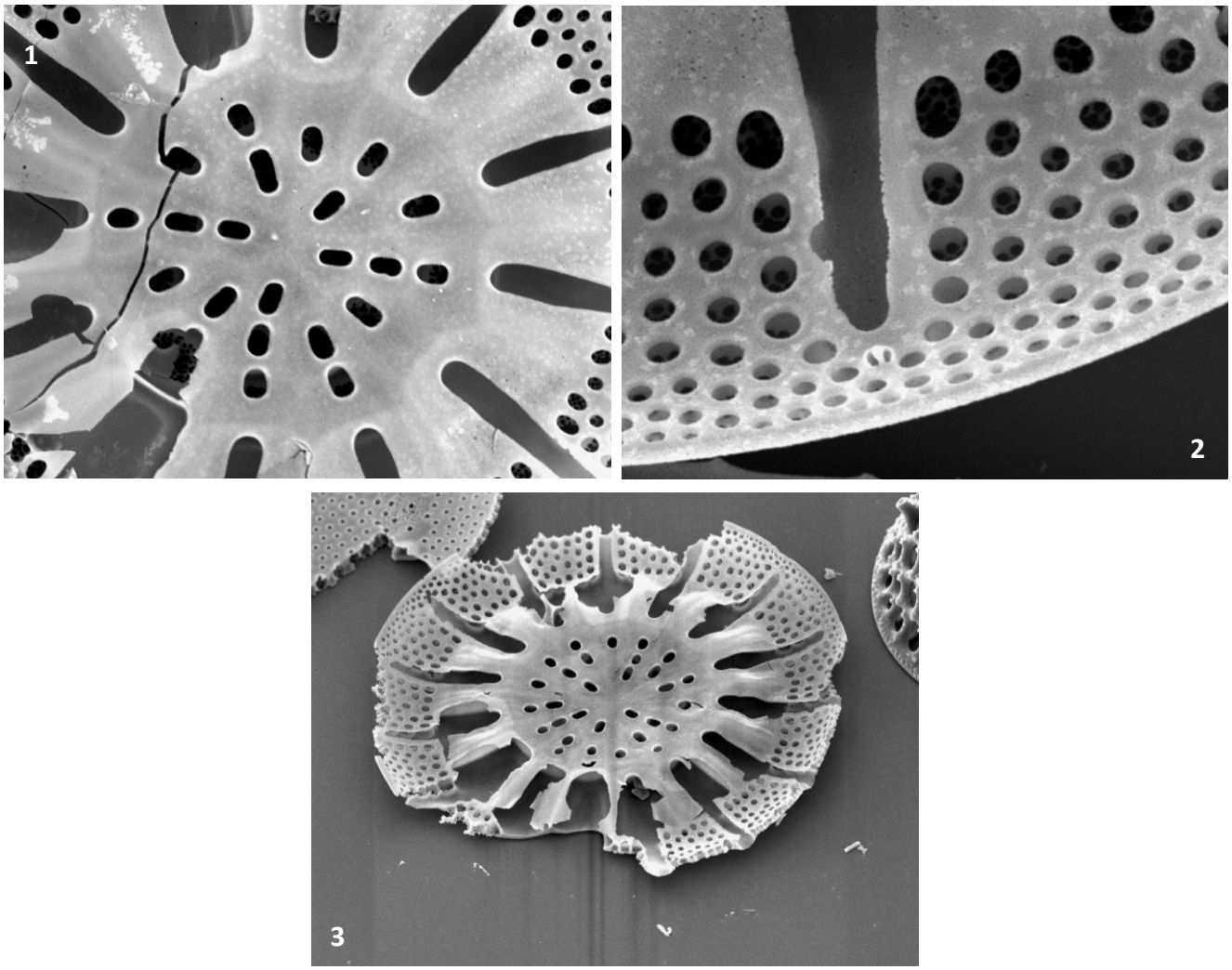

Fig 1 Internal view of central area. Detail of image oamar3a800. oamar3a2000.

Fig 2 Internal view of valve edge showing internal opening of a rimoportula at end of open chamber. Detail of image oamar3a800. oamar3a4500.

Fig 3 Internal valve view. oamaru2ftilt_1000.

Plate 20

Asterolampra insignis

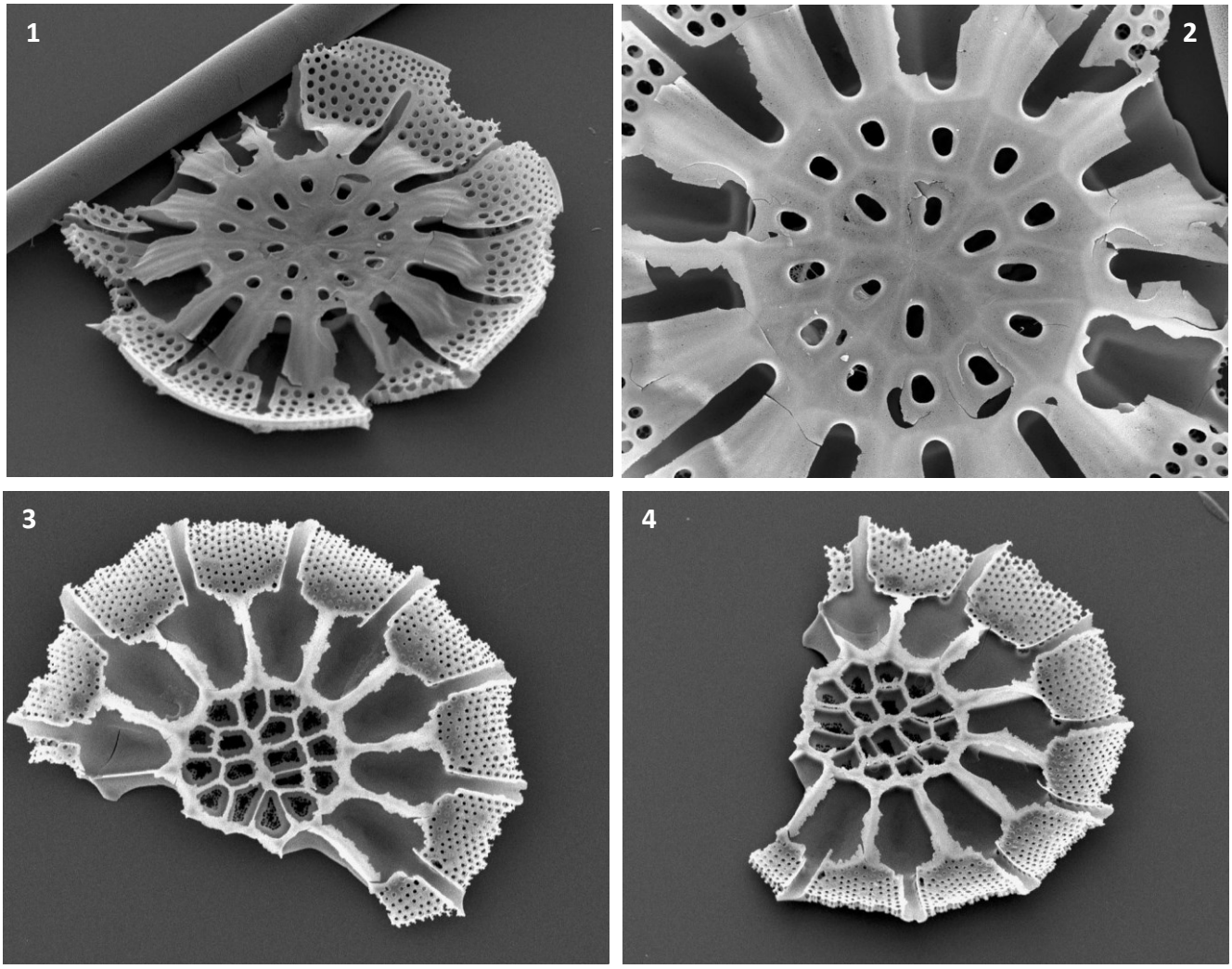

Fig 1 Detail of internal view of central area. oamaru3_b1800.

Fig 2 Internal valve view. oamaru3_btilt1100.

Fig 3 Internal view of eroded valve. oamaru3b1100.

Fig 4 Internal view of eroded valve tilted. Shows thickness of valve wall. oamaru3btilt1100.

Plate 21

Asterolampra vulgaris

Refer to Tiffany and Hernández-Becerril (2005) pg 17 pl 12 fig 5-6; D&S (1989) pg 56 pl 19 fig 1-4, recorded from Bain's Farm.

Fig 1 External valve view. Species distinguished by the pair of rows of densely packed pores on each side of the raised ray. oamaru_3a1300.

Fig 2 Detail of external valve view. Pair of densely packed rows of pores on each side of raised ray. Rimportula visible at base of eroded ray hole. oamaru_3a5000.

Fig 3 External valve view tilted. oamaru_3atilt1500.

Fig 4 External valve view detail. Two eroded ray holes each with rimoportula at its bottom lip. oamaru_3atilt3000.

Fig 5 External valve view. oamaru2ltilt1500.

Fig 6 Detail of valve edge. Visible are rows of dense pores, ray holes, and rimoportulae at base of ray holes. oamaru3_d24500.

Plate 21

Asterolampra vulgaris

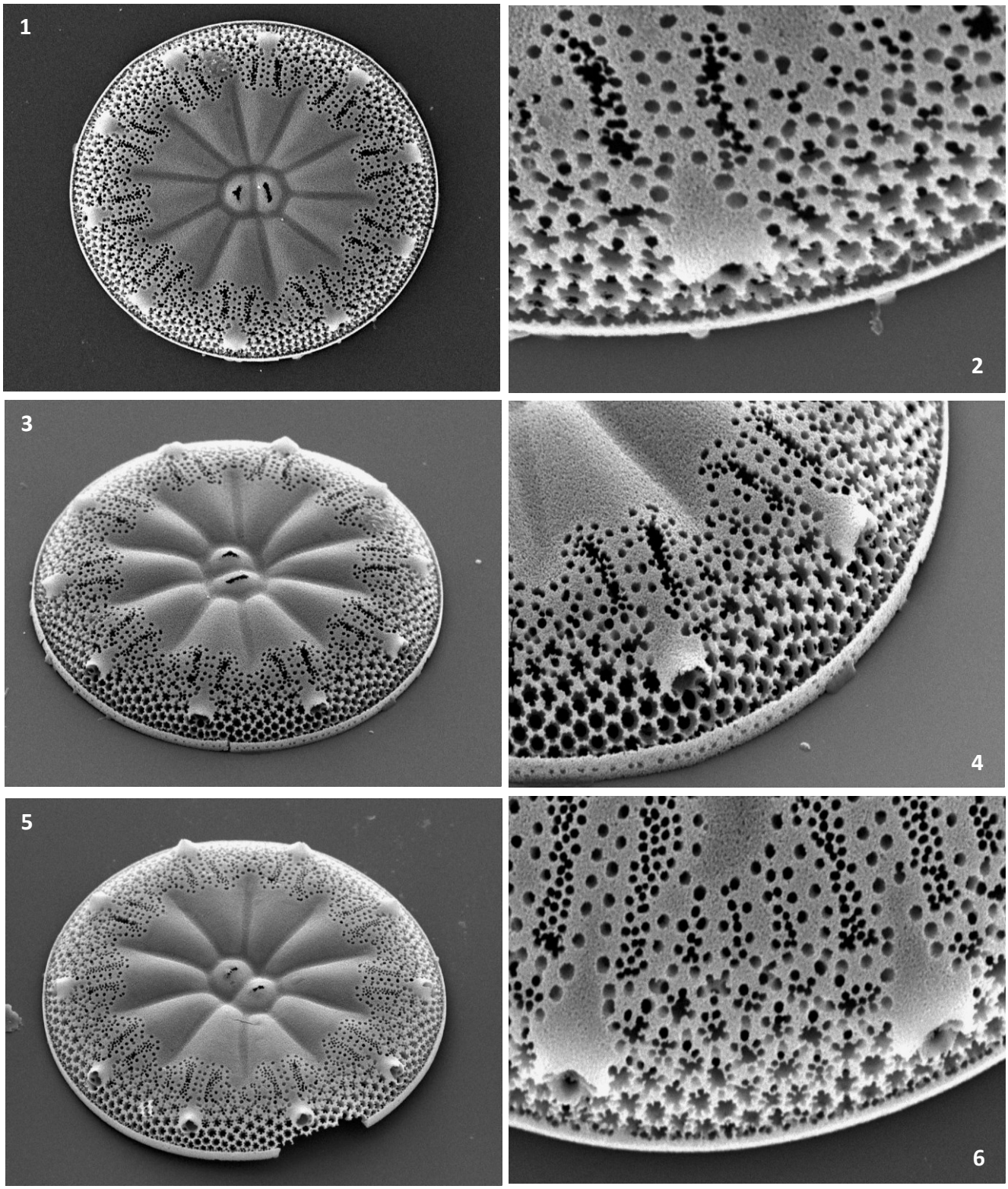

Asterolampra vulgaris

Fig 1 External valve view. Species distinguished by the pair of rows of densely packed pores on each side of the raised ray. oamaru3c1100.

Fig 2 Detail of external view of central area. oamaru3c3500.

Fig 3 Detail of external margin. oamaru3c4500.

Fig 4 External valve view. Species distinguished by the pair of rows of densely packed pores on each side of the raised ray. oamaru3ctilt1500.

Fig 5 Detail of external margin. oamaru3ctilt6000.

Fig 6 External valve view tilted. oamaru3dtilt4000.

Plate 22

Asterolampra vulgaris

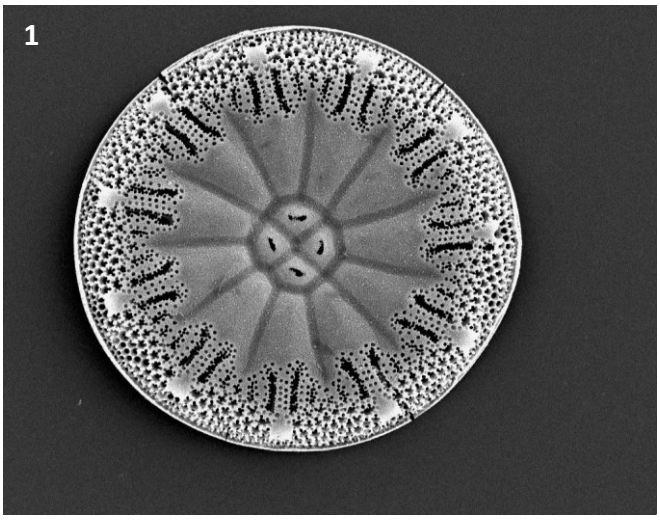

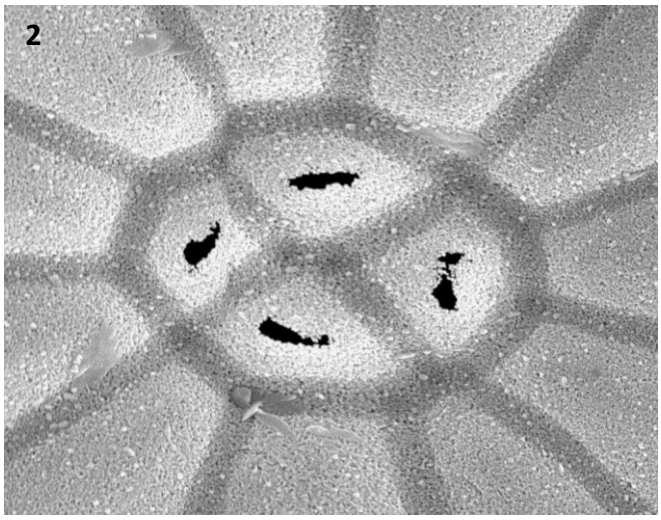

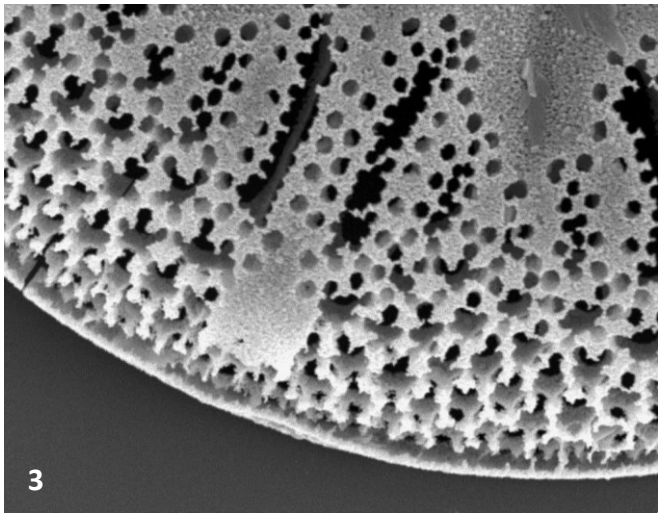

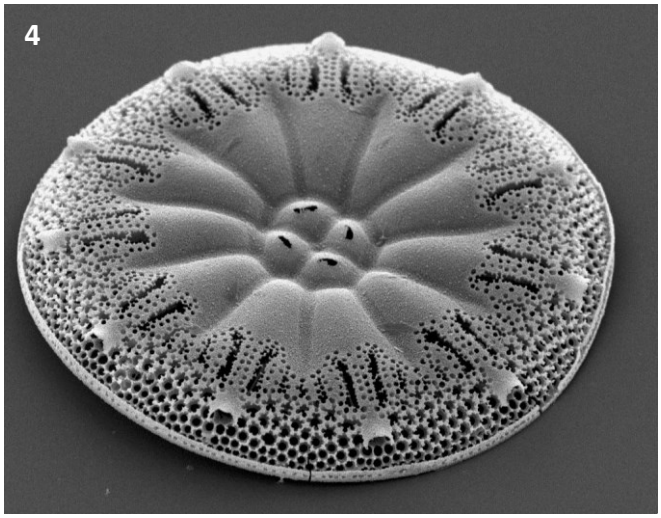

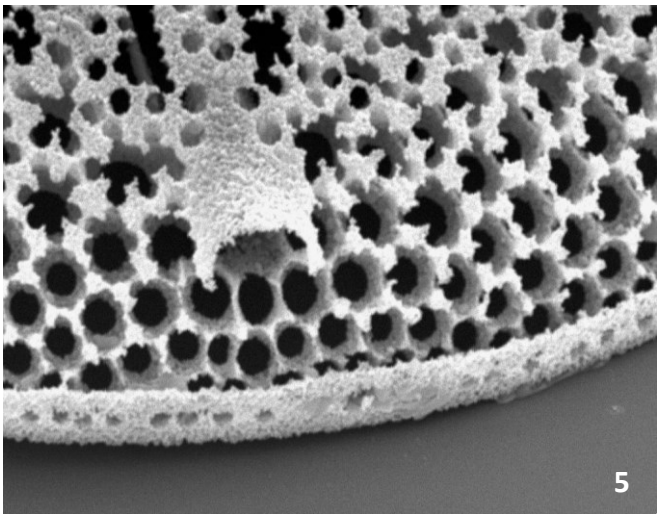

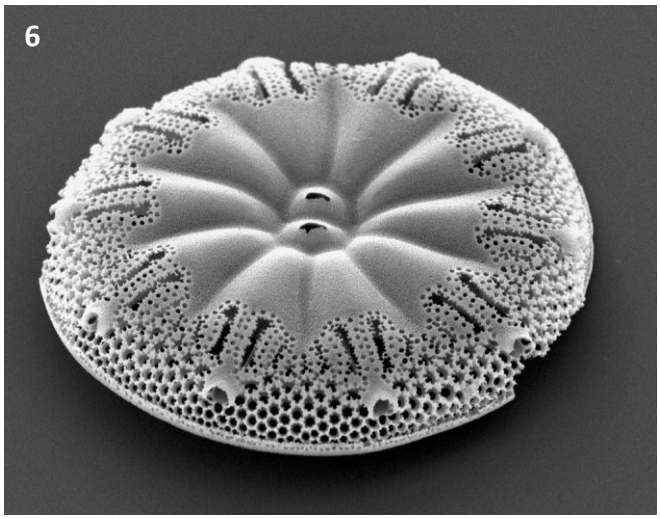

Asterolampra vulgaris

Fig 1 Internal view of eroded valve. Species distinguished by the pair of rows of closely packed pores on each side of the ray chamber. oamar3b1100.

Fig 2 Internal view of valve. Visible are long ray chambers and short chambers on either side. oamaru3_c1300.

Fig 3 Detail of internal view of valve. The short parallel chambers show pores in the external side. At end of each ray chamber is the internal opening of a rimoportula. oamaru3_c2000.

Fig 4 Detail of internal view of central area. oamaru3_c3500.

Fig 5 Internal view of valve tilted. Visible are ray chambers with ray holes at the distal ends and a cross section of the valve edge. oamaru3_ctilt1300.

Fig 6 Internal view of the valve. oamaru3_d800.

Plate 23

Asterolampra vulgaris

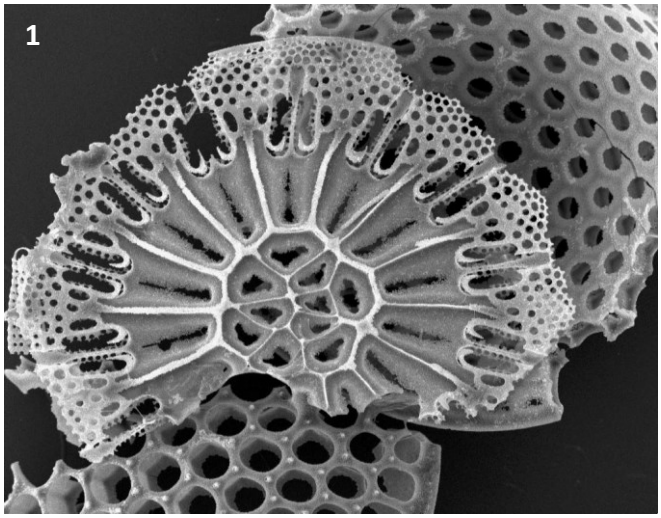

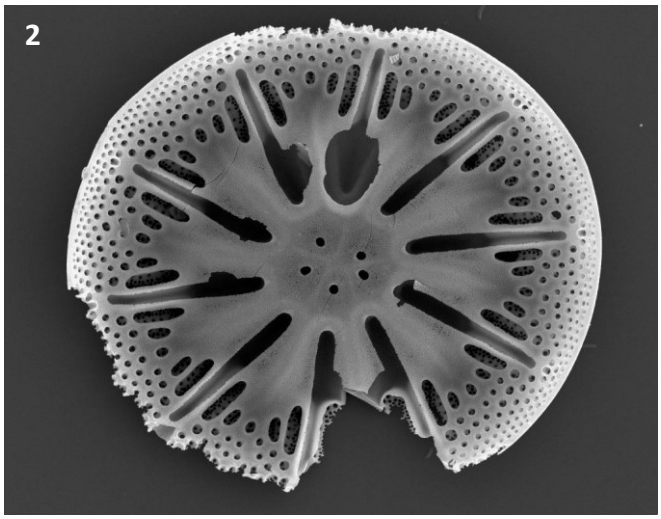

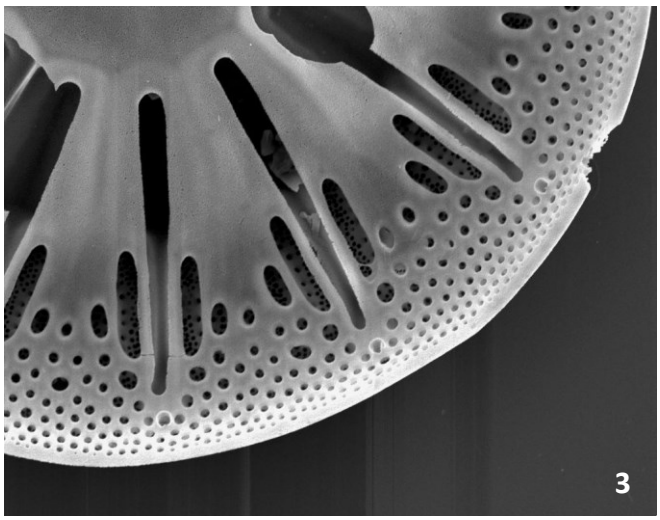

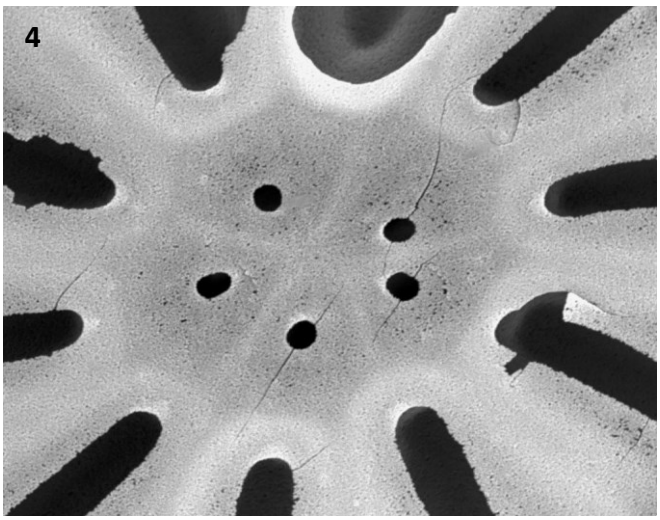

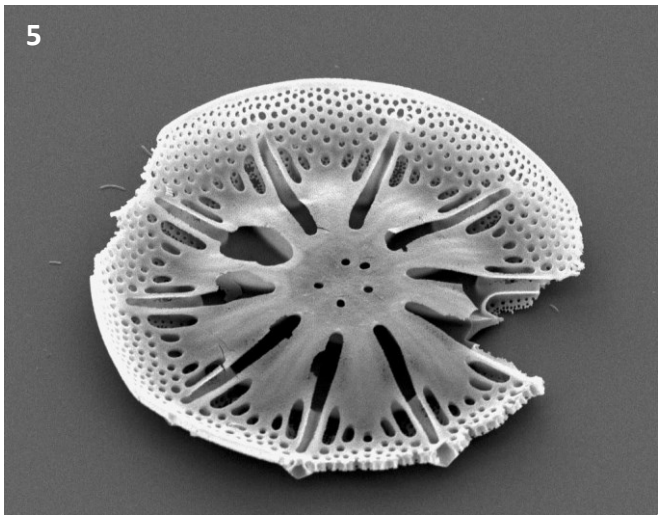

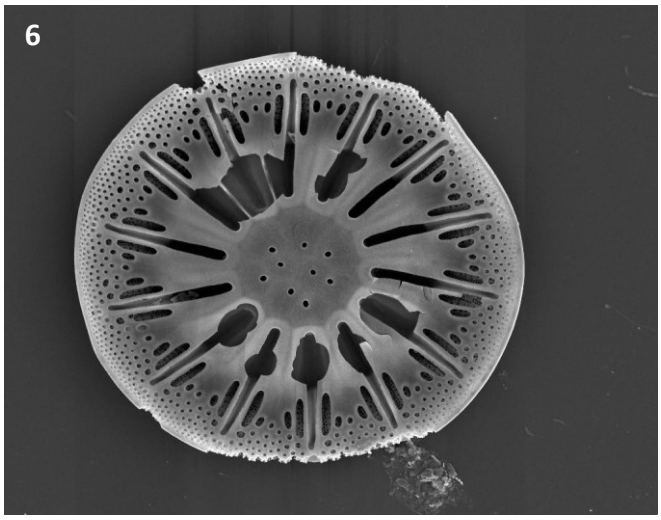

Asterolampra vulgaris

Fig 1 Internal view of valve. oamaru3e1100.

Fig 2 Detail of internal view of ray chambers and parallel side chambers with external pores visible. oamaru3e3000.

Fig 3 Detail of internal view of ray chambers and parallel side chambers with external pores visible. oamaru3e6000.

Fig 4 Detail of internal view of central area. oamaru3ee3000.

Fig 5 Internal view of valve tilted. Cross section of valve wall visible. oamaru3etilt1500.

Plate 24

Asterolampra vulgaris

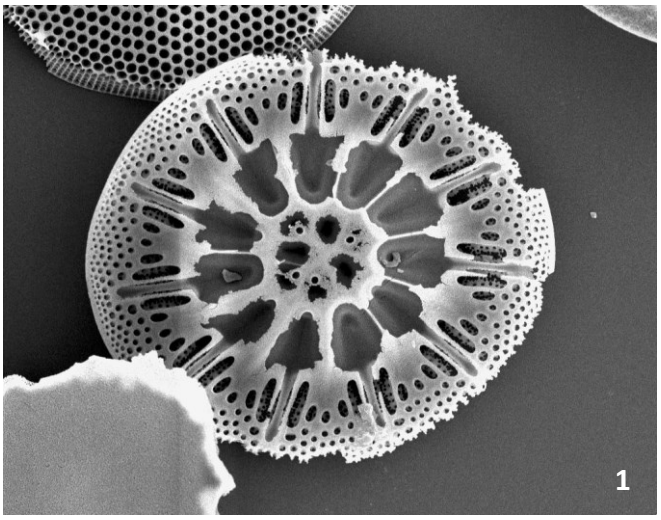

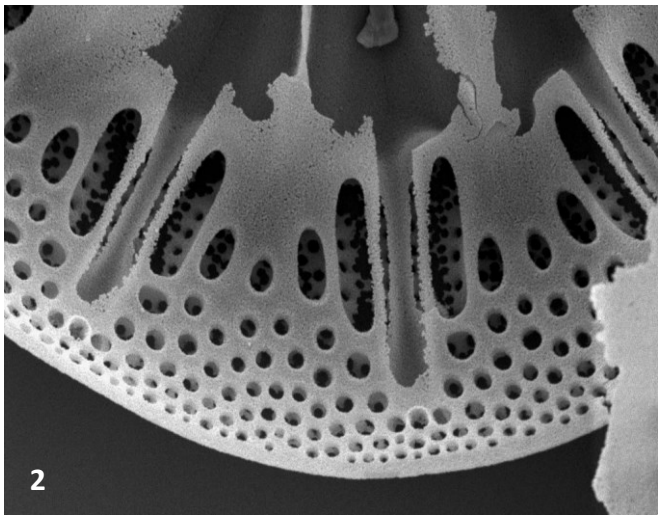

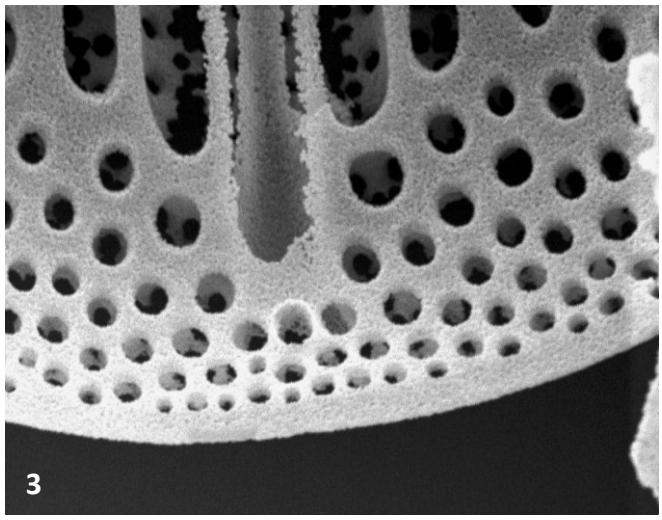

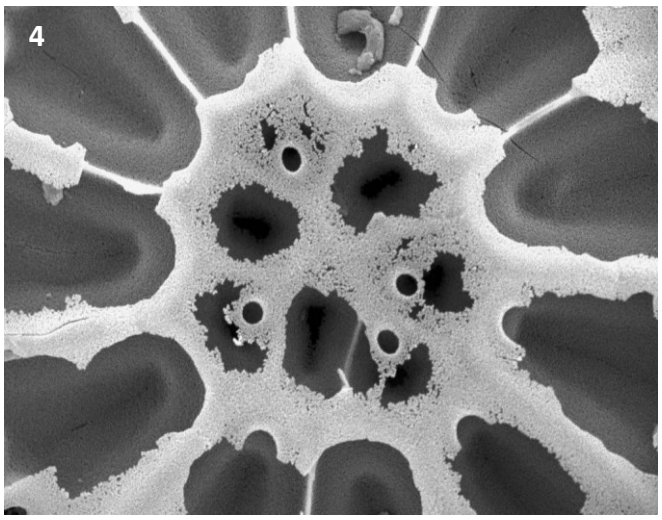

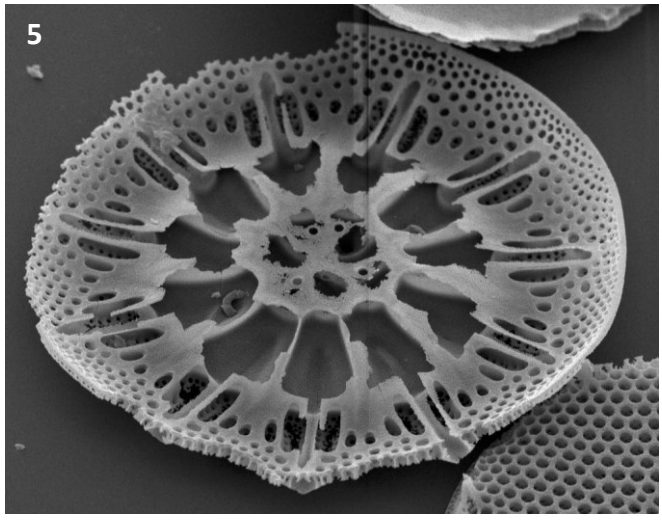

Plate 25

Aulacodiscus aemulans

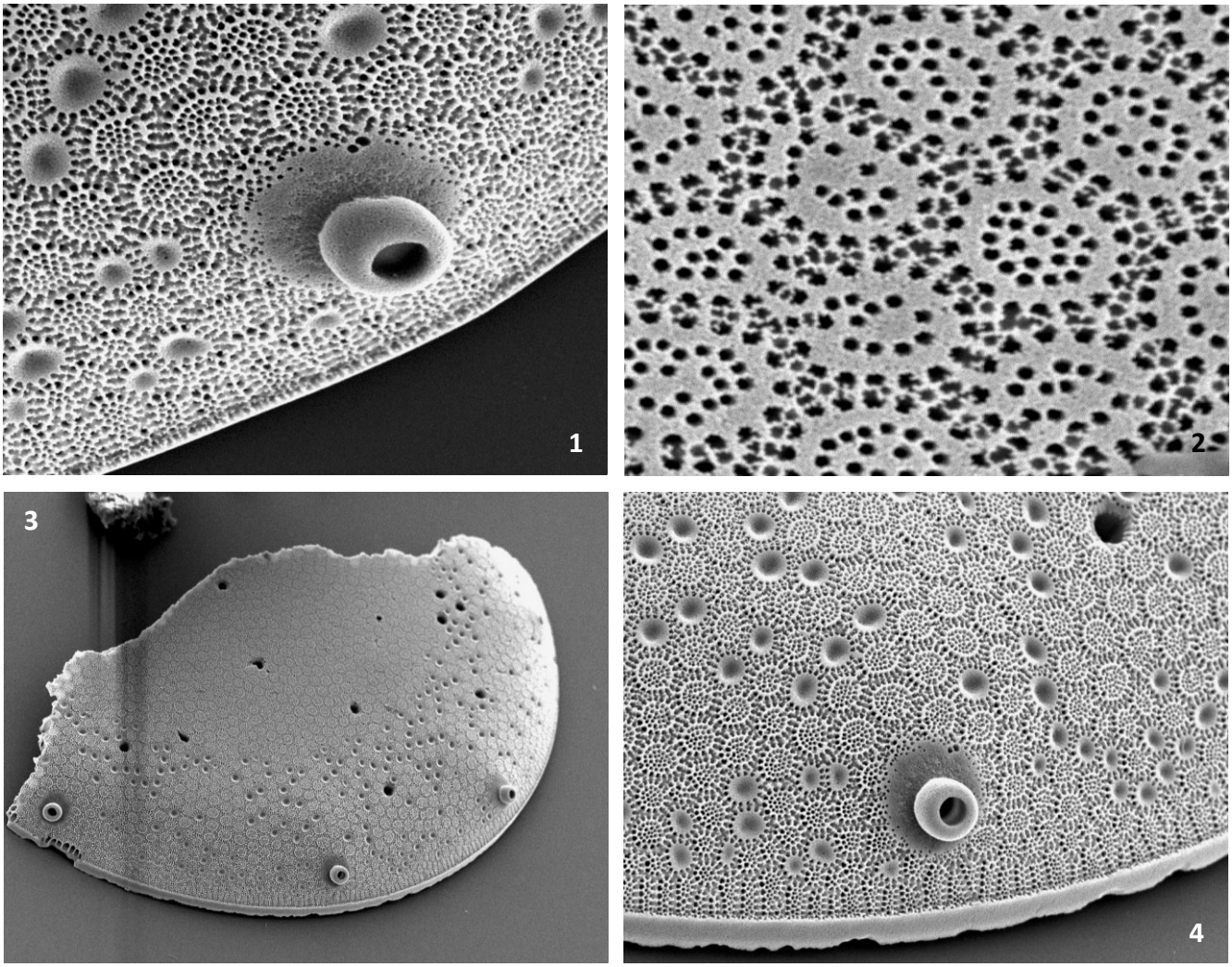

Refer to Strelnikova et al. (2004) figs 66-70.

Fig 1 Detail of external valve edge. Cribra with a daisy shape cover the areolae. One rimoportula stem visible. oamaru3_de3000.

Fig 2 Cribra with a daisy shape cover the areolae. oamaru3_e7000.

Fig 3 External view of valve. Cribra with a daisy shape cover the areolae. oamaru3_etilt600.

Fig 4 Cribra with a daisy shape cover the areolae. oamaru3_etilt2000.

Plate 26

Aulacodiscus aemulans

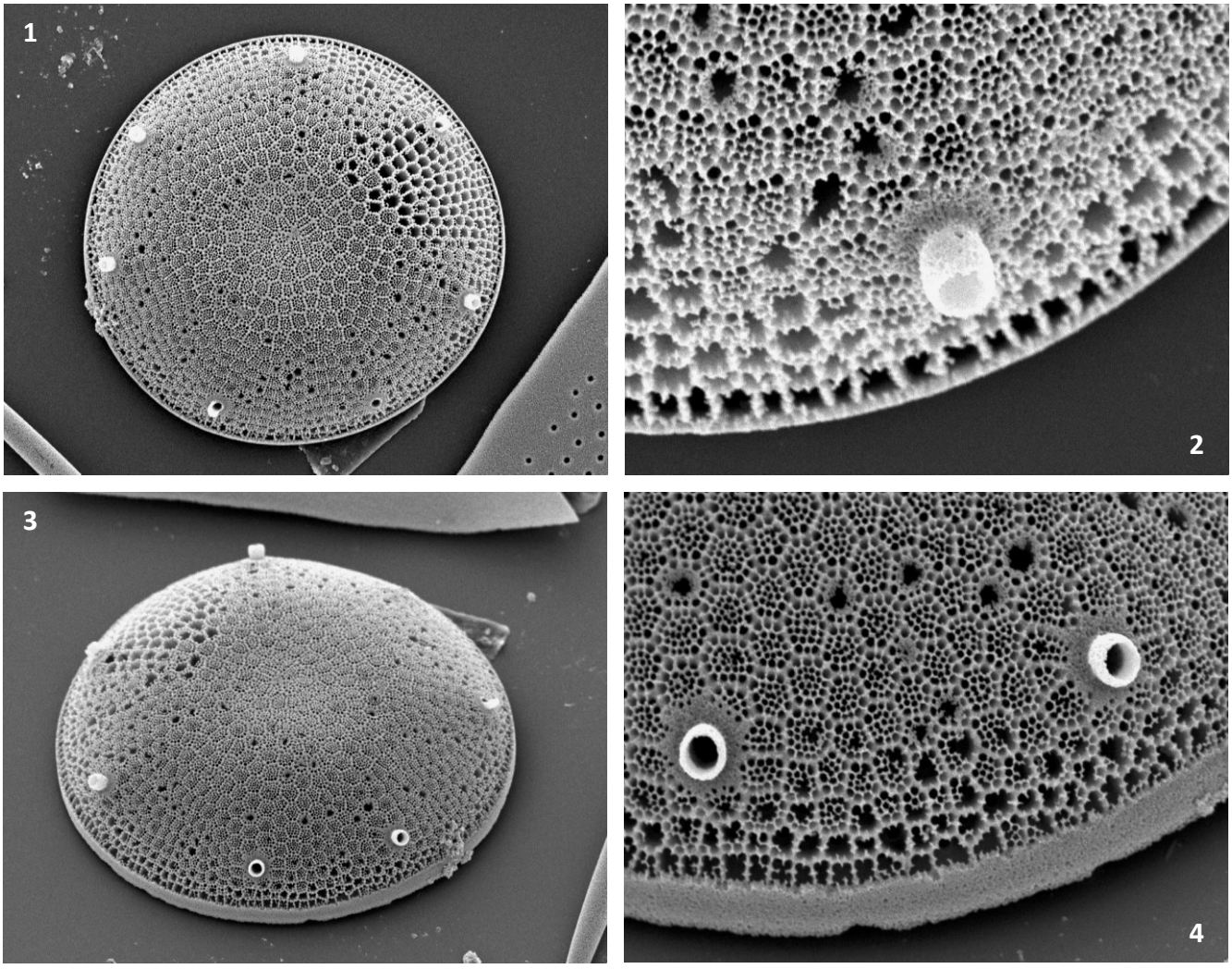

Fig 1 External view of valve. Cribra with a daisy shape cover the areolae. Some cribra have eroded showing the areolae. oamaru3i1000.

Fig 2 Detail of image oamaru3i1000. oamaru3i4500.

Fig 3 External view of valve tilted. Cribra with a daisy shape cover the areolae. Tubes of rimoportulae form a ring near the margin. oamaru3itilt1100.

Fig 4 Detail of image oamaru3itilt1100. Areola diameter ~ 2.5 µm. Diameter of pore in cribra ~ 0.4 µm. Rimoportula external opening ~ 1.9 µm. oamaru3itilt3000.

Plate 27

Aulacodiscus amoenus

Refer to Charles (2017); D&S (1989) pg 57 and pl 20 fig. 1-6, recorded from Bain's Farm.

Fig 1 External view. Valve convex in center, rising suddenly to a marginal ridge with rimoportulae protruding away from center on marginal side of the ridge. oamaru_3l450.

Fig 2 Detail of external margin with rimoportula. oamaru_3l1800.

Fig 3 External view tilted. Valve convex in center, rising suddenly to a marginal ridge with rimoportulae protruding away from center on marginal side of the ridge. oamaru_3ltilt500.

Fig 4 Detail of external margin with rimoportula. oamaru_3ltilt1800.

Fig 5 Detail of external margin with rimoportula. oamaru_3ltilt2000.

Plate 27

Aulacodiscus amoenus

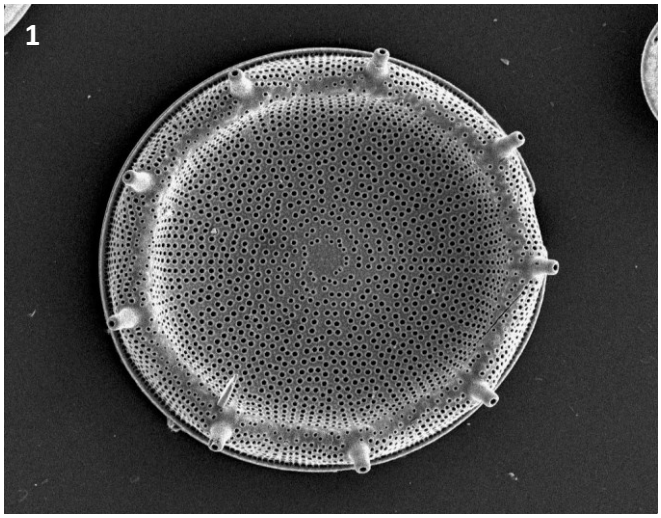

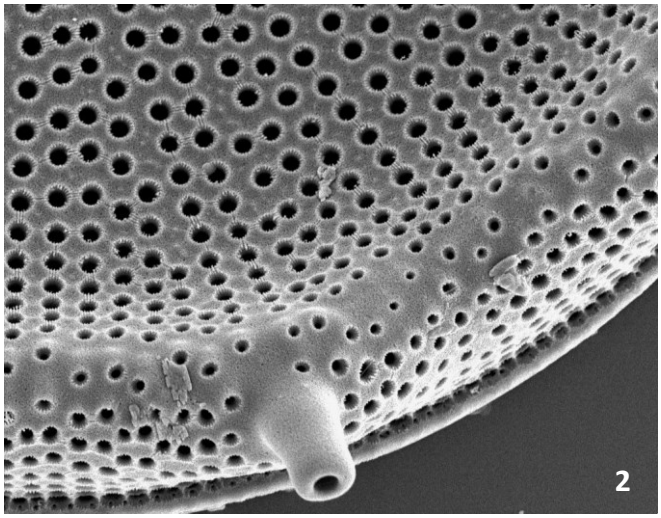

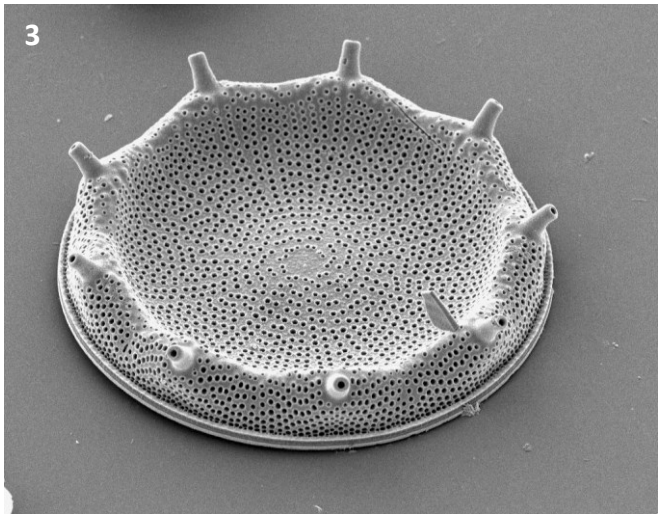

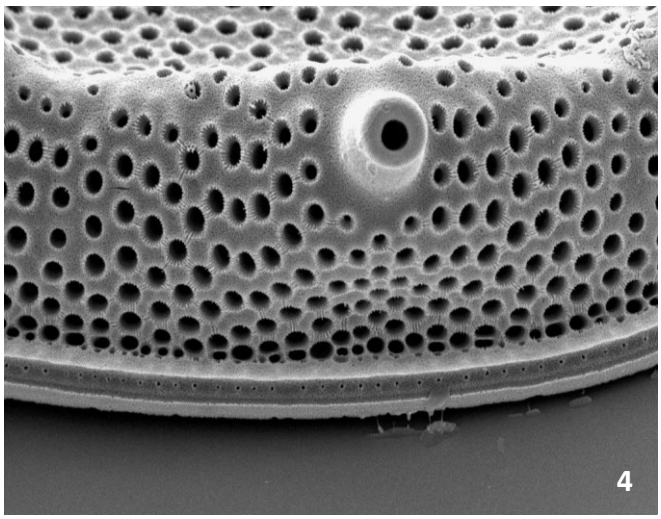

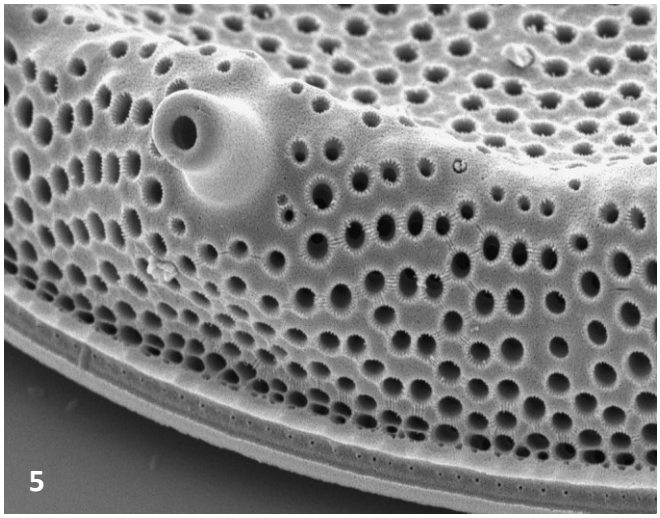

Plate 28

Aulacodiscus cellulosus

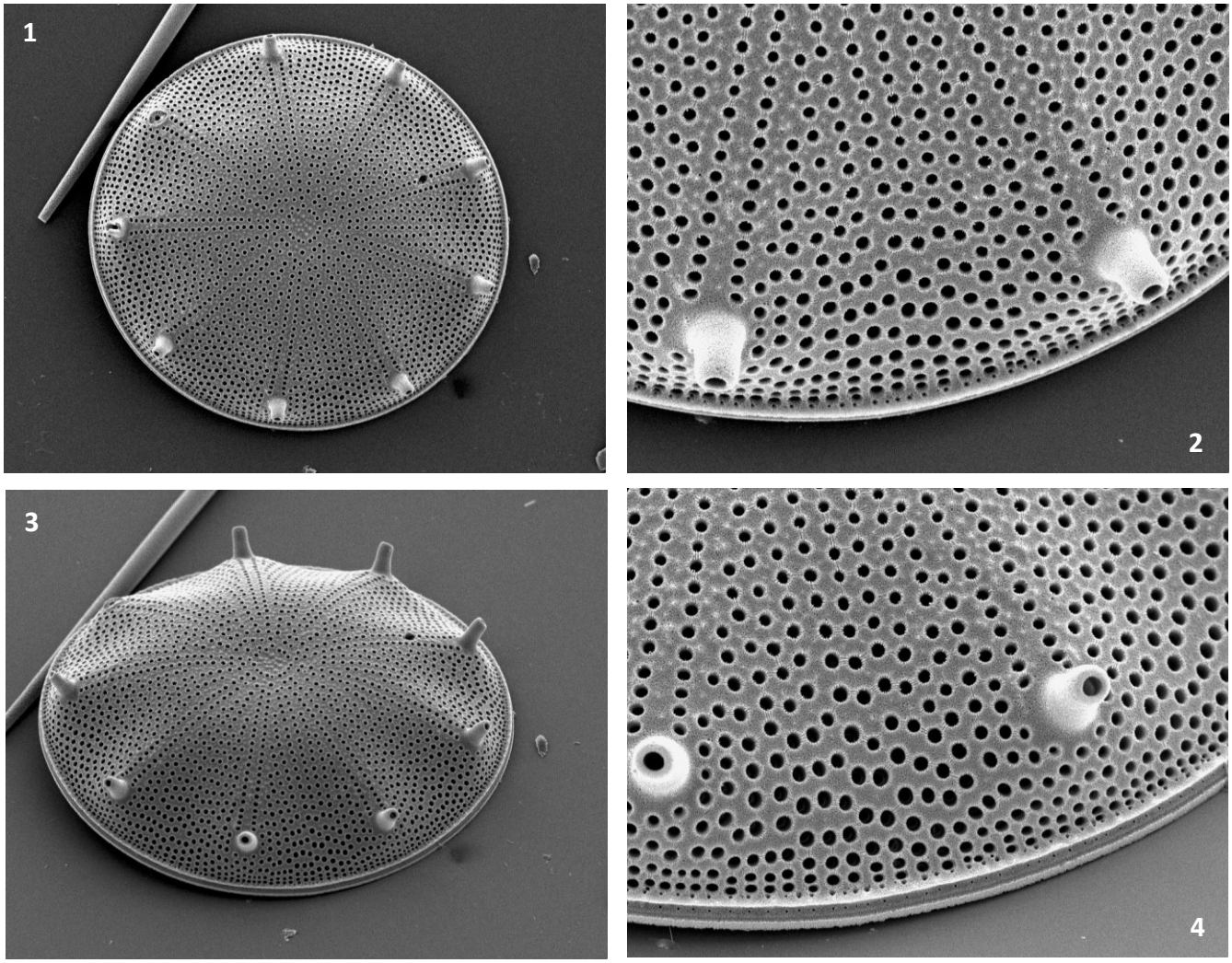

Refer to Tiffany (2023); D&S (1989) pg 62; Charles (2017); Heck (2015) bild 98,99,109.

Fig 1 External valve view. Distinctive central rosette and two parallel rows of areolae along the furrows leading to the rimoportulae. oamaru_3c450.

Fig 2 Detail of image oamaru_3c450. oamaru_3c1500.

Fig 3 External valve view. Distinctive central rosette and two parallel rows of areolae along the furrows leading to the rimoportulae. oamaru_3ctilt500.

Fig 4 External view of valve margin. oamaru_3ctilt1500.

Plate 29

Aulacodiscus cellulosus

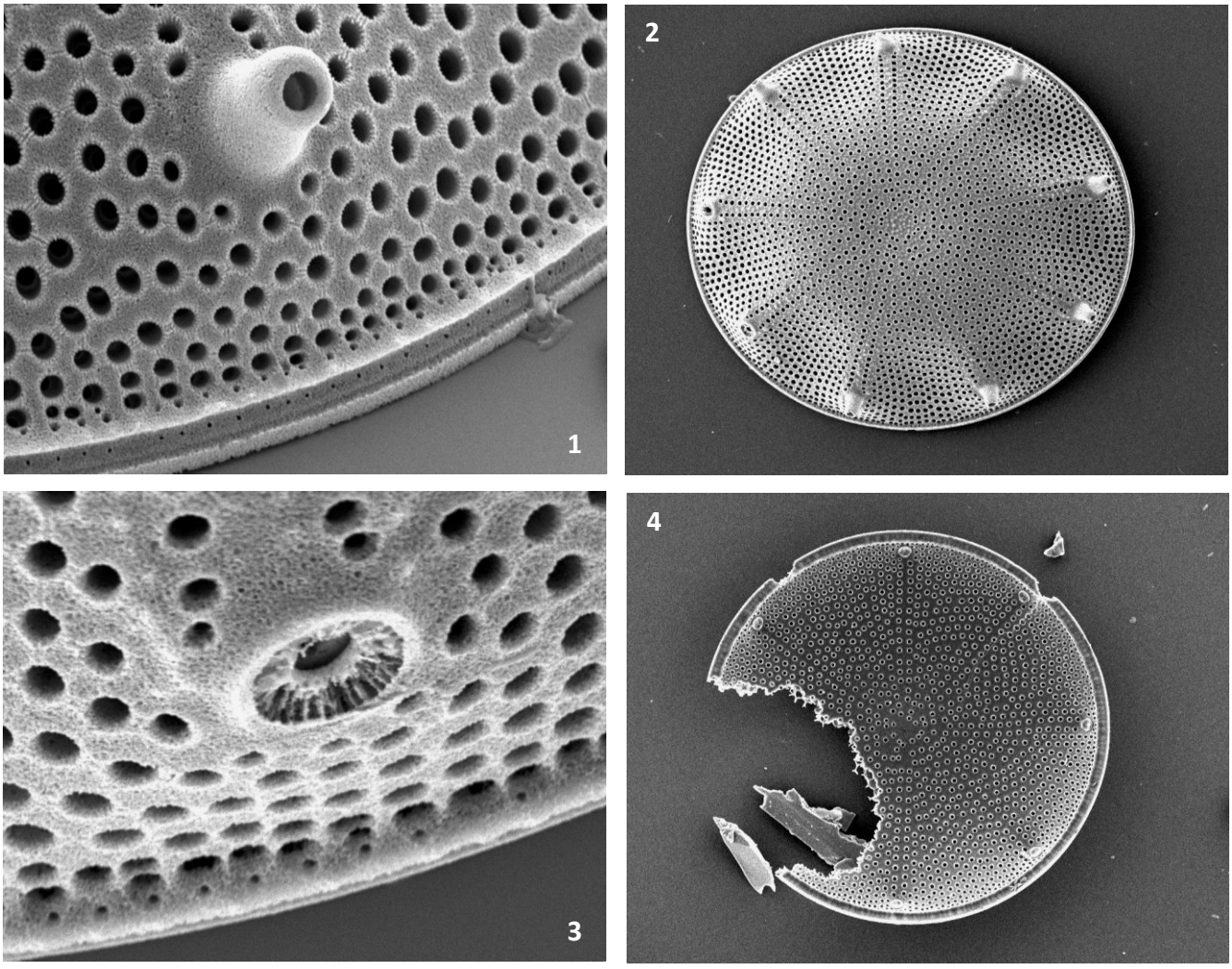

Fig 1 Detail of external opening of a rimoportula. oamaru_3ctilt2500.

Fig 2 External view of valve with two broken rimoportulae. Distinctive central rosette and two parallel rows of areolae along the furrows leading to the rimoportulae. oamaru_3e450.

Fig 3 Detail of broken rimoportula. oamaru_3e4000.

Fig 4 Internal view of valve. Distinctive ring around central area and pair of parallel rows of areolae along the rays leading to the rimoportulae. Internal openings of rimoportulae visible. oamaru_3i500.

Plate 30

Aulacodiscus cellulosus

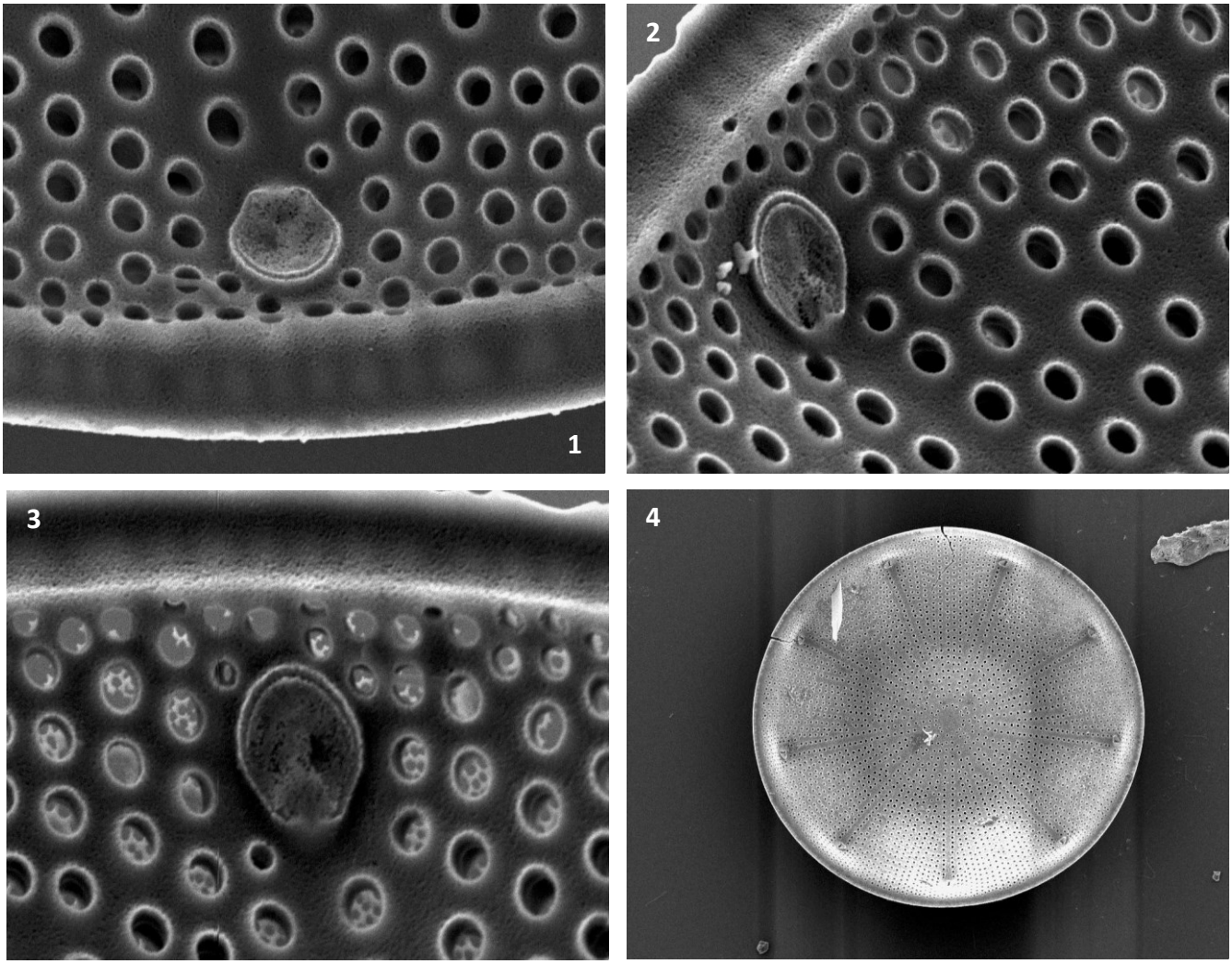

Fig 1 Internal view of valve edge showing opening of a marginal rimoportula. oamaru_3i4000.

Fig 2 Internal view of valve edge tilted showing opening of a marginal rimoportula. oamaru_3itilt4000.

Fig 3 Internal view of valve edge tilted showing opening of a marginal rimoportula. Also visible in some of the areolae are cribra covering the exterior side. oamaru_3itilt4500.

Fig 4 Internal view of valve. Distinctive ring around central area and pair of parallel rows of areolae along the rays leading to the rimoportulae. Internal openings of rimoportulae eroded in the same direction. oamaru3_a350.

Plate 31

Aulacodiscus cellulosus

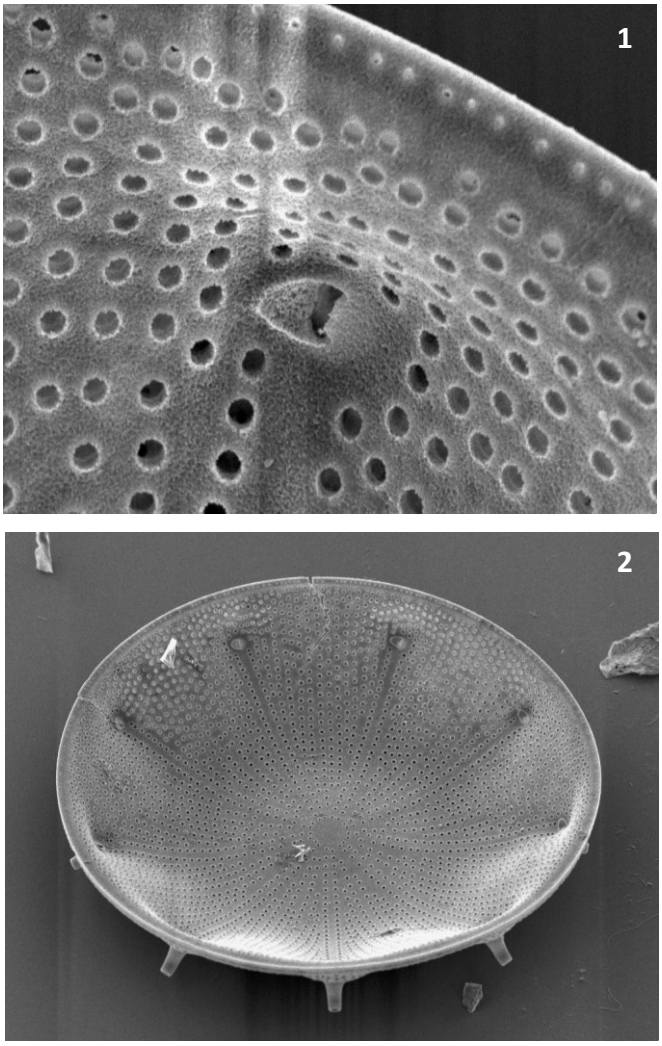

Fig 1 Detail of internal view of eroded rimoportula. oamaru3_a3000.

Fig 2 Internal view of valve tilted. Distinctive ring around central area and pair of parallel rows of areolae along the rays leading to the rimoportulae. Internal openings of rimoportulae eroded in the same direction. oamaru3_atilt450.

Plate 32

Aulacodiscus janischii

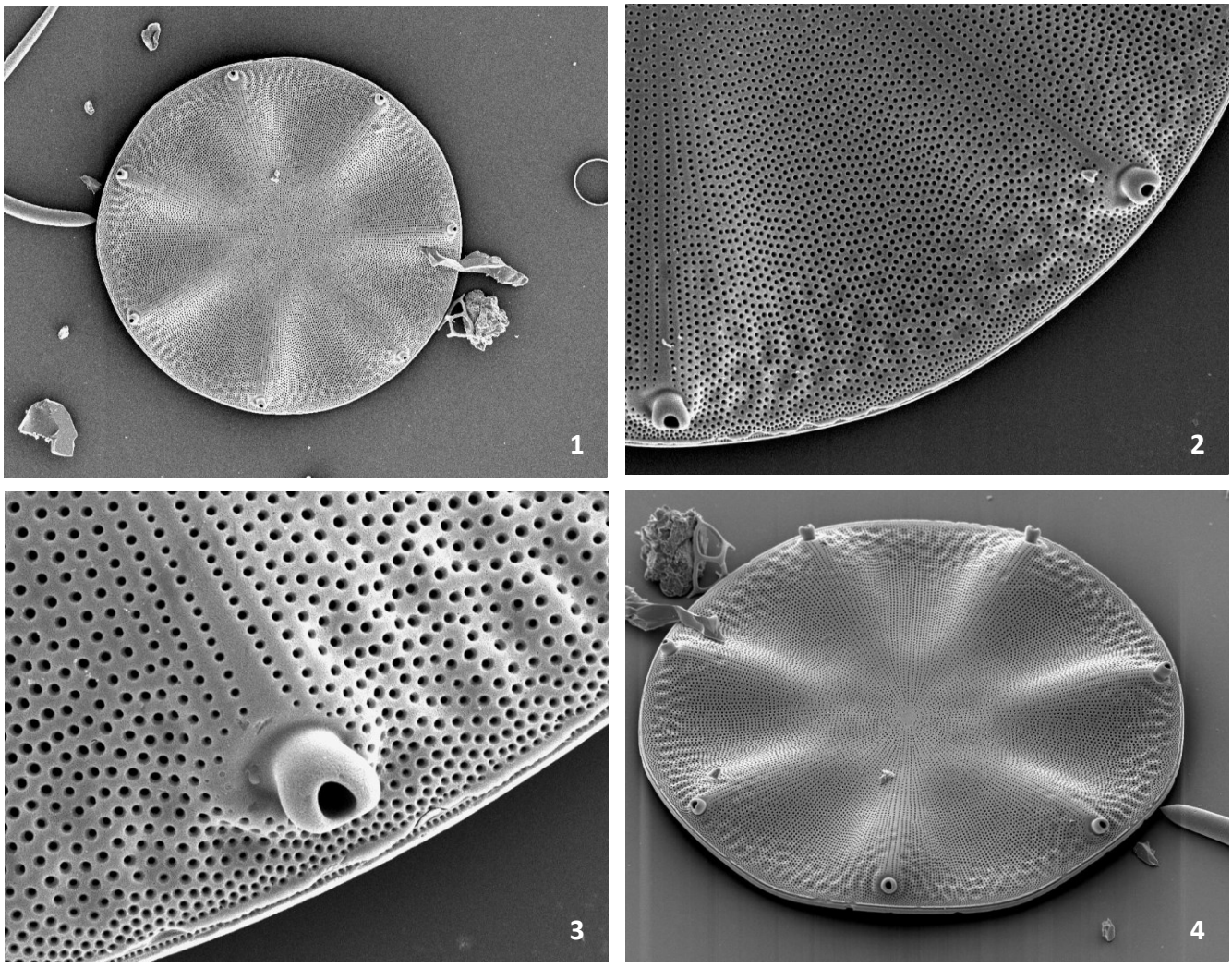

Refer to Tiffany (2023); Round et al. (1990) for the genus description; Witkowski et al. (2017) fig 34-35; Schmidt (1874-1959) pl 133,146,169; D&S (1989) pg 68 and pl 25 fig 6-7, pl 26 fig 1-5, recorded from Bain's Farm.

Fig 1 External view of valve. Diameter 354 µm. Distinguished by (a) tangentially undulating valve surface, (b) small hyaline area in the center, (c) small areolae of nearly uniform size covering the valve, (d) lack of ribs showing in SEM, (e) uniform spacing of the striae which are slightly wider on the crests, (f) rimoportulae near the margin protruding from the crests. oamaru_3j200.

Fig 2 External view of valve edge showing opening of two marginal rimoportulae. oamaru_3j700.

Fig 3 External view of valve edge showing opening of a marginal rimoportulae. oamaru_3j1800.

Fig 4 External view of valve tilted. oamaru_3jjtilt300.

Plate 33

Aulacodiscus janischii

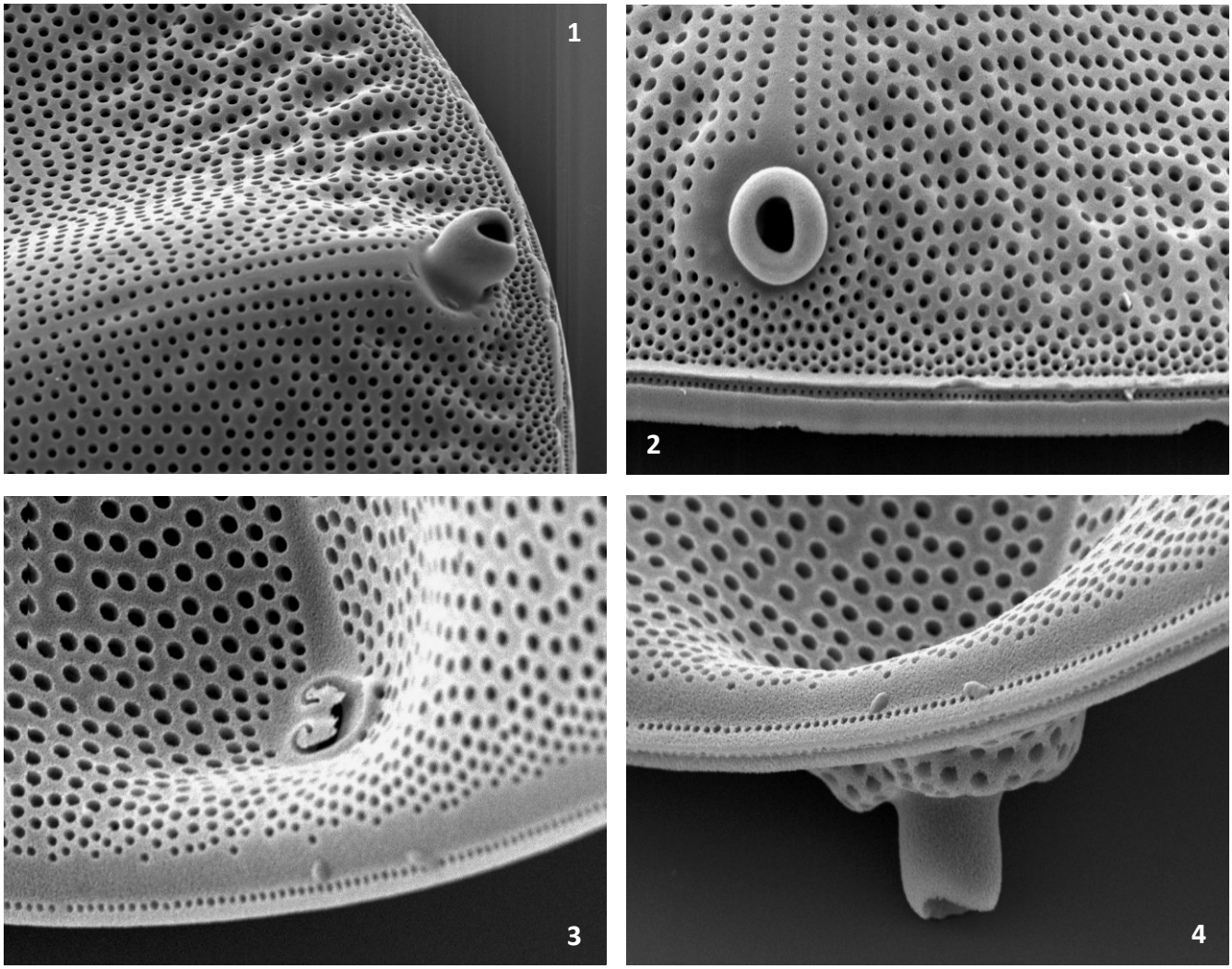

Fig 1 External view of valve edge showing opening of a marginal rimoportulae. oamaru_3jtilt1500.

Fig 2 External view of valve edge showing opening of a marginal rimoportulae. oamaru_3jtilt1800.

Fig 3 Detail of internal view of margin and inner opening of a rimoportula. oamaru_3n2500.

Fig 4 Detail of internal view tilted of margin and outer opening of a rimoportula in image oamaru_3n2500. oamaru_3ntilt2500.

Plate 34

Aulacodiscus janischii

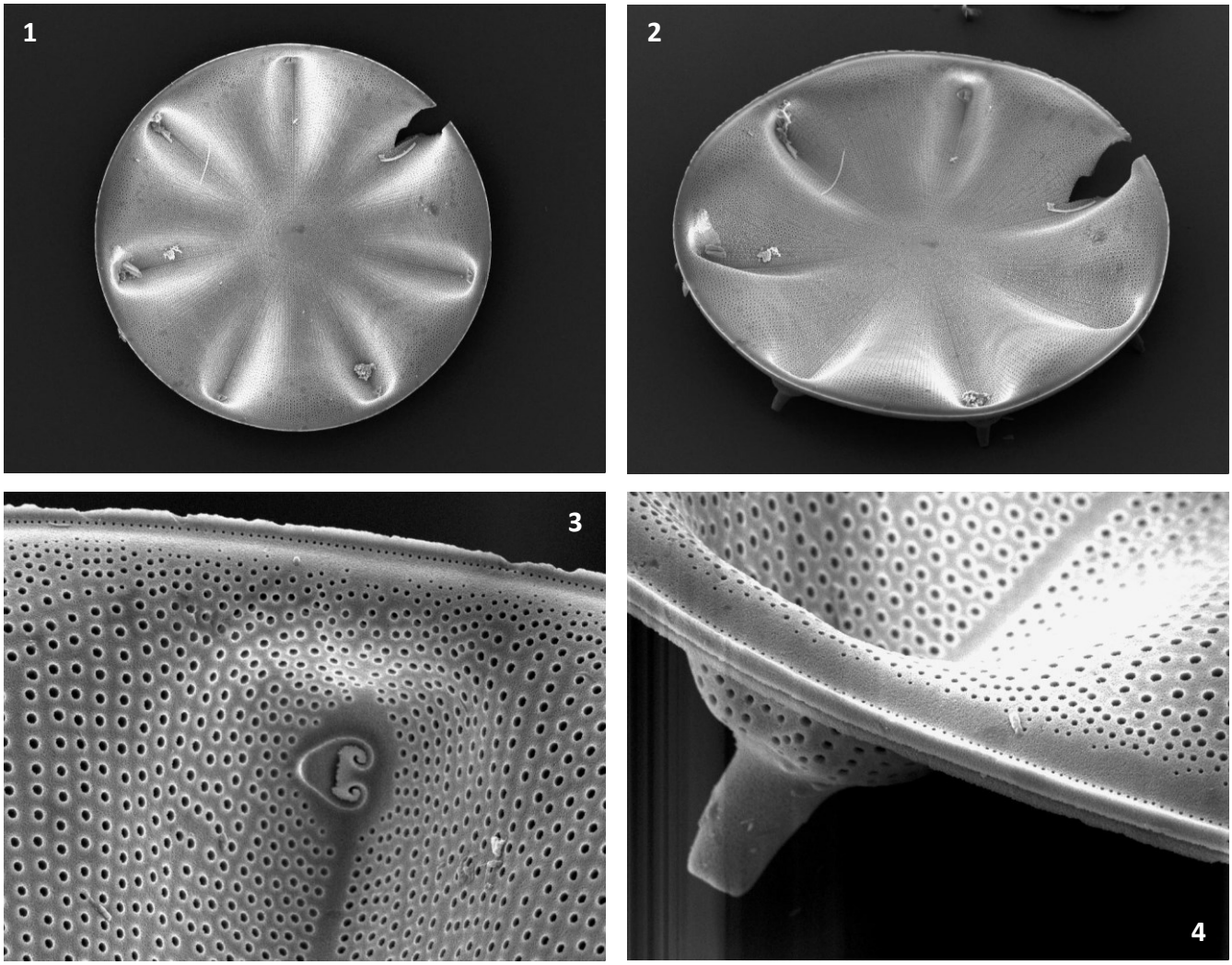

Fig 1 Internal view of valve. oamaru3_g200.

Fig 2 Internal view of valve tilted. oamaru3_gtilt250.

Fig 3 Internal view of opening of rimoportula. oamaru3_gtilt1500.

Fig 4 Internal view of valve with external view of rimoportula. oamaru3_gtilt1800.

Plate 35

Aulacodiscus sollittianus var. *novaezealandica*

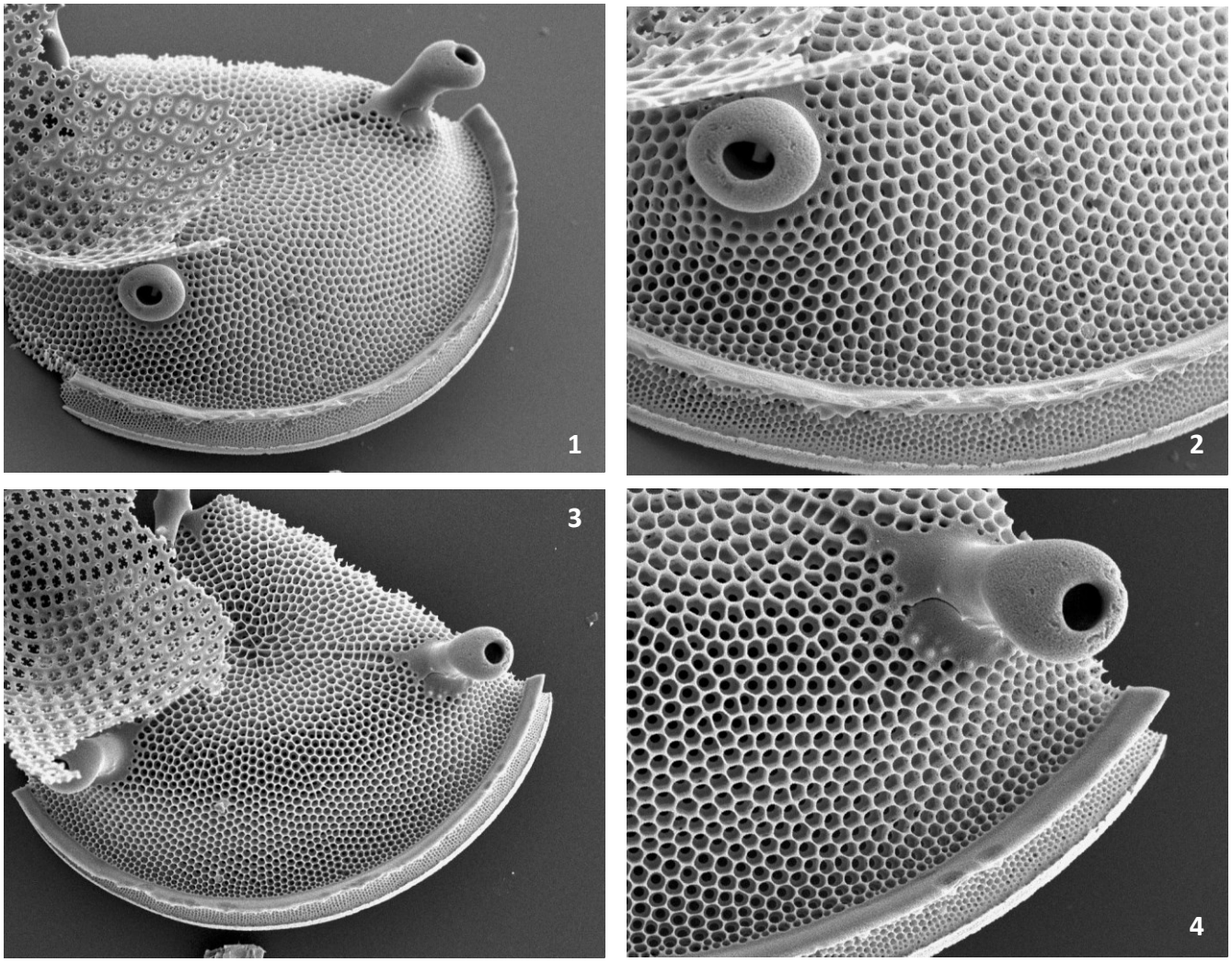

Refer to Tiffany (2023) for identification; Witkowski et al. (2017) fig 43-44; Round et al. (1990) for valvocopula and genus; Charles (2017); Heck (2015) bild 127; D&S (1989) pg 76 for description. (D&S 1989 uses alveolae instead of areolae. Areolae is used here because Round et al. has the advantage of SEM to more clearly see the structures.)

Fig 1 External valve view tilted. Distinguishing features of this species include (a) angular areolae covering surface of valve (cribra, which usually occlude areolae in this genus, appear to have eroded); (b) distal ends of rimoportulae broadly rounded; (c) collar visible at junction of mantle and valvocopula; (d) valvocopula with vertical rows of small areolae. oamaru_3d1tilt900.

Fig 2 Detail of image oamaru_3d1tilt900 showing areolae, rimoportula, mantle collar, and valvocopula. oamaru_3d1tilt1800.

Fig 3 External valve view. oamaru_3d800.

Fig 4 Detail of areolae on valve face, distal end of a rimoportula, and valvocopula below the mantle rim. oamaru_3d1800.

Plate 36

Aulacodiscus sollittianus var. *novaezealandica*

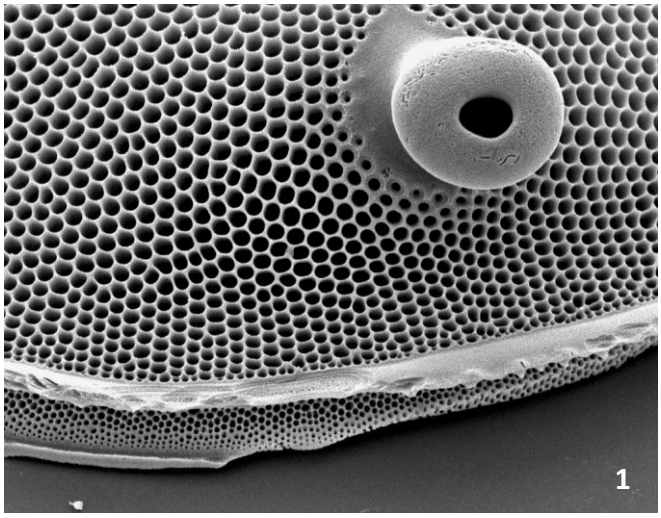

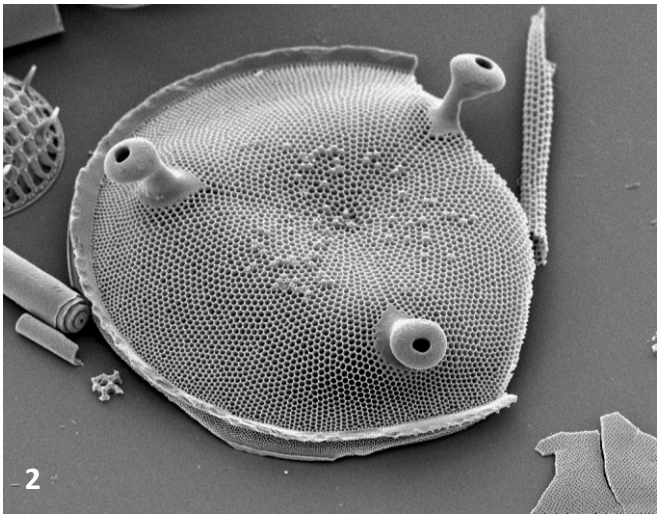

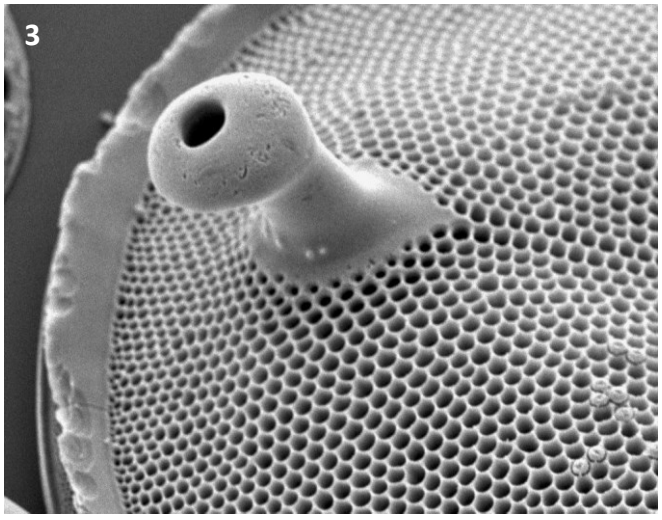

Fig 1 Detail of rimoportula in image oamaru_3otilt500. Faint lines at edge of some areolae may be remainder of cribra. oamaru_3ootilt1500.

Fig 2 External valve view tilted. Distinguishing features of this species include (a) angular areolae covering surface of valve (cribra, which usually occlude areolae in this genus, appear to have eroded); (b) distal ends of rimoportulae broadly rounded; (c) collar visible at junction of mantle and valvocopula; (d) valvocopula with vertical rows of small areolae. oamaru_3otilt500.

Fig 3 Detail of external view clearly showing the base of the rimoportula. The conchoidal fractures on flange at the mantle edge suggest broken glass. oamaru_3otilt1500.

Plate 37

Brightwellia coronata

Refer to Round et al. (1990) pg 182 for genus description, "Development of valve areolae into localised enlarged chambers seems to be a characteristic of fossil genera"; Charles (2017); Heck (2015); D&S (1989) pl 90 fig 3-4, recorded from Bain's Farm; Schmidt (1874-1959) pl 140 fig 11-12, from Oamaru.

Fig 1 External valve view. Diameter 89 µm. oamar3d900.

Fig 2 Detail of image oamar3d900. External view of ring of ovals and areolae. oamar3d4000.

Fig 3 External view of areolae and ring of ovals. More eroded than other *Brightwellia* specimens here. oamaru2etilt_3500.

Fig 4 Detail of external view of ring of ovals. Four of the ovals demonstrate the chamber beneath the oval and the corresponding single, round foramen leading to the cell interior. oamaru2ptilt3500.

Fig 5 External view of central area. oamaru3u1100.

Plate 37

Brightwellia coronata

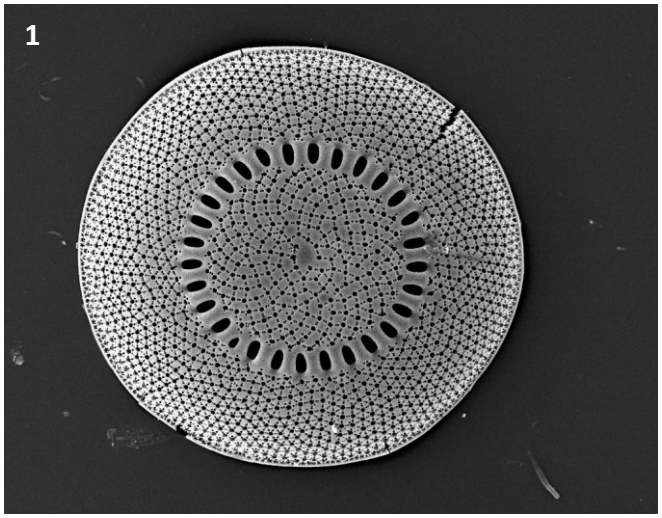

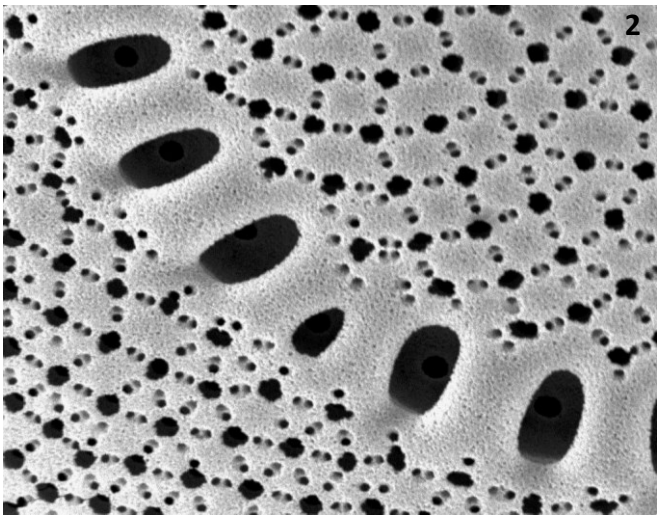

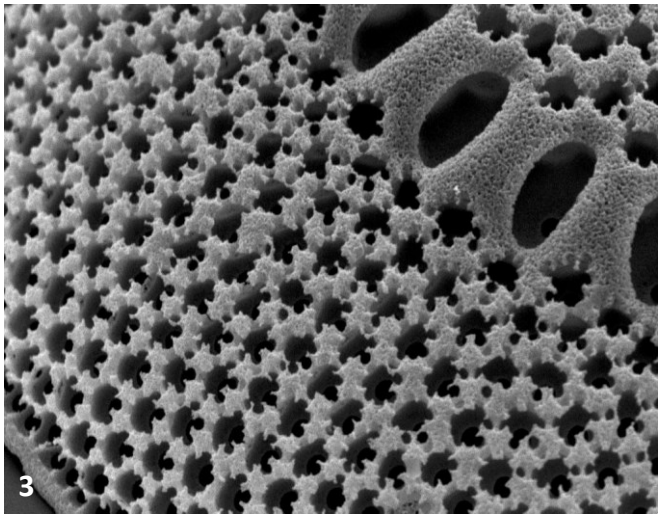

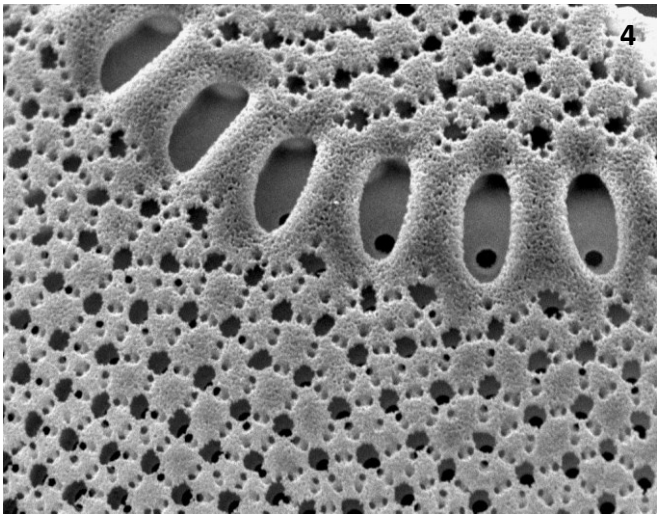

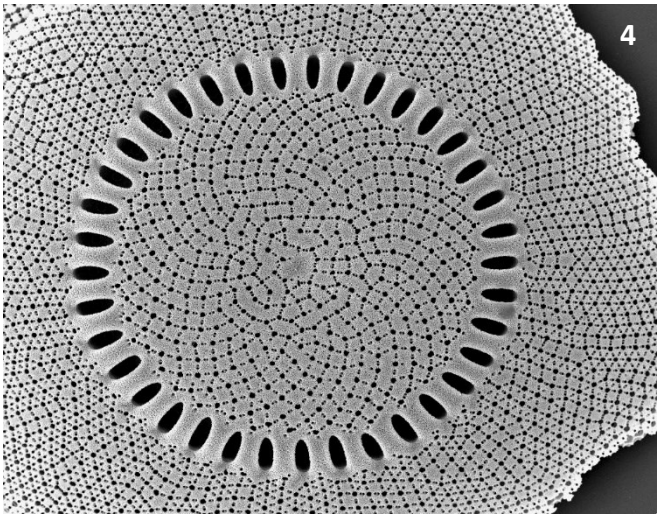

Plate 38

Cestodiscus spinifer

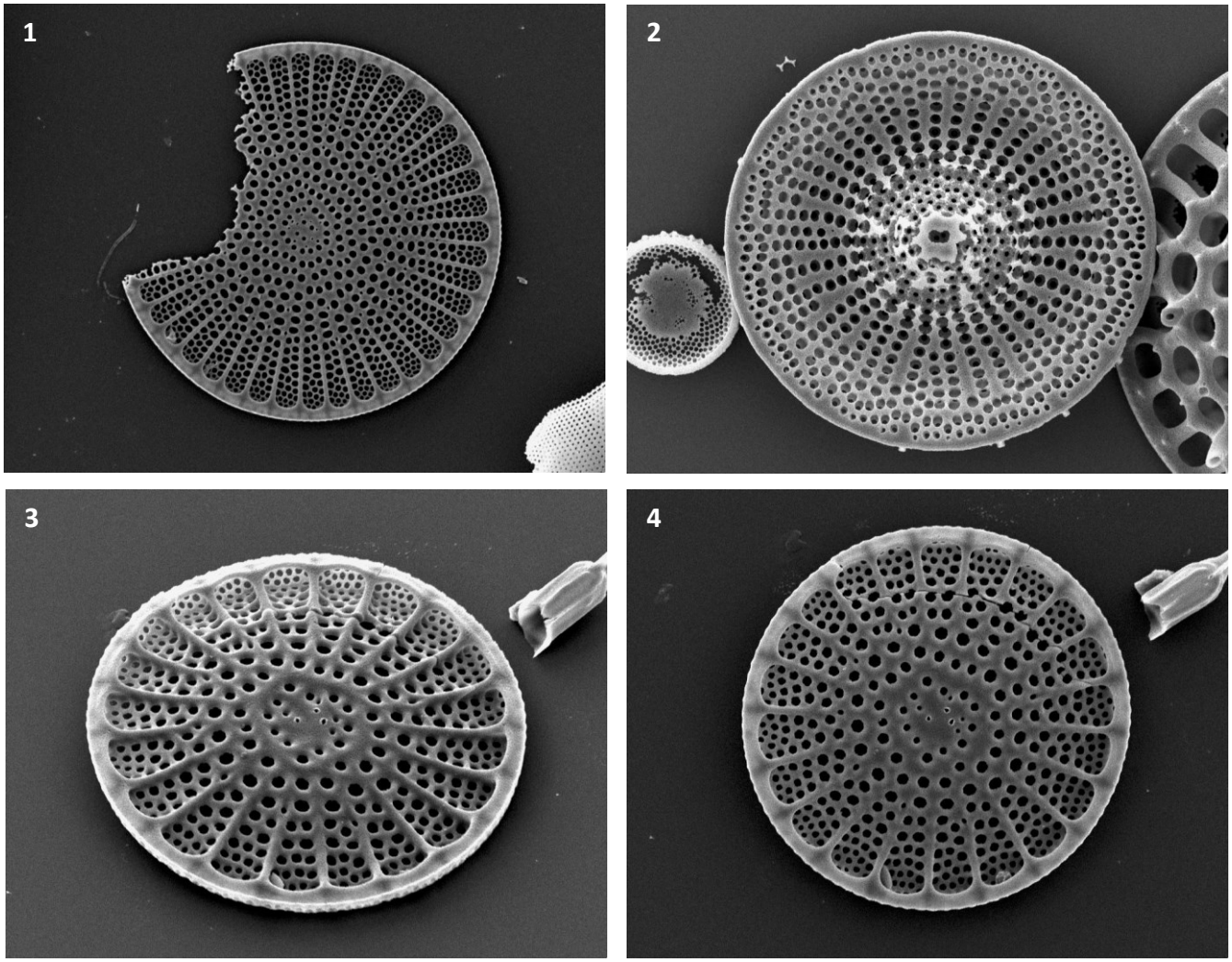

Refer to Witkowski (2023a) for identification; Witkowski (2023b) for image (https://fossil-diatoms.com/atlas/index.php?page=entry&genus=Cestodiscus&species=spinifer&id=51&requestedBy=taxa-list) ; DiatomBase for synonymy (https://www.diatombase.org/aphia.php?p=taxdetails&id=651833).

Fig 1 Internal view. Diameter 106 µm. Distinguished from *Arachnoidiscus* by having no central ring with attached flange. The interal ribs in these specimens may distinguish this from *Coscinodiscus.* oamaru2r700.

Fig 2 External view. Diameter 63 µm. oamaru2v1300.

Fig 3 Internal view. Tilted view of oamaru2ww1300. oamaru2wtilt1500.

Fig 4 Internal view. Diameter 58 µm. oamaru2ww1300.

Coscinodiscus argus

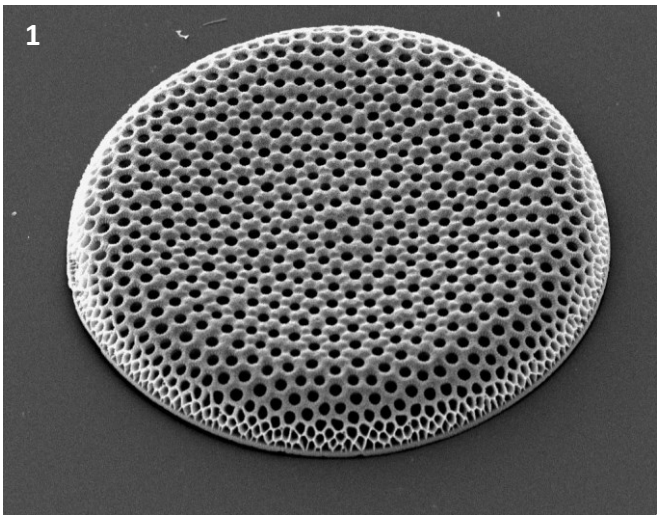

Refer to Charles (2017); Heck (2015) bild 227; Edwards (1991) plate 4 fig 44.

Fig 1 Valve diameter 97 µm. Areola diameter ~ 2.2 µm. Areolae on a radius 11-12. By comparison, *Coscinodiscus asteroides* appears to have denser areolae arranged in more distinct rows and has a more definite central area in Charles and in Heck. Edwards shows a distribution of areolae similar to this specimen. oamaru3stilt1000.

Coscinodiscus subdivicus

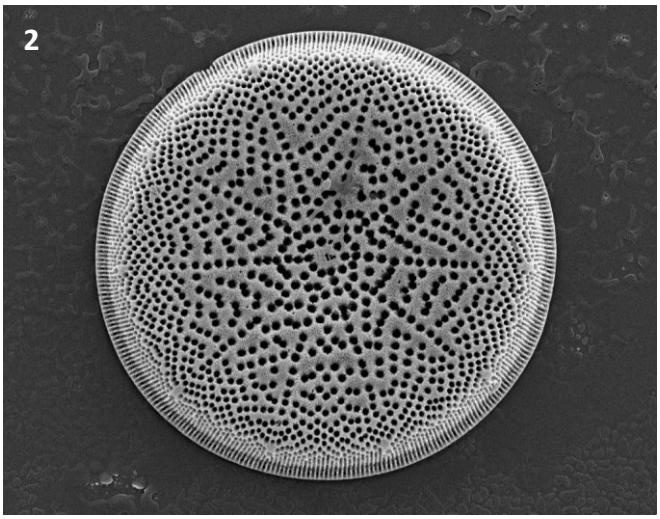

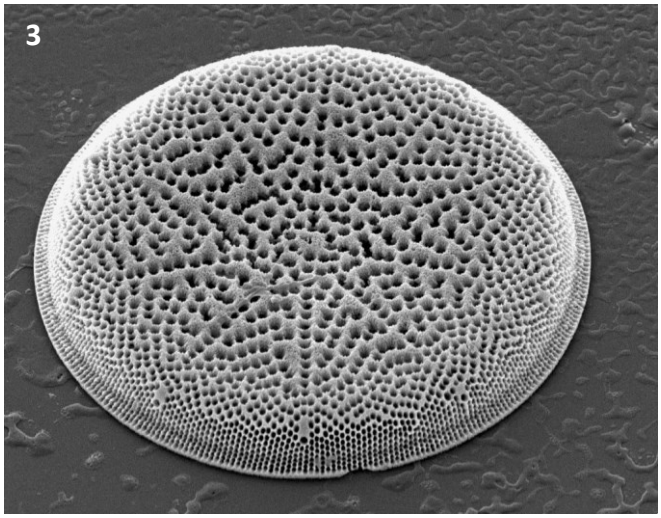

Refer to Heck (2015); Charles (2017); D&S (1989) pg 135 and pl 57 fig 10, recorded from Bain's Farm.

Fig 2 External view of valve. Radial lines of large areolae lead to the rimoportulae near margin. The marginal rimoportulae suggest an *Aulacodiscus*. oamaru3h1500.

Fig 3 External view of valve tilted. oamaru3rtilt1800.

Plate 40

Ellerbeckia clavigera

Refer to Witkowski (2023a) who provided probable identification and explained the morphology; Crawford & Sims (2006) in Miranda (2016) explains the name; Round et al. (1990) pg 168 for genus description; Edwards (1991) pl 1 fig 6; Charles (2017); Heck (2015) bild 351; D&S (1989) pg 177 pl 78 fig 1,4,8,9. Both Edwards and Charles use the synonym *Melosira clavigera*.

Fig 1 Internal view of two sibling linking valves. Diameter 44 µm. For detail, see image oamaru_3qtilt5000. For an external view, see image oamaru3qtilt1300. oamaru_3qtilt1800.

Fig 2 Detail of image oamaru_3qtilt1800. Exterior of mantles of two sibling linking valves. Intaglio valve at top. Cameo valve at bottom with the step appearing as the light line two or three pores below the links. The black marks are spaces in the interlocking ridges and grooves. oamaru_3qtilt5000.

Fig 3 External view of both mantles of image oamaru3vtilt1000. oamaru3itilt3500.

Fig 4 oamaru3itilt6000. Internal view of mantle of intaglio valve of image oamaru3vtilt1000.

Fig 5 External view of a linking valve. Diameter 71 µm. The wavy rim suggests the linking area of the two sibling valves linked in image oamaru_3qtilt1800. Round et al. (1990) has an SEM image very similar to this specimen. oamaru3qtilt1300.

Fig 6 Two sibling linking valves. Intaglio valve (internal view) at the top, cameo valve with the step in the mantle at the bottom. The wavy pattern of the ridges and grooves where the cells join matches the pattern in image oamaru3qtilt1300. oamaru3vtilt1000.

Plate 40

Ellerbeckia clavigera

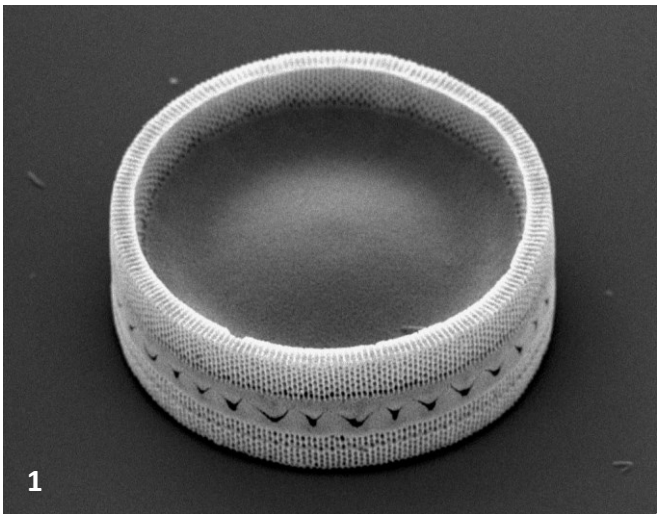

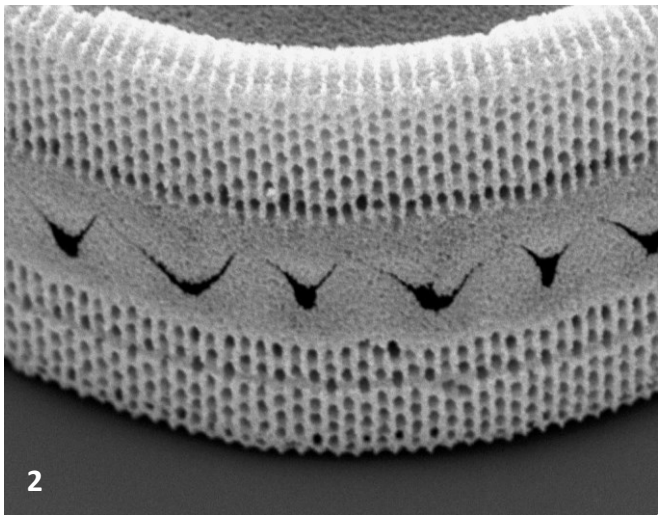

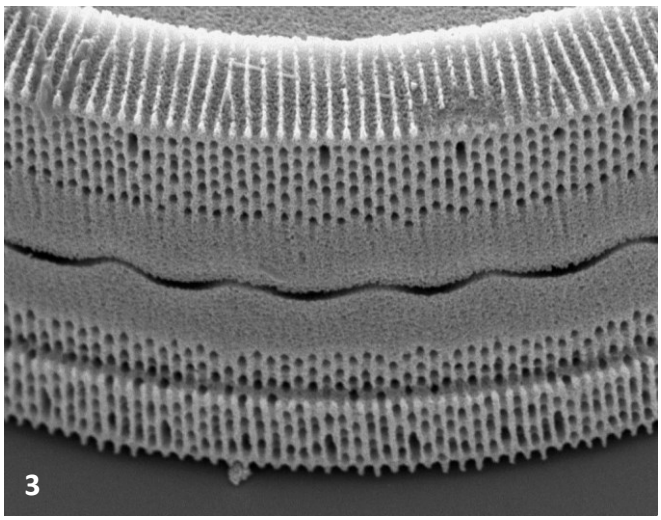

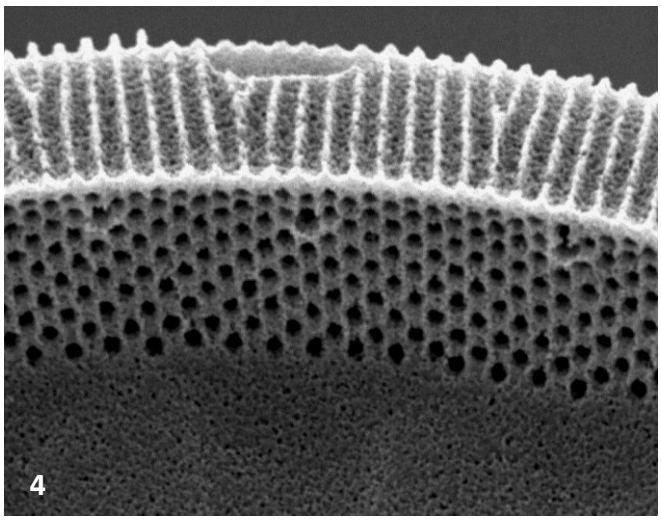

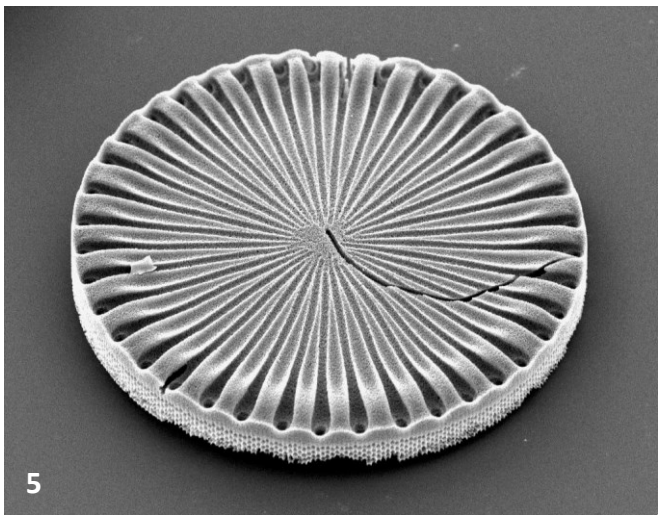

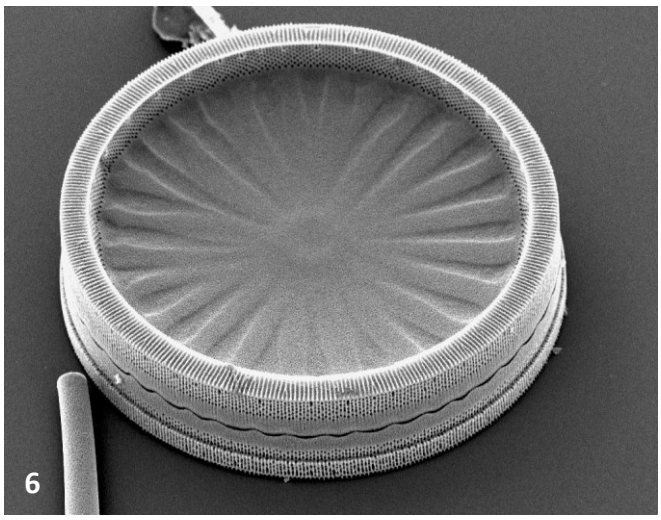

Plate 41

Ellerbeckia sp1

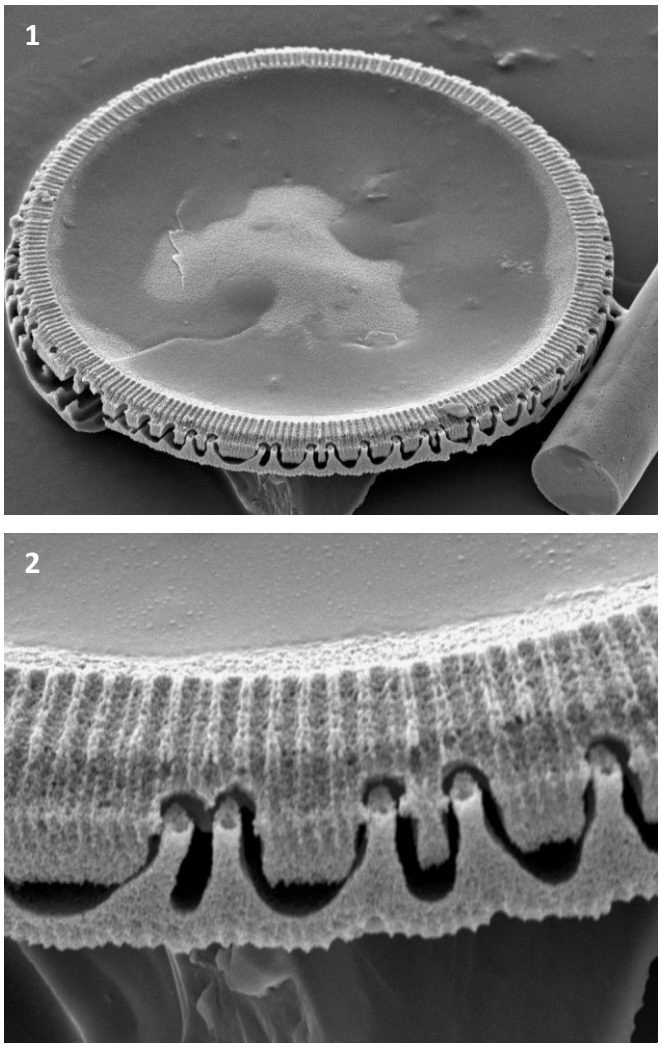

Refer to Witkowski (2023a) for morphology; Round et al. (1990) for the genus.

Fig 1 Edges of two linking valve faces, the only preserved parts of these valves. Diameter 106 µm. Edge of bottom valve and internal view of top valve. The fine rays around the upper valve are cross-sections of mantle areolae. The hollowed rim of the upper valve was caused by erosion. The ring of narrow uprights on the lower valve are costae (ridges) on the valve face visible from the side. They are interlocking with the corresponding costae on the upper valve face. oamaru3mtilt1000.

Fig 2 Detail of valve mantles. Image width 29 µm. oamaru3mtilt4000.

Endictya oceanica

Refer to Round et al. (1990) pg 160 fig a; Edwards (1991) pl 1 fig 1; Schmidt (1874-1959) tafel 65 fig 10,12,13 (oblique view); Charles (2017).

Fig 1 External view. Valve center has a few projections intact but many appear to be crushed; valve rim has narrow flange and line of pores. See also internal view of a possible *Endictya* in image oamaru2btilt1600. Witkowski et al. (2017) figs 145-146 does not appear to have enough detail to distinguish *Pyxilla* from *Endictya*. oamaru_3rtilt500.

Endictya sp1

Refer to Round et al. (1990) pg 161 fig i.

Fig 2 Internal view. Areolae on mantle variable in size in contrast to *Endictya oceanica*. Round et al. (1990, pg 160) has several examples of both areola patterns. Internal apertures of rimoportulae at angle of mantle and face. Internal pores arranged in rows radiating from valve center (similar to *Melosira* and *Stephanopyxis*). oamaru2btilt1600.

Hyalodiscus laevis

Refer to Round et al. (1990) for genus description; Heck (2015) bild 324; Charles (2017).

Fig 3 External view of valve. Diameter 112 µm. oamaru2j600.

Fig 4 External view of valve tilted. Diameter 112 µm. oamaru2jtilt800.

Fig 5 Detail of valve edge and mantle. oamaru2jtilt1800.

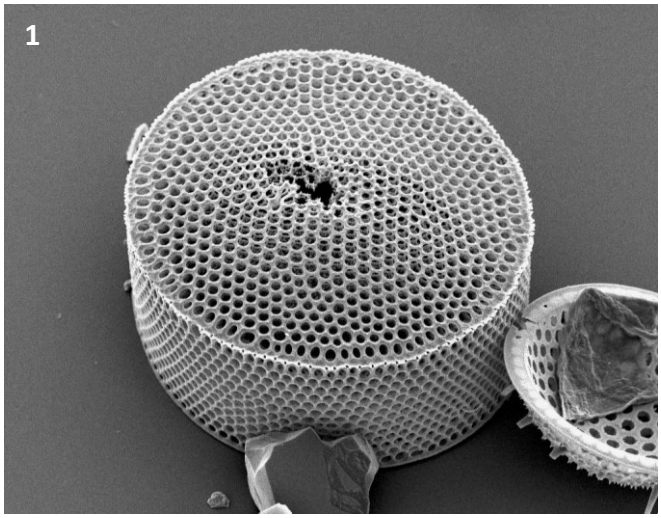
1

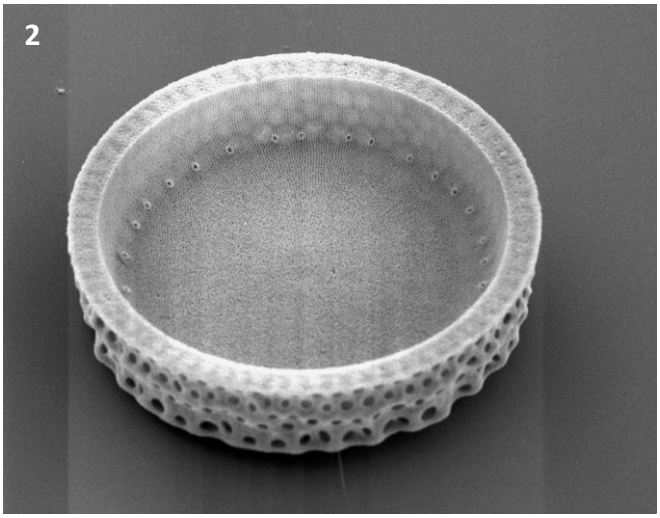
2

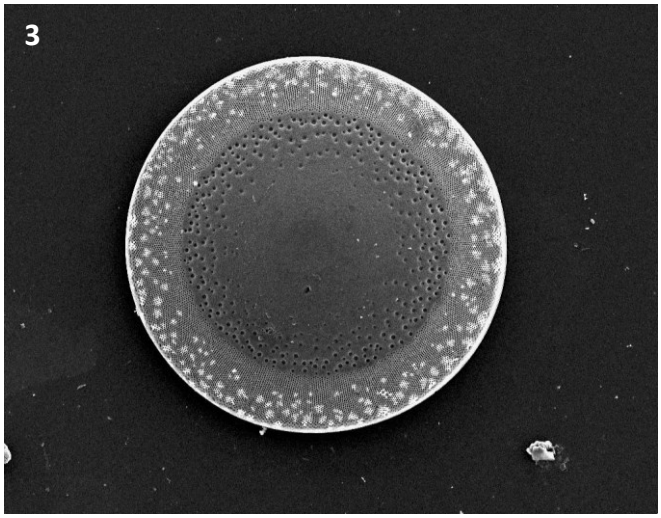
3

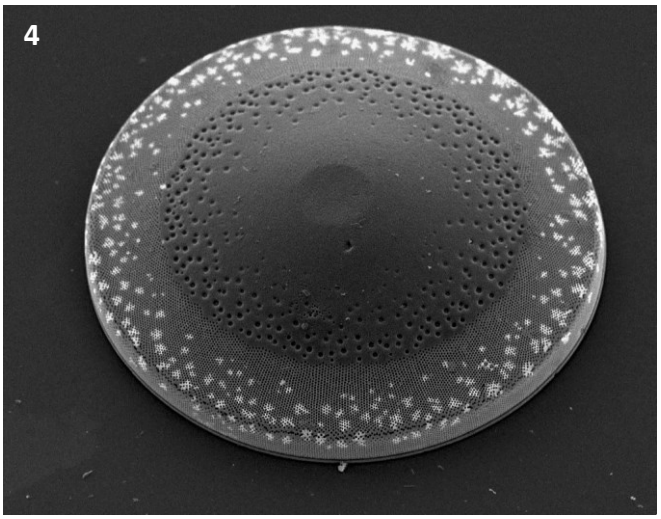
4

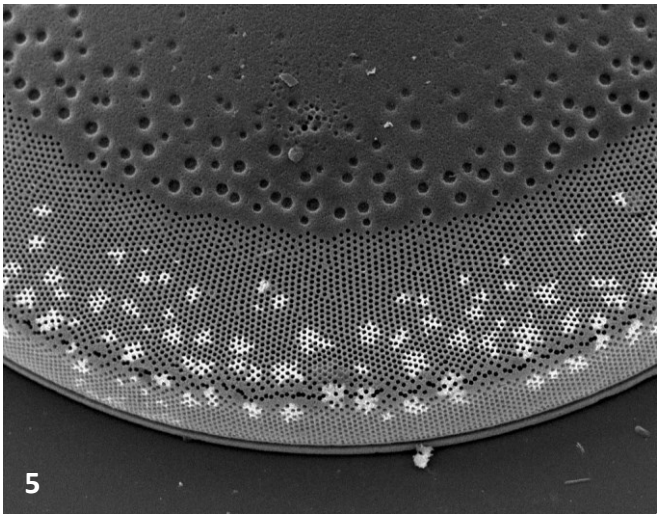
5

Plate 44

Podosira corolla

Refer to Charles (2017); Heck (2015); D&S (1989) pl 90 fig 3-4, recorded from Bain's Farm; Schmidt (1874-1959) pl 140 fig 11-12, from Oamaru; Round et al. (1990) for genus description. DiatomBase (https://www.diatombase.org/aphia.php?p=taxdetails&id=840841)

These specimens look nothing like the images for *Podosira* in Round et al. (1990, pg 164). Perhaps it is a different genus.

Schmidt calls this *P. corolla.* Charles calls it *P. corolla* on the index but *P. coronata* on the image. Charles has an excellent LM image. D&S and DiatomBase use Schmidt as the source. DiatomBase says it is recent only.

Fig 1 External view of valve tilted. oamaru2ptilt1800.

Fig 2 External view of valve tilted. oamaru2qtilt1500.

Fig 3 Detail of junction flange between valve face and mantle showing rimoportulae and striated band. oamaru2t4500.

Fig 4 External view of valve tilted. oamaru3ktilt2000.

Fig 5 Detail of external view of valve edge. Rimoportulae protrude through the striated band. The mantle is below the flange at the junction of face and mantle. oamaru3ktilt5000.

Fig 6 External view of valve tilted. Wide striated band below the flange. oamaru3otilt1800.

Plate 44

Podosira corolla

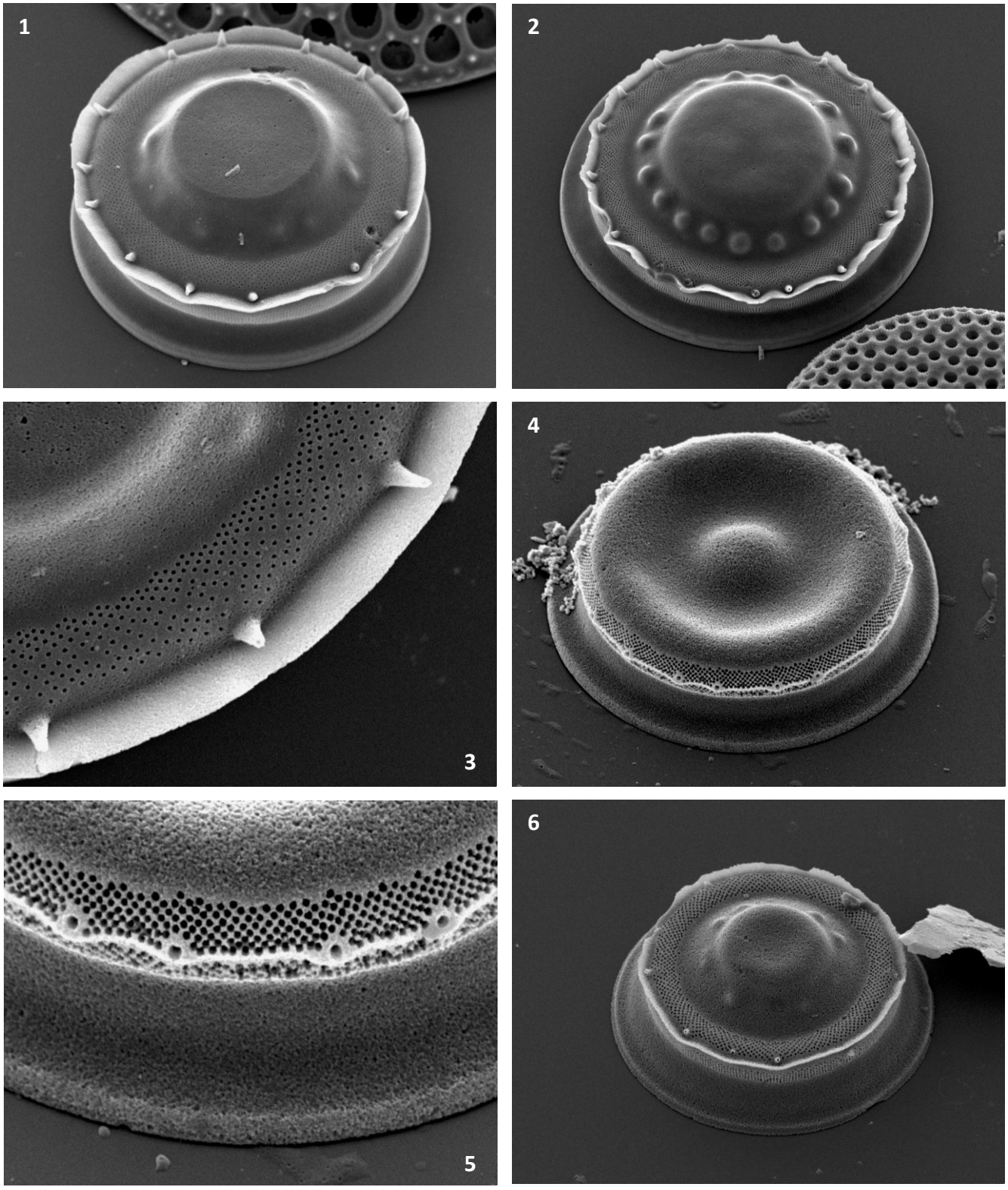

Stephanopyxis

Refer to Round et al. (1990); D&S (1989) pp 229-235 and associated plates; Charles (2017).

Stephanopyxis sp1

Fig 1 Two sibling valves joined by the valve faces. Internal openings to rimoportulae visible on the top valve. oamaru2gtilt_1500.

Stephanopyxis sp2

Fig 2 External view of valve of a domed form. oamaru3g900.

Fig 3 External view of valve tilted of a domed form. oamaru3jtilt1000.

Stephanopyxis sp3

Fig 4 External view of form with nearly flat valve. oamaru3g1500.

Fig 5 External view of form tilted with nearly flat valve. oamaru3ltilt1800.

Stephanopyxis sp4

Fig 6 External view of a form with hemispheric valve. oamaru3ntilt1800.

Oamaru Diatoms

Plate 45

Stephanopyxis

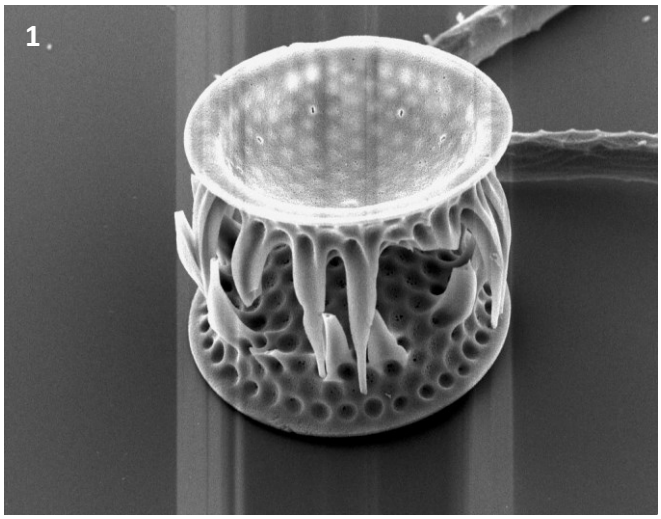

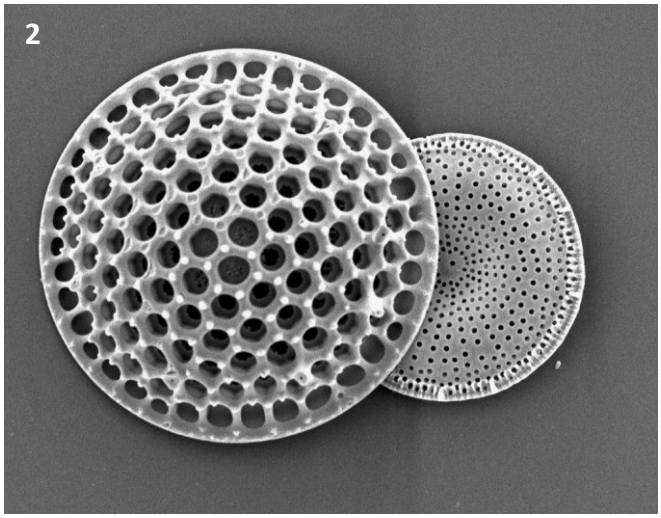

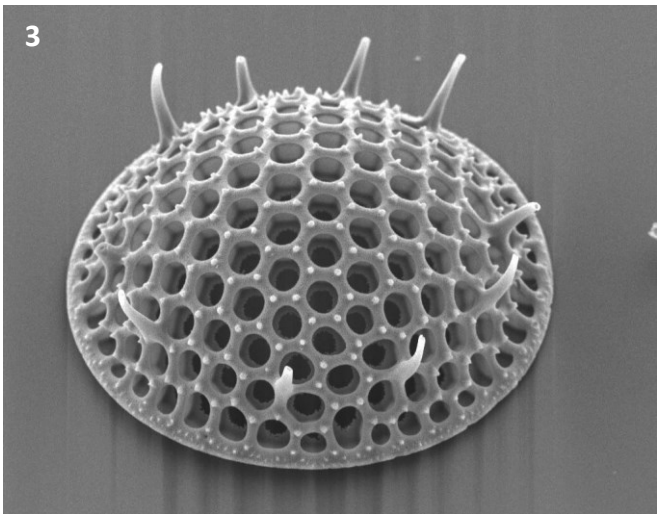

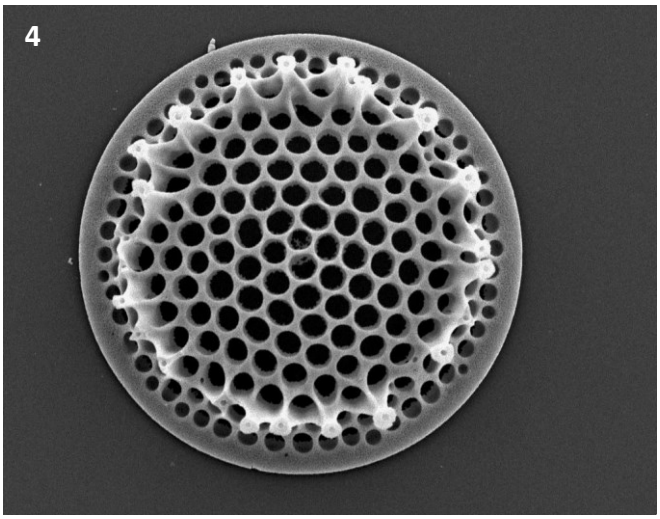

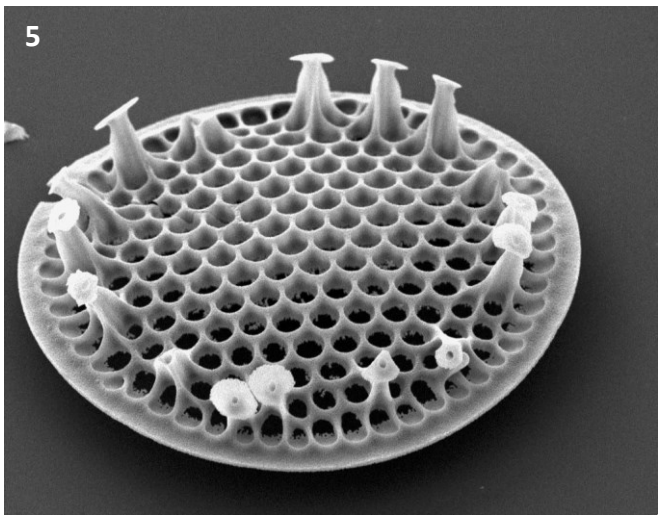

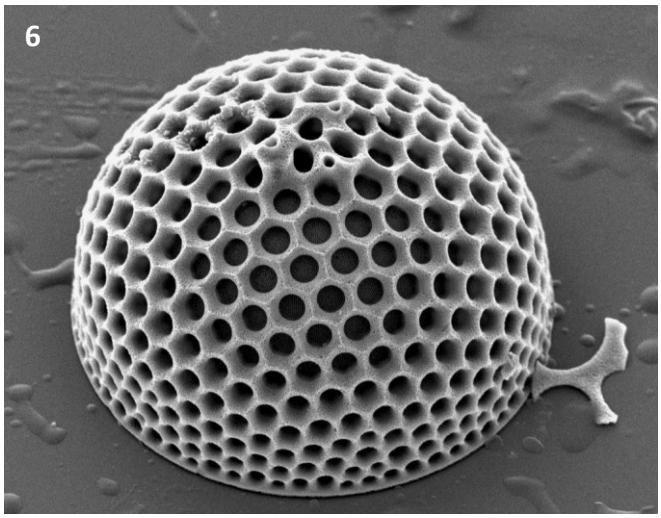

Plate 46

Stictodiscus

This genus is partly defined by the raised siliceous thickenings that often surround the areolae forming a network on the valve face. In this group of specimens, *Stictodiscus californicus* var. *nitida* seems to not fit the definition. More study is needed to better define the genus (Round et al. 1990).

Stictodiscus californicus var. *nitida*

Refer to Charles (2017); Witkowski et al. (2017) fig 159-160; D&S (1989) pg 234 and pl 102 fig 1-5, recorded from Bain's Farm.

Fig 1 External valve view. A circular species. oamaru_3btilt1800.

Stictodiscus novaezealandiae

Refer to Heck (2015) bild 466 for clear image of central area; Schmidt (1874-1959) band 1 tafel 131 fig 10 for a clear drawing; Charles (2017); D&S (1989) pl 105 fig 1,4,5,7-9.

Fig 2 Internal view of valve. Distance between apices across center 163 µm. A quadrangular species. oamaru3_ftilt600.

Fig 3 Internal view of an apex. oamaru3_ftilt3000.

Fig 4 Internal view of rimoportulae in central area. oamaru3_ftilt4000.

Stictodiscus splendidus

Refer to D&S (1989) pl 106 fig 1,6 are a good match; Heck (2015) bild 465; Charles (2017); Round et al. (1990) for discussion of taxonomic difficulties of the genus.

Fig 5 External view. Distance between apices 208 µm! A triangular species. Pore fields at apices. Very clear example of the raised thickenings surrounding the areolae that define the genus. This specimen defies the category of a Centric Radial diatom. oamaru3f400.

Fig 6 Detail of external view of apical pore field. Width of image 58 µm. Very clear example of raised thickenings surrounding the areolae that define the genus. oamaru3ftilt2000.

Plate 46

Stictodiscus

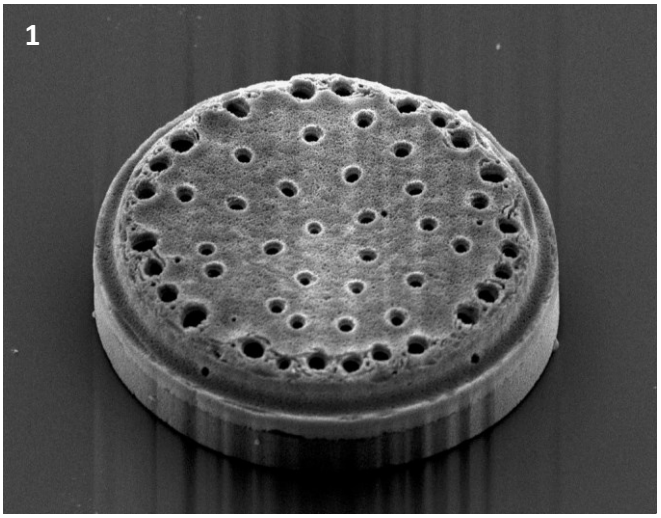

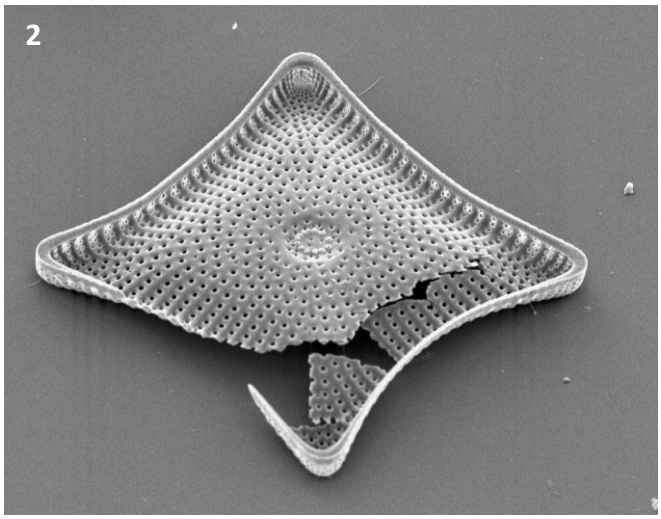

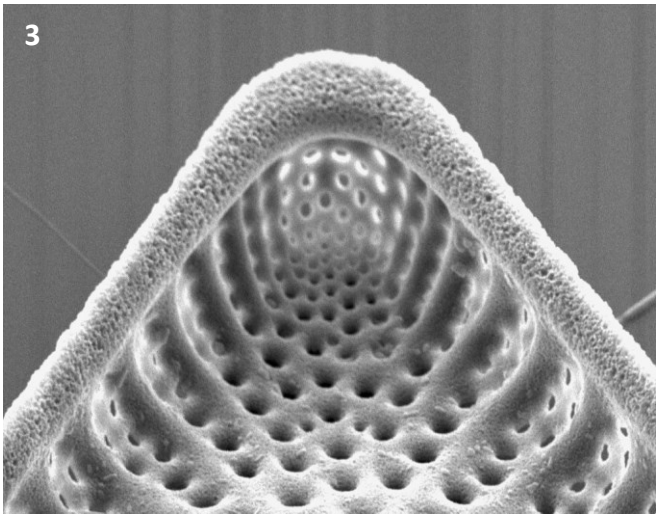

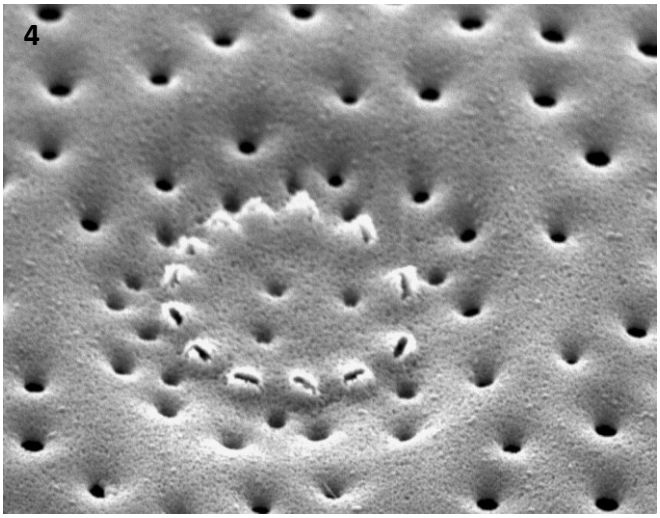

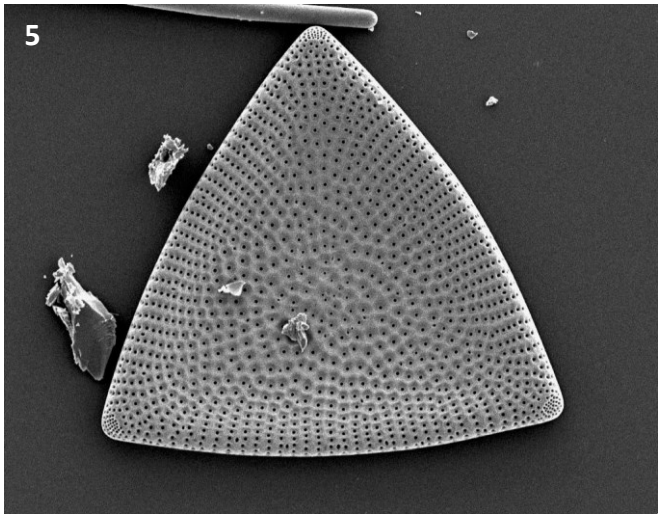

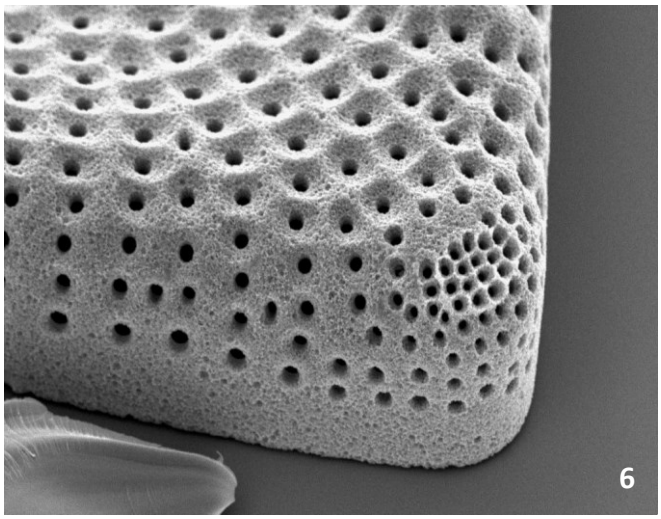

Strangulonema barbadense

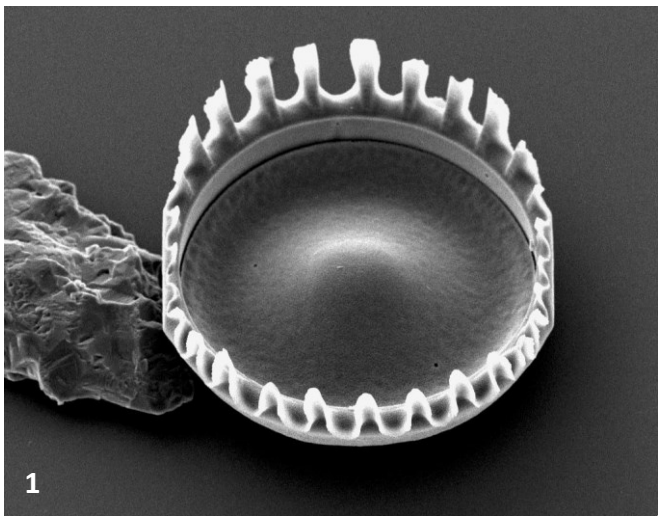

Refer to Round et al. (1990) which says this is a fossil genus; DiatomBase (https://www.diatombase.org/aphia.php?p=taxdetails&id=622698) says this is a fossil species from the Eocene to Oligocene, the time of Oamaru; Witkowski (2023b) has an excellent LM image that resembles the SEM in Round et al. (https://fossil-diatoms.com/atlas/index.php?page=entry&id=61&genus=Strangulonema&requestedBy=taxa-list).

This identification was a guess based on illustrations in Round et al. (1990) and on limited experience with fossil diatoms. Assumptions were made about the structures visible.

Fig 1 External view of valve face with collar at edge giving rise to spines. Round et al. (1990) for the genus has these spines as flattened and furcate (forked) though they do not appear forked here, perhaps because of erosion. oamaru3stilt1100.

Acknowledgements

Bill Dailey (US) provided the cleaned sample and the single list of the images used for the first edition gallery. Rob Kimmich (US) provided text and code for the page. Mary Ann Tiffany (US) provided the images, magnification table, identifications, as well as the inspiration to attempt this project. David Walker (UK) hosted the project on Micscape Magazine. Bill and David provided testing and comments on design and content. These collaborators are members of Diatom Forum. Jakub Witkowski (University of Szczecin, Poland) helped greatly with naming specimens and provided insights into problems of working with fossil diatom names.

Appendix

Version History The First Edition was started in February 2023 and completed in March 2023. It was an HTML web page. This Second Edition was started in March 2023 and completed in June 2023 as a PDF document which provided more flexibility for use. It contains many name changes and additional comments.

References

As often happens, diatom references may be out of print or behind various pay walls, though some may be in the public domain. Authors are often willing to share copies of their work.

Brown, N.E. (1933) Arachnoidiscus. Watson & Sons, Ltd, London. http://www.microscopy-uk.org.uk/diatomist/Arachnoidiscus.pdf.

Charles, Nigel (2017). Oamaru diatoms. https://www.oamarudiatoms.co.uk/index.html. [Nigel died in 2018. His website is now maintained by Anne Gleich.]

Crawford, R.[M.] & Sims, P.A. (2006). The diatoms Radialiplicata sol (Ehrenberg) Glezer and R. clavigera (Grunow) Glezer and their transfer to Ellerbeckia Crawford, thus a genus with freshwater and marine representatives. Nova Hedwigia Beiheft 130: 137-162.

Dailey, W. (2004) Oamaru diatomite collection sites. https://diatomsamples.weebly.com/oamaru-diatomite.html.

Desikachary, T.V., and P.M. Sreelatha (1989) Oamaru diatoms. Bibliotheca Diatomologica, Berlin, Band 19, 330 pp plus 145 plates. [Abbreviated here as D&S.]

Edwards, A.R. (compiler) (1991) The Oamaru diatomite. New Zealand Geological Survey Paleontological Bulletin 64, 260 pp.

Guiry, M.D. in Guiry, M.D. & Guiry, G.M. (2016) Rattrayella oamaruensis. AlgaeBase, National University of Ireland, Galway. https://www.algaebase.org; retrieved on 28 February 2023. https://www.algaebase.org/search/species/detail/?species_id=136831

Heck, Paul-Rainer (2015) Die fossilen Diatomeen Oamarus (Neuseeland) aus den Sammlungen von Bernard Hartley und Nigel Charles. Self-published in PDF form.

Kociolek, J.P.; Blanco, S.; Coste, M.; Ector, L.; Liu, Y.; Karthick, B.; Kulikovskiy, M.; Lundholm, N.; Ludwig, T.; Potapova, M.; Rimet, F.; Sabbe, K.; Sala, S.; Sar, E.; Taylor, J.; Van de Vijver, B.; Wetzel, C.E.; Williams, D.M.; Witkowski, A.; Witkowski, J. (2023). DiatomBase. Accessed at https://www.diatombase.org on 2023-04-30. doi:10.14284/504 [Here, Kociolek et al. (2023)]

Miranda, Salvador Valenzuela in Guiry, M.D. & Guiry, G.M. (2016) *Ellerbeckia clavigera*. AlgaeBase https://www.algaebase.org/search/species/detail/?species_id=147257

Refsnes Data (1999-2023) A school for web developers. https://www.w3schools.com/about/default.asp. [Very useful for writing web applications. Contains many up to date examples of code for web pages.]

Richman, David B and Carter, Richard (2007). Oamaru Diatoms. http://www.microscopy-uk.org.uk/mag/imgjun07/dr-rc-oamaru.pdf.

Ross, Robert (1995) A revision of *Rutilaria* Greville (Bacillariophyta). Bulletin of the Natural History Museum. Botany series 25(1), 1–93. https://www.biodiversitylibrary.org/item/128057

Round, F.E., Crawford, R.M. & Mann, D.G. (1990). The diatoms: biology and morphology of the genera. pp. [i-ix], 1-747. Cambridge: Cambridge University Press.

Schmidt, A. (0) (1874-1959). Atlas der Diatomaceen-Kunde, von Adolf Schmidt, continued by Martin Schmidt, Friedrich Fricke, Heinrich Heiden, Otto Muller, Friedrich Hustedt. Reprint 1972, 480 plates.

Sims, P.A. (2006) A REVISION OF THE GENUS RATTRAYELLA DE-TONI INCLUDING A DISCUSSION ON RELATED GENERA, Diatom Research, 21:1, 125-158, DOI:10.1080/0269249X.2006.9705656

Spaulding et al. (2021) Glossary. Retrieved on 27 Feb 2023 from https://diatoms.org/glossary.

Spaulding et al. (2023) Taxa by Morphology. Retrieved on 23 Feb 2023 from https://diatoms.org/morphology.

Strelnikova, N.I., Fourtanier, E., and Kociolek, J.P. (2004) MORPHOLOGICAL STUDIES OF AULACODISCUS SPECIES FROM THE "RUSSIAN COLLECTION" OF THE CALIFORNIA ACADEMY OF SCIENCES, Diatom Research, 19:2, 283-310, DOI: 10.1080/0269249X.2004.9705876

Tiffany, Mary Ann (2023) numerous personal communications to identify specimens.

Tiffany, Mary Ann and Hernández-Becerril, David U. (2005) Valve development in the diatom family Asterolampraceae H. L Smith 1872. Micropaleontology, vol. 51, no. 3.

Williams, D.M. (1988) An illustrated catalogue of the type specimens in the Greville diatom herbarium. Bulletin of the British Museum (Natural History), Botany Series Vol 18 No 1.

Witkowski, Jakub (2023a) personal communication.

Witkowski, Jakub (2023b) Fossil diatom atlas (https://fossil-diatoms.com/atlas/index.php?page=atlas-home)

WITKOWSKI, JAKUB, PATRICIA A. SIMS, NINA I. STRELNIKOVA & DAVID M. WILLIAMS (2015) Entogoniopsis gen. nov. and Trilamina gen. nov. (Bacillariophyta): a survey of multipolar pseudocellate diatoms with internal costae, including comments on the genus Sheshukovia Gleser. Phytotaxa 209 (1): 001–089. http://dx.doi.org/10.11646/phytotaxa.209.1.1 [Here, Witkowski et al. (2015).]

Witkowski, Jakub, Patricia A. Sims & David M. Williams (2017) Typification of Eocene–Oligocene diatom taxa proposed by Grove & Sturt (1886–1887) from the Oamaru Diatomite, Diatom Research, 32:4, 363-408. [Here, Witkowski et al. (2017)]

Wikipedia (2023) https://en.wikipedia.org/wiki/Variety_(botany) which refers to the ICN: McNeill, J.; Barrie, F.R.; Buck, W.R.; Demoulin, V.; Greuter, W.; Hawksworth, D.L.; Herendeen, P.S.; Knapp, S.; Marhold, K.; Prado, J.; Prud'homme Van Reine, W.F.; Smith, G.F.; Wiersema, J.H.; Turland, N.J. (2012). International Code of Nomenclature for algae, fungi, and plants (Melbourne Code) adopted by the Eighteenth International Botanical Congress Melbourne, Australia, July 2011. Vol. Regnum Vegetabile 154. A.R.G. Gantner Verlag KG. ISBN 978-3-87429-425-6. Chapter I. Article 4

Second Edition
Published in the June 2023 issue of Micscape Magazine.
www.micscape.org

Send comments and questions to Rob Kimmich.
Email rkimmich12 AT gmail DOT com

(First Edition published in February 2023.)